Alma Mater Studiorum · Università di Bologna

facoltà di scienze matematiche, fisiche e naturali

Corso di Laurea Magistrale in Fisica

RENORMALIZATION GROUP FLOW OF NON-LOCAL EFFECTIVE AVERAGE ACTIONS

Tesi di Laurea in Fisica Teorica

Relatore:
Prof. GIOVANNI VENTURI

Presentata da:
ALESSANDRO TICCHI

Correlatore:
Dr. GIAN PAOLO VACCA

II Sessione

Anno Accademico 2010/2011

.

To Ilenia

Contents

Introduction

In a Quantum Field Theory, all the physically relevant information is contained in the correlation functions, which can be conveniently obtained from the generating functional using the functional integration. The functional integration can be interpreted as a d-dimensional generalization of the path-integral, and from the beginning scientist approached to this task with a perturbative expansion of the field fluctuations around the fundamental configuration. In such a way, we became able to deal with many little-interacting models, and we developed some advanced techniques in order to solve the technical and conceptual issue of divergences arising in the calculations, through an intuitive redefinition of the physical quantities. But as many theories revealed to be easily manageable using renormalization techniques, others manifested pathological behaviors making them impracticable, such as it is the case of a QFT concerning General Relativity.

Luckily, the perturbative expansion is not the only way of integrating out the field fluctuations, and an alternative approach to the functional integration, first developed by K.G. Wilson [23] and reformulated by J. Polchinsky and by C. Wetterich [22] in a different form, allows to achieve non-perturbative results and is particularly useful to introduce a new definition of renormalizability called Asymptotic Safety, that includes a wider range of theories. Such a new approach is based on the concept of the Effective Average Action, that can be interpreted as the effective action we would achieve integrating out all the field fluctuations averaged over a finite volume, and allows to perform the functional integration momentum shell by momentum shell through the Exact Renormalization Group Equation, a non-perturbative integro-differential equation which describe the RG flow of the EAA.

We can interpret the EAA also as the effective action describing our system at a

particular energy scale k, providing us an alternative tool to compute the quantum effective action as the result of a flow in an infinite-dimensional theory space. But we are evidently unable to work with infinite many base elements, and if we are interested in non-numerical results we are forced to project this infinite dimensional space on an arbitrary finite dimensional subspace. Such a process is called truncation, and despite it is a non-perturbative approximation and it allows to work with a wider range of theories than the perturbative expansion do, it has the disadvantage of being arbitrary, and there is in principle no way to know a priori if a truncation is accurate. When we set a truncation, we must try to keep all the physically relevant degrees of freedom neglecting only the basis elements which do not considerably modify the flow of the investigated ones, and the only way we can check the accuracy of a truncation is to compare its outcomes with the ones achieved using a wider truncation or other asserted techniques.

Since now, people mainly investigated local truncations, by expanding the EAA in powers of the fields and focusing on the small momenta behavior of the result. This is the case of the Local Potential Approximation and of the Derivative Expansion. Such a class of truncations reveals to be accurate because, as a consequence of the particular structure of the ERGE, only the field fluctuations with momentum smaller than the reference energy scale contributes to the RG flow of the EAA.

But we could also be interested in the non-local structure of the effective average n-point vertices, as they are necessary for the calculation of the cross sections and of the scattering amplitudes, and the local truncations reveal to be unsuitable to achieve such a results for arbitrary momenta. The most useful approach for a non-perturbative evaluation of the momentum dependent n-point vertices has been developed by J.-P. Blaizot, R. Mendez-Galain and N. Wschebor [6] [2] [5], but it requests the numerical evaluation of an integro-differential equation and exploit many approximations.

Therefore, it would be interesting to find an appropriate non-local truncation able to describe the momentum-dependent structure of the correlation functions in the theory under investigation. Moreover, there are many situations in which the non-local structure of the EAA is fundamental in order to achieve meaningful results, such as it is the case of low energy QCD correlators close to the confinement phase or the computation of the contribution to the vacuum energy flow for interacting massless fields. In

fact, in both cases the non-local structure of the 2-point function plays a fundamental role. Finally, an adequate non-local truncation would allow to obtain more accurate results than the LPA without introducing an high order derivative expansion, which reveals to be quite complicate.

In order to achieve all these results, we need to find a non-polynomial analytical function dependent from few k-dependent parameters able to accurately fit the non-local structure of the n-point vertices for every energy scale k, in order to project the exact EAA flow on a subspace as close as possible to the real trajectory. We tried to find such a function and we developed two non-local truncations for a d-dimensional real scalar field theory, comparing the outcomes with the results achieved using other asserted techniques. Finally, we numerically implemented the BMW technique in order to test the 2 and 4 point vertices structure obtained using the non-local truncation we developed.

In Chapter 1, the main concepts about the non-perturbative approach to the RG are introduced. The Average Effective Action is defined and it's flow equation (ERGE) is derived. Finally, the concept of Asymptotic Safety is introduced. All the results are compared with their analogues in perturbation theory, in order to check their validity and to better understand the physical meaning of this approach.

In Chapter 2 the LPA truncation is introduced in a d-dimensional interacting real scalar field framework and the RG flow equations for the couplings are derived. The anomalous dimension of the scalar field is investigated together with the flow of the VEV and, finally, for the 1-dimensional case corresponding to the Quantum Mechanical anharmonic oscillator, the vacuum energy outcomes are compared with the corresponding results in perturbation theory.

In Chapter 3 most of our original work is collected. A non-local ansatz for the 2-point vertex is introduced in a real scalar field framework, supported by the 1-loop results given in appendix A, and the RG flow equations for the couplings are derived. An approximation scheme is developed in order to define a consistent non-local truncation also for a Z-2 invariant real scalar field theory and, under these approximations, the differential equations for the couplings are derived under the new truncation. Finally, the vacuum energy results for the QM anharmonic oscillator are compared with the LPA results and with the most accurate numerical ones.

Finally, in Chapter 4, the BMW integro-differential equation describing the RG flow of the momentum dependent 2-point vertex is derived through some approximations. The case of a real scalar field theory is numerically solved by us for different bare actions both in 1 and 4 dimensions and the results are compared to the ones achieved using the non-local truncations, in order to test the validity of the ansatz we introduced. Some analytical results concerning the BMW technique are given in appendix B.

In the Conclusions the main achieved results are summarized, some improvements and further tests are suggested and some suggestive future applications for this technique are pointed.

Chapter 1

The Exact Renormalization Group Equation

In this chapter we introduce the Effective Average Action in the framework of QFT and we develop a non-perturbative RG equation describing it's flow in the theory space. The effective average action $\Gamma_k[\phi]$ can be thought as the result of having integrated out all the field fluctuations with momentum higher than k from the bare action S. The RG flow of the EAA can be investigated through the Exact Renormalization Group Equation, which affords to integrate out the field fluctuations momentum shell by momentum shell and therefore is a non-perturbative equation despite it present a one-loop structure. We will compare the derived achievements with the perturbative loop expansion ones and we will introduce a useful non-perturbative approximation scheme, called truncation, focusing on the scheme dependence of our results. Finally, we will show how this non-perturbative approach to QFT shall introduce a new and more general definition of renormalizability under the name of AS.

1.1 Physical meaning of the Effective Action

We will now give a brief introduction about the physical meaning of the effective action and it's possible interpretation in a QFT framework [18], [28]. All the physically relevant information of a quantum field theory can be derived from the n-point Green's

functions

$$\begin{aligned} G_d^n(x_1,...,x_n)_{A_1...A_N} &= \langle 0|T\phi_{A_1}(x_1)...\phi_{A_n}(x_n)|0\rangle_{J=0} \\ &= \int D\phi\, \phi_{A_1}(x_1)...\phi_{A_n}(x_n)\, e^{-\mathcal{S}[\phi]} \end{aligned} \tag{1.1}$$

that can be obtained with n $\phi-$derivate acting on the generating functional

$$Z[J] = \int D\phi\, e^{-\mathcal{S}[\phi]+\langle \phi_A, J^A\rangle} \tag{1.2}$$

$$\text{where} \quad \langle \phi_A, J^A\rangle = \sum_A \int d^dx \phi_A(x) J^A(x)$$

$$G_d^n(x_1,...,x_n)_{A_1...A_N} = \left|\frac{\delta Z[J]}{\delta J^{A_1}(x_1)...\delta J^{A_n}(x_n)}\right|_{J=0} \tag{1.3}$$

where, for notational semplicity, we omit the A subscript in ϕ and J where possible. Diagrammatically speaking the disconnected Green's functions contains completely disjointed pieces [1], but when we deal with the calculation of cross sections we are really interested only in the connected Green's functions, which can be obtained from the functional $W[J]$ where

$$W[J] = \log[Z[J]] \tag{1.4}$$

$$G_c^n(x_1,...,x_n)_{A_1...A_N} = \left|\frac{\delta W[J]}{\delta J^{A_1}(x_1)...\delta J^{A_n}(x_n)}\right|_{J=0} \tag{1.5}$$

The relation between disconnected and connected Green's functions is illustrated in figure 1.1 and can be clarified if we invert 1.4 and expand the exponential

$$Z[J] = \sum_{n=0}^{\infty} \frac{1}{n!}(W[J])^n \tag{1.6}$$

For our purpose it is necessary to go one step further, and in place of W[J] work with the sum of all connected one particle irreducible vacuum-vacuum graphs. We introduce the classical field $\bar{\phi}_j$ as the vacuum expectation value of the operator ϕ in the presence of the current J

$$\bar{\phi}_{JA}(x) = \frac{\langle 0|\phi_A(x)|0\rangle_J}{\langle 0|0\rangle_J} = \frac{\delta W[J]}{\delta J^A} \tag{1.7}$$

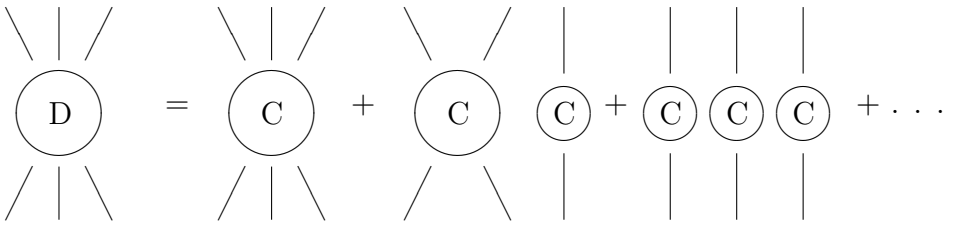

Figure 1.1: Diagrammatic representation of the relation between the Disconnected and the Connected 6-vertex Green's functions.

and inverting this relation we can obtain $J_{\bar{\phi}}$ and define the quantum effective action by the Legendre transform

$$\Gamma[\bar{\phi}] = \left\langle \bar{\phi}_A, J^A_{\bar{\phi}} \right\rangle - W[J_{\bar{\phi}}] = \min_J \left(\left\langle \bar{\phi}_A, J^A \right\rangle - W[J] \right) \tag{1.8}$$

We will now show that $\Gamma[\phi]$ is an effective action in the sense that $W[J]$ may be calculated as a sum of connected tree graphs for the vacuum-vacuum amplitude, with vertices calculated using $\Gamma[\phi]$ instead of $\mathcal{S}[\phi]$. For this purpose we introduce $W_\Gamma[J, g]$ as follow [20]

$$Z_\Gamma[J, g] = e^{W_\Gamma[J,g]} = \int D\phi \, e^{-\frac{1}{g}\left(\Gamma[\phi] - \left\langle \phi_A, J^A \right\rangle\right)} \tag{1.9}$$

Extracting the Feynman rules from our modified action $g^{-1}\Gamma[\phi]$ we find that the propagator is proportional to g while all vertices make a contribution proportional to g^{-1}. It is easy to show that for any connected graph the number of loops is $L = I - V + 1$ where I is the number of internal lines, including those connected to the J vertices, and V is the number of vertices, including those produced by the current J. So we can extract the g-dependence for the L-loop components

$$W^L_\Gamma[J, g] = g^{I-V} W^L_\Gamma[J, 1] = g^{L-1} W^L_\Gamma[J] \tag{1.10}$$

and expand

$$W_\Gamma[J, g] = \sum_{L=0}^{\infty} g^{L-1} W^L_\Gamma[J] \tag{1.11}$$

so, in the $g \to 0$ limit, we get

$$\lim_{g \to 0} \; g \, W_\Gamma[J, g] = W^0_\Gamma[J] \tag{1.12}$$

If now we rewrite equation 1.9 in Minkowsky formulation we find that in the small g limit the path integral is dominated by the point of stationary phase where $\phi = \bar{\phi}_J$ and we have

$$\lim_{g\to 0} g\, W_\Gamma[J,g] = \left\langle \bar{\phi}_{JA}, J^A \right\rangle - \Gamma[\bar{\phi}_J] = W[J] \tag{1.13}$$

therefore, from 1.12

$$W^0_\Gamma[J] = W[J] \tag{1.14}$$

where $W^0_\Gamma[J]$ is the sum of tree vacuum-vacuum grapgs calculated with vertices and propagators derived from $\Gamma[\bar{\phi}]$. We can write with symbolic formulation

$$W[J] = \int_{\text{sum of connected tree graphs}} D\phi\; e^{-\Gamma[\phi]+\left\langle \phi_{AJ}, J^A \right\rangle} \tag{1.15}$$

meaning that $W[J]$ can be calculated from a sum over all the tree level graphs with fundamental vertices and propagators obtained using the effective action instead of the bare one. But we also know that the same functional $W[J]$ can be achieved from the sum over the connected graphs with bare vertices and propagators, and, as every connected graph can be view as a tree level sum using the 1PI n-point functions as vertices connected by the 2-point green functions, we can infer that the opposite effective action $-\Gamma[\phi]$ is the result of a sum over the 1PI connected graphs in presence of the external field ϕ. This can be achieved formally using a background field technique.

$$-\Gamma[\bar{\phi}] = \int_{\text{sum of 1PI connected graphs}} D\phi\; e^{-\mathcal{S}[\phi+\bar{\phi}]} \tag{1.16}$$

$\Gamma[\bar{\phi}]$ is an effective action also in the sense that provide a quantum-corrected field equation. In fact, if we take a variational derivative of $\Gamma[\bar{\phi}]$, we find

$$\frac{\delta\Gamma[\bar{\phi}]}{\delta\bar{\phi}(x)} = J_{\bar{\phi}}(x) \tag{1.17}$$

and, for $\bar{\phi} = \bar{\phi}_J$ with $J = 0$

$$\left|\frac{\delta\Gamma[\bar{\phi}]}{\delta\bar{\phi}(x)}\right|_{\bar{\phi}=\bar{\phi}_0} = 0 \tag{1.18}$$

meaning that all the possible classical fields in the absence of external current are given by the stationary points of Γ.

Another interesting interpretation of the physical meaning of the effective action comes from the analysis of the effective potential, defined as the opposite of the density of effective action when the classical field $\bar{\phi}_0$ is supposed to be constant

$$\Gamma[\bar{\phi}_0] = -V(\bar{\phi}_0) \int d^d x \tag{1.19}$$

It is possible to show that $V(\bar{\phi}_0)$ is the minimum of the expectation value of the energy density for all states constrained by the conditions that the fields ϕ have expectation value $\bar{\phi}_0$. For the complete demonstration see [20].

1.2 The Effective Average Action

The starting point of the framework we are developing is due to Wilson and consists of performing a functional integration over a subspace of all the possible field fluctuations, discriminated by a selection in the allowed fluctuations momentums [23] . The final result will be the same as if a complete integration is performed, provided the bare action to be adjusted in order to consider the neglected field fluctuations. In such a prospective, we are allowed to integrate out the field fluctuations piecemeal and the central point of this approach to QFT is the idea that the effective theory describing physical phenomena at a momentum scale k can be thought as the result of having integrated out all the fluctuations of the field with momentum larger than k from the bare action. This can be easily obtained, as if we are using the functional integration framework to quantize the classical action we can directly select which field modes will give the greatest contribution to the generating functional. It is sufficient to add a momentum dependent term $\Delta_k \mathcal{S}[\phi]$ to the bare action $\mathcal{S}[\phi]$ acting as a weight in the path integral and suppressing all the contributions from field fluctuations with Fourier modes lower than k.

$$Z_k[J] = \int D\phi \; e^{-\mathcal{S}[\phi] - \Delta_k \mathcal{S}[\phi] + \langle \phi_A, J^A \rangle} \tag{1.20}$$

$$\text{where} \quad \langle \phi_A, J^A \rangle = \sum_A \int d^d x \phi_A(x) J^A(x)$$

The simplest choice for the regulator is

$$\Delta_k \mathcal{S}[\phi] = \frac{1}{2} \int d^d x \phi_A(x) \mathbb{R}_k^{AB}(-\nabla^2) \phi_B(x) \tag{1.21}$$

where

$$\mathbb{R}_k^{AB}(-\nabla^2) = Z^{AB} \bar{R}_k(-\nabla^2) \tag{1.22}$$

with $\bar{R}_k$ shape function satisfying the following requirements:

$$\bar{\mathbb{R}}_k(p^2) \to \begin{cases} \infty & \text{for } \left(\frac{p}{k}\right)^2 \to 0 \quad \& \quad k^2 \to \infty \\ 0 & \text{for } \left(\frac{p}{k}\right)^2 \to \infty \quad \& \quad k^2 \to 0 \end{cases} \tag{1.23}$$

We can now use our modified generating functional to get a modified average action. We obtain $W_k[\phi]$ from the generating functional

$$W_k[J] = \log[Z_k[J]] \tag{1.24}$$

and then, with a modified Legendre transform, we get the effective average action

$$\Gamma_k[\bar{\phi}] \equiv \left\langle \bar{\phi}_A, J^A_{k,\bar{\phi}} \right\rangle - W_k[J_{k,\bar{\phi}}] - \Delta_k \mathcal{S}[\bar{\phi}] \tag{1.25}$$

where, now, the $\Delta_k \mathcal{S}[\phi]$ term belong to the classical field, while the cutoff term in in 1.20 depends on the field fluctuations.

In the low k limit the functional integration is unconstrained and we have

$$\lim_{k\to 0} \Delta_k \mathcal{S}[\phi] = 0 \quad \Rightarrow \quad \lim_{k\to 0} W_k[J] = W[J] \tag{1.26}$$

the modified Legendre transform coincide with the standard one and we get the standard effective action. The need of a modified Legendre transform can be easily understood if we try to analyse the high k limit. If we use a standard Legendre transform to get our effective average action

$$\tilde{\Gamma}_k[\bar{\phi}] = \left\langle \bar{\phi}_A, J^A_{k,\bar{\phi}} \right\rangle - W_k[J_{k,\bar{\phi}}] \tag{1.27}$$

exponentiating and substituting 1.24 and 1.20 we get to the integro-differential equation

$$\exp\{-\tilde{\Gamma}_k[\bar{\phi}]\} = \int D\phi \, \exp\{-\mathcal{S}[\phi] - \Delta_k \mathcal{S}[\phi] + \int d^d x (\phi_A - \bar{\phi}_A) \frac{\delta \tilde{\Gamma}_k[\bar{\phi}]}{\delta \phi_A} \, \} \tag{1.28}$$

From the definition of the regulator 1.21 we can see that, when $k \to \infty$, $\Delta_k \mathcal{S}[\phi]$ reduces to a non-normalized Gaussian with vanishing width and suppress all the contributions in the integral except the ones from null ϕ, acting as a no-normalized delta-functional. The problem of the correct normalization will be explored and solved in chapter 1.6 with a more rigorous approach to the path integral called "Balanced Coarse-Graining". For now it is sufficient to show that, under the normalization assumption, the high k limit of the average effective action obtained with a regular Legendre transform reduces to

$$\tilde{\Gamma}_k[\bar{\phi}] \approx \mathcal{S}[\bar{\phi}] + \Delta_k \mathcal{S}[\bar{\phi}] \tag{1.29}$$

But in Wilsonian approach $k \to \infty$ limit should mean no functional integration, and so no quantization. Therefore we want to recover the bare action as high k limit of the average effective action. It is easy to show that this can be obtained with the modified Legendre transform we introduced in 1.25. In fact, proceeding as before, we can write the integro-differential equation

$$\exp\{-\Gamma_k[\bar{\phi}]\} = \int D\phi \, \exp\{-\mathcal{S}[\phi] - \Delta_k \mathcal{S}[\phi - \bar{\phi}] + \int d^d x (\phi_A - \bar{\phi}_A) \frac{\delta \Gamma_k[\bar{\phi}]}{\delta \phi_A} \, \} \tag{1.30}$$

and, for $k \to \infty$

$$\Gamma_k[\bar{\phi}] \approx \mathcal{S}[\bar{\phi}] \tag{1.31}$$

We have now introduced a new functional interpolating between the bare action $\mathcal{S}$ and the full effective action Γ. But we could also ask if the effective average action has a physical significance also for arbitrary k. We can try to answer this question remembering the interpretation of the effective action we gave in 1.1. We find that the effective average action $\Gamma_k[\bar{\phi}]$, used at three level, gives an accurate description of processes occurring at momentum scales of order k, where k behaves like a physical IR cutoff suppressing all the fluctuations with lower momentum. The characteristic physic scale k has to be defined case by case and depend on the particular situation we are interested in. An example of this could be a particle physics scattering amplitude, where the center of mass energy of the process behaves like an IR-cutoff and the effective

average action used at tree-level would allow to properly calculate the cross sections. The effective average action is so called because, as we understand from Wilson's approach to QFT, it is closely related to the effective action for fields that have been averaged over volumes of order k^{-d}, this imposing the momentum of the fluctuations to be higher than k. Additionally, the average effective action allows a good description of phenomena with characteristic scale k in the sense that it allows to derive classical equation of motion containing also quantum effects relevant for the scale of interest k. For notational simplicity we considered a fundamental theory, where the complete functional integration includes the field fluctuations with arbitrary momentum, but the generalization to an effective theory is straightforward and can be achieved simply introducing the UV cutoff term Λ in our theory and taking it into account.

1.3 Shape function and cutoff scheme dependence

In this section we have a brief excursus on the possible cutoff term choices that have been mainly used in the literature, considering a general environment with arbitrary curved spacetime, arbitrary number of fields and eventual gauge internal degrees of freedom of the fields. There are obviously several regulator choices we can do and we expect all the physical meaningful results to be independent of our arbitrary choice of it, provided it's right asymptotic behavior. This would be the case if we could get an exact evaluation of our equations. But, as we will see in section 1.7, when dealing with a flow equation for our average effective action we are forced to introduce some approximations, such as a non-perturbative one called truncation, and this introduces an inevitable cutoff scheme dependence. We faces a disappointing situation, where observable property of nature seems to depend on our personal choice of implementing an interpolation between 0 and ∞. But, as we saw, this is only the result of our approximations and, luckily, there are several observed results that reassure in believing in this approach. In fact, all the perturbative results about QFT performed with the effective average action technique are consistent with the perturbative ones for every choice of the regulator. Moreover many qualitative results obtained for the first time with this non-perturbative approach in a specific truncation are consistent and quite independent of any reasonable choice of the cutoff term. Therefore it seems reasonable to accept the scheme dependence, also

considering that it introduces an approximation in our result usually negligible when compared to the other necessary approximations.

The most natural choice for constructing a reasonable shape function is starting from the inverse propagator $\Gamma^{(2)}$ of our general theory

$$\Gamma_k^{(2)}(x,y)^{AB} = \frac{\delta^2\Gamma_k[\bar{\phi}]}{\delta\bar{\phi}_B(y)\delta\bar{\phi}_A(x)} \tag{1.32}$$

The reason is that a correct cutoff should appear everywhere the derivative of the kinetic term does, acting as a conventional mass-like IR regulator dependent from the eigenvalues of the derivative operator. For generality purpose, we will now consider the case of a covariant derivative, but everything keep valid if we deal with a standard one. The fluctuation matrix $\Gamma_k^2(x,y)^{AB}$ may contain kinetic terms also in the off diagonal entries and in such a case we need $\mathbb{R}_k^{AB}$ not to be diagonal. The simplest way to solve this problem is replacing

$$-\nabla^2 \;\longrightarrow\; P_k(-\nabla^2) \equiv -\nabla^2 + \bar{\mathbb{R}}_k(-\nabla^2) \tag{1.33}$$

everywhere it appears in the inverse propagator, where $\bar{R}(p^2)$ is a scalar function verifying 1.23 and ∇ is a covariate derivative, both with respect to the gravitational field and to other gauge connections coupled to the internal degrees of freedom. In such a way we get

$$\Gamma_k^{(2)}(x,y)^{AB} \;\longrightarrow\; \hat{\Gamma}_k^{(2)}(x,y)^{AB} \tag{1.34}$$

and we can define

$$\mathbb{R}_k(x,y)^{AB} \equiv \hat{\Gamma}_k^{(2)}(x,y)^{AB} - \Gamma_k^{(2)}(x,y)^{AB} \tag{1.35}$$

If we work with flat spacetime and without gauge internal degrees of freedom, the covariant derivative reduces to the standard one, and if we deal with only one field we can write

$$\mathbb{R}_k(x,y)^{AB} \equiv z_\phi \bar{\mathbb{R}}_k(-\partial^2) \tag{1.36}$$

where z_ϕ is called "field strength" and correspond to the factor multiplying the kinetic term in the effective average action. We are now left with the arbitrary choice of the shape function $\bar{R_k}$. Such a choice must get to terms with our possible different purposes.

The most intuitive and radical choice is that of a divergent cutoff

$$\bar{\mathbb{R}}_k(p^2) \approx \begin{cases} \infty & \text{if } p^2 << k^2 \\ 0 & \text{if } p^2 >> k^2 \end{cases} \tag{1.37}$$

for example a simple choice is the "sharp cutoff"

$$\bar{\mathbb{R}}_k(p^2) = \lim_{\Lambda\to\infty} \Lambda\, \theta(k^2 - p^2) \tag{1.38}$$

This kind of cutoff completely suppress all the fluctuations of momenta out of our rang of interest. But such a cutoff family with a singular behavior result problematic for calculations and often less adapted to imitate physical cutoff appearing in many physical situations. Therefore in the literature it is often utilized a cutoff with the following asymptotic behavior

$$\bar{\mathbb{R}}_k(p^2) \approx \begin{cases} k^2 & \text{if } p^2 << k^2 \\ 0 & \text{if } p^2 >> k^2 \end{cases} \tag{1.39}$$

If we deal with a shape function of this kind, it is often comfortable to write

$$\bar{\mathbb{R}}_k(p^2) = k^2 \mathbb{R}^0(\frac{\partial^2}{k^2}) \tag{1.40}$$

where the dimensionless shape function $R^0(p^2)$ interpolates between 0 for small k^2 and 1 for large k^2. The most common choices are that of the "optimized cutoff"

$$\mathbb{R}^0(z) = (1-z)\theta(1-z) \tag{1.41}$$

and the "exponential cutoff", parametrized by the shape parameter s

$$\mathbb{R}^0(z,\alpha) = \frac{\alpha z}{e^{\alpha z} - 1} \tag{1.42}$$

The optimized cutoff is better for analytical evaluation of many integrals while the exponential one affords more precise calculations and allows to check the scheme dependence of the results thanks to the shape parameter s. Another suitable family of cutoff functions derived from the optimized one is

$$\mathbb{R}^0(z,\alpha) = (z^{-\alpha} - z)\theta(1-z) \tag{1.43}$$

which are quite easy to handle for calculations, in particular with the choice of $\alpha = d/2$. Finally, another often used cutoff term is the so called "Callan-Zymanzic cutoff"

$$\bar{\mathbb{R}}_k(p^2) = k^2 \tag{1.44}$$

A worrying doubt about the consistency of the cutoffs satisfying 1.37 shall arise from the system of units choice. In fact, as we will see in 1.8, it is often reasonable and sometimes necessary to set k as dimensional reference unit. In such a case, the dimensionless cutoff term loose it's divergent asymptotic behavior for large k and, in the $k \to \infty$ limit, there is still quantization [24].

1.4 Exact Renormalization Group Equation

Now we are ready to develop a functional flow equation governing the behavior of the average effective action with respect to the sliding scale k [22] [3] [21]. As a first step we introduce the dimensionless parameter $t = \log \frac{k}{k_0}$, called RG time, which will parametrize the k-dependence of $\Gamma_k[\bar{\phi}]$ in our flow equation. It is also useful to rewrite the cutoff term in momentum space

$$\Delta_k \mathcal{S}[\phi] = \frac{1}{2} \int \frac{d^d p}{(2\pi)^d} \phi_A(-p) \mathbb{R}_k^{AB}(p^2) \phi_B(p) \tag{1.45}$$

where the trace Tr mean a continuous momentum integration as well as a matrix trace and we omitted the Fourier transform label $\tilde{\phi_A}$ for notational semplicity. Considering the source J as k-independent and calculating the t-derivate of $Z_k[J]$, from 1.20 we get

$$\begin{aligned} \partial_t Z[J] &= -\frac{1}{2} \int D\phi \int \frac{d^d p}{(2\pi)^d} \phi_A(-p) \partial_t \mathbb{R}_k^{AB}(p^2) \phi_B(p) e^{-\mathcal{S}[\phi] - \Delta_k \mathcal{S}[\phi] + <\phi_A J^A>} \\ &= -\frac{1}{2} \int \frac{d^d p}{(2\pi)^d} \frac{\delta}{\delta J^A(-p)} \partial_t \mathbb{R}_k^{AB}(p^2) \frac{\delta}{\delta J^B(p)} Z_k[J] \end{aligned} \tag{1.46}$$

from 1.24 we have

$$\partial_t W_k[J] = -\frac{1}{2} \mathrm{Tr} \left[\partial_t \mathbb{R}_k \{ \frac{\delta^2 W_k[J]}{\delta J \delta J} + \frac{\delta W_k[J]}{\delta J} \frac{\delta W_k[J]}{\delta J} \} \right] \tag{1.47}$$

where, using the relation shown in figure1.3, we recognize

$$\begin{aligned} \frac{\delta^2 W_k[J]}{\delta J^A(x) \delta J^B(y)} + \frac{\delta W_k[J]}{\delta J^A(x)} \frac{\delta W_k[J]}{\delta J^B(y)} &= G^{(2)}_{c,AB}(x,y) + \bar{\phi}_A(x) \bar{\phi}_B(y) \\ &= G^{(2)}_{d,AB}(x,y) \end{aligned} \tag{1.48}$$

and so we can write

$$\partial_t W_k[J] = -\frac{1}{2}\mathrm{Tr}\left[\partial_t \mathbb{R}_k G_d^{(2)}[J]\right] \tag{1.49}$$

From 1.27 it is easy to show that $G_k^{(2)}\tilde{\Gamma}_k^{(2)} = 1$ and, using 1.27 again, we can obtain

$$\partial_t \tilde{\Gamma}_k[\bar{\phi}] = \frac{1}{2}\mathrm{Tr}\left[\partial_t \mathbb{R}_k \ \left(\tilde{\Gamma}_k^{(2)}[\bar{\phi}]\right)^{-1}\right] + \partial_t \Delta_k \mathcal{S}[\bar{\phi}] \tag{1.50}$$

and, finally, using 1.25 and 1.27, we get the exact RG flow equation

$$\partial_t \Gamma_k[\bar{\phi}] = \frac{1}{2}\mathrm{Tr}\left[\partial_t \mathbb{R}_k \left(\Gamma_k^{(2)}[\bar{\phi}] + \mathbb{R}_k\right)^{-1}\right] \tag{1.51}$$

It is interesting to note that, thanks to the regulator $\mathbb{R}_k$, the ERGE is always well defined. In fact, the presence of $\mathbb{R}_k$ in the denominator together with 1.23 guarantees the IR regularization of the trace integration, while the UV regularization is preserved thanks to the derivative $\partial_t \mathbb{R}_k$, which force the main contribution of the integration to lie on a momentum shell near $p^2 \sim k^2$.

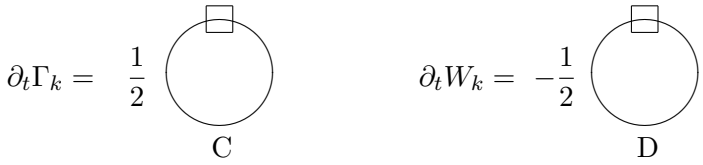

Figure 1.2: Diagammatic representation of equations 1.47 and 1.51. The straight line represent the modified propagator G_k^2 respectively connected C and disconnected D (fig.1.3) while the square vertex represent the t-derivative of the cutoff term $\partial_t R_k$.

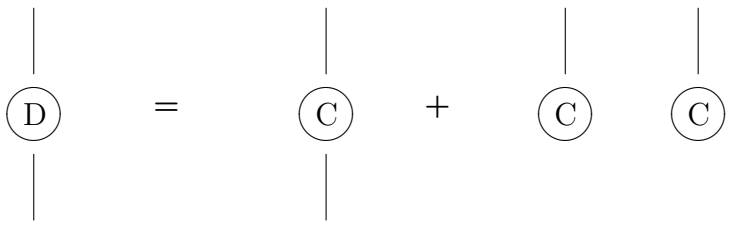

Figure 1.3: Diagrammatic representation of the relation between the Disconnected and the Connected 2-points Green's functions.

1.5 ERGE and perturbative loop expansion

Although the flow equation we obtained has a one-loop structure, as a consequence of $\Delta_k\mathcal{S}$ being quadratic in the field, it is nevertheless an exact and non-perturbative equation, thanks to the presence of the exact propagator in the loop integration. Perturbative loop expansion can be derived from the ERGE simply expanding the average effective action in $\hbar$

$$\Gamma_k[\bar{\phi}] = \Gamma_k^{0-l}[\bar{\phi}] + \hbar\Gamma_k^{1-l}[\bar{\phi}] + \hbar^2\Gamma_k^{2-l}[\bar{\phi}] + \dots \tag{1.52}$$

remembering the presence of $\hbar$ in the rhs of the ERGE (we omitted while working in natural units) we get

$$\begin{aligned} \partial_t\Gamma_k^{0-l}[\bar{\phi}] &= 0 \\ \Gamma_k^{0-l}[\bar{\phi}] &= \mathcal{S}[\bar{\phi}] \end{aligned} \tag{1.53}$$

In the same way we can derive the 1-loop approximation

$$\begin{aligned} \partial_t\Gamma_k^{1-l}[\bar{\phi}] &= \frac{1}{2}\mathrm{Tr}\left[\partial_t\mathbb{R}_k\left(\frac{\partial^2\mathcal{S}}{\partial\bar{\phi}\partial\bar{\phi}} + \mathbb{R}_k\right)^{-1}\right] \\ \Gamma_k^{1-l}[\bar{\phi}] &= \frac{1}{2}\mathrm{Tr}\log\left[\frac{\partial^2\mathcal{S}}{\partial\bar{\phi}\partial\bar{\phi}} + \mathbb{R}_k\right] + \text{Const.} \end{aligned} \tag{1.54}$$

which, for $k \to 0$, coincide with the standard one loop approximation of the effective action. We can see the analogy between the ERGE and the one loop equation for the effective action, the latter being an improved version of the former, obtained simply replacing the bare action with the effective one in the loop integration and adding a cutoff term. We can push forward our expansion to every perturbative order.

1.6 Balanced Coarse-Graining

The generating functional $Z[J]$ can be achieved through a functional integration over the field fluctuations, which can be seen as a d-dimensional generalization of the path integral in phase space. The integration, having place over the configuration variables q and their conjugate momenta p, is performed with a Liouville measure $\mu(q,p)$ and, under the hypothesis of an Hamiltonian quadratically dependent on the conjugate momenta, the p-integration can be performed separately reducing the path integral to an

integration of the Lagrangian action over the configuration space with a new measure, symbolically represented by $\mu(q) = \mu(q,p)(det(-\partial_t^2))^{\frac{1}{2}}$. In the path integral there are many sources of divergences, coming from the integrations over both the configuration and momentum variables and from the path integral Liouville measure, that, in a skeletonized version, can be seen as the product of infinite many phase space Liouville measures, everyone being the square root of the determinant of the symplectic form. In QM, all these singular contributions need to cancel each other in order to get a finite path integral result. In our approach to the functional integration, we simply forgot about the momentum integration and we derived the EAA by modifying the Lagrangian action and performing the q integration leaving the measure unchanged. But such a procedure does not preserve the mutual cancellation process of the divergences arising in the integration, and the finiteness in QM of the result is no more guaranteed. We will now introduce an alternative way to achieve a weighted functional integration without altering the pattern of cancellations of the divergences. This approach, called "Balanced Coarse-Graining", was firstly introduced by Vacca and Zambelli [24] and consists in the introduction of a regularization term in the functional integration as a consequence of the insertion of a mode-dependent operator in the symplectic structure. After the momentum integration has been performed, this more general approach will bring to a configuration space measure with an implicit momentum scale dependence related to the cutoff term, and this will allow to achieve a modified Wetterich RG flow equation which will bring to many comforting results.

1.6.1 Balanced Coarse-Graining and Quantum Mechanics

As a first step we will now introduce a Balanced Coarse-Graining framework for a quantum mechanical bosonic oscillator, corresponding to the QM transposition of a 0+1 dimensional real scalar field theory. We introduce an Hamiltonian quadratically dependent on the momentum p

$$H[p,q] = \frac{1}{2}p^2 + V[q] \tag{1.55}$$

and the unmodified Euclidean path integral

$$Z[J] = \int DqDp\ \mu(q,p)\ e^{\int dt[ip(t)\partial_t q(t) - H[q(t),p(t)] + J(t)q(t)]} \tag{1.56}$$

We can now change the integration variables introducing $P(t) = p(t) - i\partial_t q(t)$ and simplify

$$\begin{aligned} Z[J] &= \int DqDP\ \tilde{\mu}(q,P)\ e^{\int dt[-\frac{1}{2}(\partial_t q(t))^2 - V[q(t)] - \frac{1}{2}p(t)^2 + J(t)q(t)]} \\ &= \int Dq\ \mu(q)\ e^{-S[q]+\langle q,J\rangle} \end{aligned} \tag{1.57}$$

where

$$\langle q, J\rangle = \int dt J(t)q(t) \tag{1.58}$$

$$S[q] = \int dt \left(\frac{1}{2}\left(\partial_t q(t)\right)^2 + V[q(t)]\right) \tag{1.59}$$

$$\mu(q) = \mu(q,p)(det(-\partial_t^2))^{\frac{1}{2}} \tag{1.60}$$

as can be achieved performing the path integral for a free particle.

In chapter 1.2 we introduced a modified generating functional

$$Z_k[J] = \int dq\ \mu(q)\ e^{-\mathcal{S}[q]-\Delta_k\mathcal{S}[q]+\langle q,J\rangle} \tag{1.61}$$

simply adding to the bare action $S[q]$ a regulator term

$$\Delta_k\mathcal{S}[q] = \frac{1}{2}\int dt\ q(t)\mathbb{R}_k(-\partial_t^2)q(t) = \frac{1}{2}\int dt\ q(t)\frac{\Delta_k(-\partial_t^2)}{-\partial_t^2}q(t) \tag{1.62}$$

acting as a weight in the functional integration over the configuration variable q. In such a way, we regularize the integration over the configuration variable leaving the momentum integration and the Liouville measure unchanged, and therefore we modify the pattern of cancellations of the divergences in an inconsistent way. It is possible to show that equation 1.61 can be achieved starting from a k-dependent phase space path-integral

$$Z[J] = \int DqDp\ \mu(q,p)\ e^{\int dt[i\sqrt{1+\Delta_k(-\partial_t^2)}p(t)\partial_t q(t) - H[q(t),p(t)] + J(t)q(t)]} \tag{1.63}$$

and substituting

$$P(t) = (1+\Delta_k(-\partial_t^2))^{\frac{1}{4}}p(t) - i(1+\Delta_k(-\partial_t^2))^{\frac{3}{4}}\partial_t q(q) \tag{1.64}$$

Therefore, the introduction of the regularization term in the path integral can be interpreted as the result of implementing a modified Legendre transform leaving the bare

Hamiltonian unchanged. But the Legendre transform and the Liouville measure μ are not independent, as the Legendre transform term $p(t)\ \partial_t q(t)$ is the pull back of the Liouville 1-form $\lambda = p\ dq$ and the Liouville measure μ is just the square root of the determinant of the symplectic form $\sigma = d\lambda$.

$$\mu = (\mathrm{Det}\sigma)^{\frac{1}{2}} = (\mathrm{Det}(d\lambda))^{\frac{1}{2}}$$

In order to get the required modified Legendre transform, we must introduce the modified quantities

$$\lambda_k = \sqrt{1+\Delta_k}\ \lambda \qquad \sigma_k = \sqrt{1+\Delta_k}\ \sigma \qquad \mu_k = \sqrt{\mathrm{Det}(1+\Delta_k)}\ \mu \tag{1.65}$$

Therefore, we are forced to introduce a modified Liouville measure in the path integral in order to get a balanced an coherent regularization. If we work with canonically conjugated variables q, p such as $[q,p]=1$, the unmodified Liouville phase space measure reduces to $\mu(q,p)=1$ and we get to the final formulation for the average generating functional

$$Z_k[J] = \int Dq\,(\mathrm{Det}(1+\Delta_k))^{\frac{1}{2}}\left(\mathrm{Det}(\partial_t^2)\right)^{\frac{1}{2}} e^{-S[q]-\Delta_k\mathcal{S}[q]+\langle q,J\rangle} \tag{1.66}$$

and, proceeding as in section 1.4, we can get a balanced version of the Wetterich RG flow equation

$$\partial_t\Gamma_k[\bar{\phi}] = \frac{1}{2}\mathrm{Tr}\left[\partial_t\mathbb{R}_k\left(\Gamma_k^{(2)}[\bar{\phi}]+\mathbb{R}_k\right)^{-1}\right] - \frac{1}{2}\mathrm{Tr}\left[\partial_t\mathbb{R}_k\left(-\partial_t^2+\mathbb{R}_k\right)^{-1}\right] \tag{1.67}$$

1.6.2 Balanced Coarse-Graining and QFT

The generalization of the Balanced Coarse-Graining framework to a d-dimensional QFT is straightforward. We firstly introduce the Hamiltonian describing our system

$$H[\phi,\pi] = \int d^dx\ \frac{1}{2}\pi(x)^2 + \frac{1}{2}|\nabla\phi(x)|^2 + V[\phi(x)] \tag{1.68}$$

and we write the generating functional through the Euclidean path integral

$$\begin{aligned} Z[J] &= \int D\phi D\pi\mu[\phi,\pi]e^{\int d^dx\ i\pi\partial_0\phi(x)-H[\phi,\pi]+\langle\phi,J\rangle} \\ &= \int D\phi\ \mu[\phi]\ e^{-S[\phi]+\langle\phi,J\rangle} \end{aligned} \tag{1.69}$$

with

$$S[\phi] = \int d^d x \, \frac{1}{2} \left(\partial_0 \phi(x)\right)^2 + \frac{1}{2} |\nabla \phi(x)|^2 + V[\phi(x)] \tag{1.70}$$

As we did in the QM framework, we can introduce a modified k-dependent Legendre transform in order to introduce a regulator term in the functional integration

$$\int d^d x \; i\pi \partial_0 \phi(x) \quad \longrightarrow \quad \int d^d x \; i\pi (1 + \Delta_k)^{\frac{1}{2}} \partial_0 \phi(x) \tag{1.71}$$

and, consequently, introducing the modified Liouville measure and proceeding as before, we get

$$Z[J] \;\; = \;\; \int D\phi \; \mu[\phi] \; \left(\mathrm{Det}(1 + \Delta_k)\right)^{\frac{1}{2}} e^{-S[\phi] - \frac{1}{2} \int d^d x \partial_0 \phi \Delta_k \partial^0 \phi + \langle \phi, J \rangle} \tag{1.72}$$

But while in a QM theory this is sufficient to fully regularize the functional integration, now the modified Legendre transform is not able to weight the spatial field oscillating modes $\partial_i \phi \partial^i \phi$, and the only way to achieve this result is to introduce a k-dependent term the bare Hamiltonian

$$\tilde{H}[\phi, \pi] = H[\phi, \pi] + \frac{1}{2} \int d^d x \; \partial_i \phi(x) \tilde{\Delta}_k \partial^i \phi(x) \tag{1.73}$$

and, therefore

$$Z[J] = \int D\phi \; \mu[\phi] \; \left(\mathrm{Det}(1 + \Delta_k)\right)^{\frac{1}{2}} e^{-S[\phi] - \frac{1}{2} \int d^d x \partial_0 \phi \Delta_k \partial^0 \phi - \frac{1}{2} \int d^d x \partial_i \phi \tilde{\Delta}_k \partial^i \phi + \langle \phi, J \rangle} \tag{1.74}$$

Generally, the regulators terms Δ_k and $\tilde{\Delta}_k$ are independent and we intentionally omitted their arguments, as many choices are possible [24]. We will now restrict to the most natural choice of a Lorentz invariant cutoff simply setting $\Delta_k = \tilde{\Delta}_k$ and making them dependent on the Lorentz invariant D'Alembert operator $-\partial^2 = -\partial_\mu \partial^\mu$. Under these assumptions, we can derive the modified Wetterich equation

$$\partial_t \Gamma_k[\bar{\phi}] = \frac{1}{2} \mathrm{Tr} \left[\partial_t \mathbb{R}_k \left(\Gamma_k^{(2)}[\bar{\phi}] + \mathbb{R}_k \right)^{-1} \right] - \frac{1}{2} \mathrm{Tr} \left[\partial_t \mathbb{R}_k \left(-\partial^2 + \mathbb{R}_k \right)^{-1} \right] \tag{1.75}$$

with the usual notation

$$\mathbb{R}_k(-\partial^2) = -\partial^2 \; \Delta_k(-\partial^2) \tag{1.76}$$

1.6.3 Effective Average Action and high k limit

If we are quantizing a classical theory, it is obviously necessary to satisfy the high energy limit

$$\lim_{k\to\infty} \Gamma_k[\phi] = \mathcal{S}[\phi] \tag{1.77}$$

in order to have an accessible boundary condition in the evaluation of the RG flow. Moreover, such a condition is also fundamental if we want to derive AS conclusions about the model we are developing and, finally, it is necessary if we want to get some informations about the classical theory we are quantizing, to start from the knowledge of the effective one. But, as we saw in section 1.2, using the standard derivation for the EAA the regulator term act as a non-normalized delta function in the high k limit. This problem is naturally solved using the balance approach to the coarse-graining. In fact, starting from the modified path integral, we can get the following formulation for the EAA

$$e^{-\Gamma_k[\phi]} = \int D\phi\ \mu_k[\phi]\exp\{-\mathcal{S}[\phi] - \Delta_k\mathcal{S}[\phi-\bar{\phi}] + \int d^dx(\phi-\bar{\phi})\frac{\delta\Gamma_k[\bar{\phi}]}{\delta\phi}\ \} \tag{1.78}$$

and in the high k limit, under the assumption of $\mathbb{R}_k \to \infty$ for $k \to \infty$ and working with canonically conjugated variables, we find

$$\int D\phi\ \left(\mathrm{Det}(\partial^2)\mathrm{Det}(1+\Delta_k)\right)^{\frac{1}{2}} e^{-\frac{1}{2}\int d^dx(\phi-\bar{\phi})\mathbb{R}_k(\phi-\bar{\phi})} \longrightarrow 1 \tag{1.79}$$

and the classical limit is restored. Unfortunately, the condition $\mathbb{R}_k \to \infty$ for $k \to \infty$ is not always granted, as we saw in 1.3, and many often used smooth cutoff terms do not satisfy this request when we set k as fundamental unit.

1.7 RG trajectory in theory space and truncation

In the previous section we introduced a non perturbative differential functional equation describing the flow of the effective average action under the variation of k. Now we are going to address the main properties of this flow and to introduce an approximation necessary for a non perturbative approach to the analysis of it's trajectory. As a consequence of the physical meaning we attributed to the average effective action, we understand that this functional contains all the relevant information describing a

QFT at a fixed characteristic scale. Therefore we can interpret the flow of Γ_k as a flow in the space of all physically acceptable theories, represented by the set of all functionals possessing the symmetry properties characterizing our physical system. We can parametrize this infinite dimensional manifold Q introducing the basis operators $\Theta_{i,k}[\phi]$, comprising all local and non-local operators constructed with the fields and their derivatives and compatible with the symmetries of our system. The existence of a complete basis for the space of the allowed functionals is not guaranteed, but we will always assume this to be the case. Generally the basis elements can flow with k, as expressed from the k-label we introduced in our notation, but for simplicity we will now assume them to be k-independent without loosing generality, because of the arbitrary choice of the basis. We can now identify every functional with a particular set of the couplings $\{g_i\}$, which are the basis elements of the dual of the operators space, and write

$$\Gamma_k[\phi] = \sum_i g_{i,k}\Theta_i[\phi] \tag{1.80}$$

Taking the k derivative of Γ we get

$$\partial_t\Gamma_k[\phi] = \sum_i \partial_t g_{i,k}\Theta_i[\phi] = \sum_i \beta_{i,k}\Theta_i[\phi] \tag{1.81}$$

and, using the ERGE, we can get an infinite-dimensional differential system

$$\beta_i = \beta_i(g,k) \tag{1.82}$$

Dealing with such a system of infinite equation is technically impossible, and the only chance we have to get quantitative results from it is to reduce the number of the basis elements to an arbitrary finite quantity N. In such a way we force the flow to lie on a N-dimensional hypersurface W projecting the real trajectory on the finite dimensional subspace [1]. This approximation is called "truncation" and is evidently unnatural, as in every momentum variation δk infinite many non-zero terms are generated from the ERGE. There is no rigorous way to discriminate a good truncation from a bad one, the only thing we can do is to use many different truncations and check the reliability

[1] Also a finite dimensional subspace could be used instead of a finite dimensional one. In such a case, it is not possible to achieve a differential system of coupled equations for the couplings, but it is nevertheless possible to investigate the system using other numerical techniques.

of the results. Although there are many natural prescriptions helping us to build a reasonable truncation; first of all, our truncation must be consistent, in the sense that, for example, if we expand the effective average action in an arbitrary way end we choose the maximal order of the expansion to keep in the truncation, we also must keep in the truncation all terms up to that order. A second useful prescription is that of trying to include in the truncation all the physically relevant degrees of freedom. It is not enough if we try to include in our truncation all the couplings which mainly differ from zero during the flow: a good truncation is not one for which neglected terms are small but one for which the effect of the neglected terms on the included ones is small. A direct and easy way to check the quality of a truncation is that of measure the cutoff scheme dependence of our observable quantities. We will now show this analysing the effect of truncation on the cutoff scheme dependence of our trajectory in the theory space.

While dealing with the complete space theory and the exact ERGE solution, the internal points of our trajectory possess a natural cutoff scheme dependence, as we can understand considering that different cutoff terms means different field fluctuations integrated out, while the initial and final points of our flow are obviously independent of $\mathbb{R}_k$, as they represent the bare and effective action, this thanks to the imposition that all the cutoff terms have the same asymptotic behavior 1.23. Moreover, all the universal and observable quantities, implicitly independent of any characteristic scale k, must also be scheme independent as, for example, happen of the characteristic exponentials. But when we project our flow on a finite-dimensional subspace, different trajectories with the same asymptotic behavior could turn into till different trajectories belonging to the same subspace but now with different asymptotic behavior. This happens because it is quite different to project the exact trajectory obtained with the ERGE on a subspace than constructing an approximated flux forced to lie on the same subspace. As a consequence all the universal quantities acquire a cutoff scheme dependence which will be as wide as the truncation is unable to describe the correct flow and forces the trajectory to lie on a subspace distant from it.

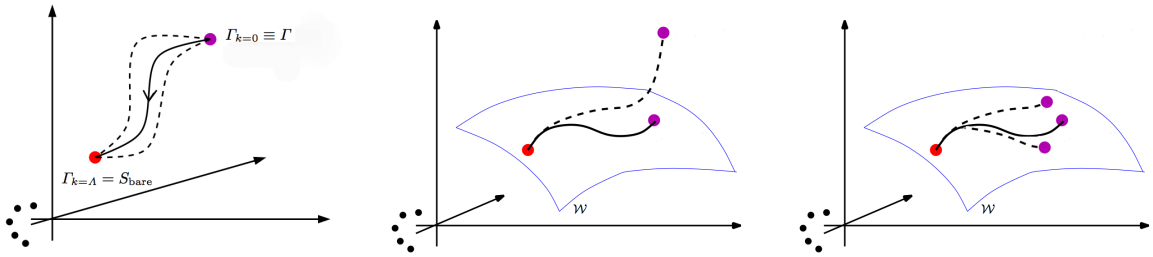

(a) **(b)** **(c)**

Figure 1.4: Graphical representation of (a) the cutoff scheme dependence of the RG trajectory in theory space obtained without any truncation; (b) the truncation effects on the RG trajectory. (c) the cutoff scheme dependence of the RG trajectory in the theory space after a truncation is introduced.

1.8 Field redefinition and system of units

In the previous section we asserted the space of all functionals compatible with the required symmetries to be equivalent with the space of all physically acceptable theories. We will now specify our assertion, showing that actually the latter is equivalent with a subspace obtained dividing the former through classes of equivalence. Indeed it is possible to build a group of allowed functional transformations leaving unaffected the physical meaning of our theory [25]. First of all we shall consider our functional $\Gamma_k(\phi, g_i)$ as actually acting on the Cartesian product $\mathcal{F} \times \mathcal{Q}$, where $\mathcal{F}$ is the infinite-dimensional space of all field configurations with the fields $\phi_A(x)$ as coordinates. As the fields ϕ are involved in our calculations only as integration variables, it is clear that shall exist a group $\mathcal{G}$ of allowed field redefinition leaving unaffected the theory we are developing. $\mathcal{G}$ must evidently submit all the symmetry requirements of our system and, as $\Gamma[phi]$ is the most general functional satisfying the required symmetries, we can always find a representation $\mathcal{D}$ of $\mathcal{G}$ acting on the space of all the coupling constant $\mathcal{Q}$ such as

$$\Gamma_k(T\phi, g_i) = \Gamma_k(\phi, \mathcal{D}(\mathcal{T}^{-1})g_i) \tag{1.83}$$

In such a way we get an equivalence relationship acting on the space of the coupling constants and this allows us to work in a subspace with n dimensions less than $\mathcal{Q}$, where n is the dimension of the group $\mathcal{G}$. We will call the coordinates of the reduced subspace

essential coupling constants, in contrast with the redundant ones we eliminated. Thus, we are able to fix the value of arbitrary n couplings $g_1...g_n$ to a constant arbitrary value $\bar{g}_1...\bar{g}_n$ for all the flow of our functional and to study the trajectory parametrized by the only essential couplings. Actually, the choice of the n couplings to be fixed and considered as redundant is not completely arbitrary. In fact we must choose n linearly independent couplings which are not invariant under the action of $\mathcal{D}$, as an invariant coupling constant is independent from the equivalence transformations an can not be fixed with an opportune choice of $\mathcal{T}$. The most simple field redefinition is that of a field rescaling $\phi'_{A(x)} = c^{-1}\phi_{A(x)}$, where c is an arbitrary dimensionless parameter. Such a transformation of the field leave unaffected the physical meaning of the theory we are developing and we can simply construct a representation of this transformation acting in the space of couplings and, through it, designate a redundant coupling.

We can make a similar observation about the system of units we are dealing with [14]. A very common an useful choice is that of using the so called natural units, where we impose $\hbar = c = 1$. In this way, all the dimensional units become linearly dependent to only one fundamental and arbitrary unit. There are several reasonable choices we can make about our reference unit and obviously our final physical theory will be independent of the arbitrary choice we make. We can show this exploiting the scale invariance of any bare action

$$\mathcal{S}(b^{d_A}\phi_A, b^{d_i}g_i) = \mathcal{S}(\phi_A, g_i) \tag{1.84}$$

where b is an arbitrary dimensionless parameter and $d_{A/i}$ are called the canonical dimensions of ϕ_A/g_i. The scale invariance can be exported to the average effective action, provided we rescale also the scale parameter k with the factor b.

$$\Gamma_{bk}(b^{d_A}\phi_A, b^{d_i}g_i) = \Gamma_k(\phi_A, g_i) \tag{1.85}$$

We usually choose the system of units to work with case by case, according to our purposes. The most common and intuitive choice for it is that of using a dimensional universal measurable quantity independent from our theory such as the electron mass if we are dealing with QCD. This choice is called of "external units". But such a choice isn't always possible. Sometimes there is no scale-independent dimensional quantity, as

for example happens when dealing with a QFT concerning gravity, and we are forced to choose an internal fundamental unit. The most natural choices are that of using the UV cutoff Λ, when present, that is the limit of validity of an effective theory, or otherwise the scale parameter k, parametrizing the flow of our average effective action. We will use this last choice in the rest of our work, a choice that will reveal to be the most useful and natural for the study of the ERGE flow. Choosing to use k as internal unit means we have to evaluate all the dimensional quantities comparing them with the scale of our theory, and affords as natural consequence the choice of the RG time $t = \log \frac{k}{k^o}$, introduced in 1.4 and parametrizing the flow equation, as we see from

$$\frac{\partial}{\partial t} = k \frac{\partial}{\partial k} \tag{1.86}$$

Using k as fundamental unit is equivalent to associate to each coupling the corresponding dimensionless parameter

$$\check{g}_{i,k} = g_{i,k} k^{-d_i} \tag{1.87}$$

and to study their flow according to the dimensionless beta functions.

$$\check{\beta}_{i,k} = \partial_t \check{g}_{i,k} = -d_i \check{g}_{i,k} + k^{-d_i} \beta_i \tag{1.88}$$

These dimensionless couplings are more fundamental than the dimensional ones, and there are many physical, mathematical and statistical arguments justifying the use of them [26] .

We have shown that the physical meaning of our theory is preserved under field redefinition and under scale transformations and that we can exploit this feature to fix once and for all the value of n irrelevant coupling constants and to set the scale parameter $k = 1$, working with dimensionless couplings rather than with dimensional ones. We can technically implement this introducing a complete RG transformation structured in three phases:

- The ERGE evaluation under an infinitesimal scale variation δk. In this way we account the contribution to the average effective action variation coming from the functional integration over field fluctuations.

- A field rescaling, adapted to set the value of the redundant couplings to the prefixed one.

- A scale redefinition associated to the spacetime, allowing to restore $k = 1$ and equivalently to study the flow of the dimensionless couplings instead of the dimensional ones.

It is interesting to mark that, if we deal with a QFT concerning gravity and we quantize the metric tensor $g_{\mu,\nu}$, the second and third point belong to the same transformation, as a metric redefinition means a rescaling of the space and is equivalent to a scale redefinition. In this situation, we are forced to abandon the point two with regard to the metric tensor and to evaluate the flow of all the gravitational coupling constants in our truncation.

Another interesting remark belonging to the choice of setting $k = 1$ through a scale redefinition was already introduced in section 1.3. In fact, if we define a cutoff satisfying conditions 1.39, such as, for example, cutoff 1.40 with 1.41 or 1.42 inserted, if we use k as dimensional reference unit we find that the regulator loose its asymptotic behavior for $k \to \infty$. This means that in the high energy limit there is still quantization and we loose the $\Gamma_k \to \mathcal{S}$ limit, as we already mentioned in 1.6.3 [24].

1.9 Asymptotic Safety

We will now come back to an exact model in the absence of truncation and we will try to introduce some criteria establishing when an effective theory could be well defined at every energy scale (fundamental) and predictive. For this purpose we consider the absence of any UV cutoff, represented by the $\Lambda \to \infty$ limit. Since now we have been defining our QFT starting from a given bare action $\mathcal{S}$ and the generating functional, in a standard way, and we have derived the ERGE as a tool for a step by step functional integration of the field fluctuations. But we also may adopt a different perspective, and define a QFT which relies on the flow equation, once a suitable initial condition $\mathcal{S}$ is assumed. We may go one step further and, instead of the bare action, take as boundary condition of the RG flow the average effective action Γ referred to an arbitrary scale k. This means that our theory will be completely defined once the theory space has been fixed, the shape function R has been chosen and we have impose d the initial condition at an arbitrary scale k. In such a way, we could hope to measure some observable quantities of our theory at the energy scale k and use them to obtain the value of any coupling constant at the same energy scale $g_{i,k}$. We could then use the ERGE to achieve the beta functions and reconstruct the whole trajectory of our theory, getting a complete and predictive model describing the system we are interested in. Unluckily, as we saw in 1.7, there are infinitely many coupling constants to be determined, ad this can be achieved only with an infinite number of experiments. In such a situation our theory unavoidably loose its predictivity, as it is unthinkable to experimentally fix infinitely many parameters. In the following we will try to fix this issue through the requirement of a fundamental theory, in an analogue way as renormalizability prescriptions do in the perturbative approach to QFT. We call fundamental a theory which is effective at every finite energy scale k. In order to get this, our theory must be well defined for every k. There are many ways a theory could lose its effectiveness and assume pathological behavior during its flow, as for example some symmetries intrinsic in the system we are studying could be broken or new degrees of freedom could arise, making our model inadequate to describe our system at such an energy scale. But the most worrying situation is that of the divergence of some observable quantities, as a consequence of the divergent behavior of some dimensionless couplings. Therefore, a necessary condition for a fundamental theory is that all the dimensionless essential couplings should be

finite at every energy scale, therefore also in the $k \to \infty$ limit.

We know that the ERGE allows to express the beta functions in terms of Γ_k and its derivatives. This imply that we can get the infinite-dimensional system

$$\check{\beta}_i = \check{\beta}_i(\check{g}) \tag{1.89}$$

In order to deal with finite dimensionless couplings also in the $k \to \infty$ limit the must natural request, nevertheless it is not the only possible scenario [13], is that of the existence of an high energy finite limit for them

$$\begin{aligned} \check{g}_{i,k} &\to \check{g}_i^* \quad \text{for} \quad k \to \infty \\ \check{\beta}_{i,k} &\to 0 \quad \text{for} \quad k \to \infty \end{aligned} \tag{1.90}$$

We define the fixed point $\check{g}^*$ in the space of couplings as the solution of the system.

$$\check{\beta}_i(\check{g}^*) = 0 \tag{1.91}$$

Clearly there could be more than one FPs and we must analyse our system case by case if we want to have qualitative informations about them. We will call "Gaussian" a fixed point characterized by all the couplings being set to zero and it is possible to show that the Gaussian FP exist for every QFT, as it corresponds to the free theory configuration. If at a certain energy scale our system is described by a theory with couplings in a FP of the flow, the theory will remain unchanged at every energy scale and we will be dealing with a scale invariant field theory, possibly conformal. Such a theory doesn't require any RG flow equation to be described, as all the necessary information is contained in the FP. A more interesting situation is that of a theory asymptotically approaching the FP for high k. We can analyse such a situation introducing the shifted coupling constants $\tilde{g}_i = \check{g}_i - \check{g}_i^*$ and linearising the RG flow and the beta functions in the neighbourhood of the FP

$$\partial_t \tilde{g}_i = \mathcal{M}_i{}^j \ \tilde{g}_j + O\left[(\tilde{g})^2\right] \tag{1.92}$$

introducing the stability matrix

$$\mathcal{M}_i{}^j = \left.\frac{\partial \check{\beta}_i}{\partial \check{g}_j}\right|_{\check{g}=\check{g}^*} \tag{1.93}$$

This matrix is not necessary symmetric and, where diagonalizable, it may have some non real eigenvalues. Under the hypothesis of the diagonalizability we can write

$$\mathcal{M} = \sum_r P_{v^r} \theta_r \tag{1.94}$$

where $(\theta_1 ... \theta_r ...)$ are the eigenvalues of $\mathcal{M}$ and $(P_{v^1} ... P_{v^r} ...)$ are the projectors on the subspace generated by the corresponding eigenvectors $(v_i^1 ... v_i^r ...)$. We can now approximate the flow of the couplings in the proximity of the FP with

$$\check{g}_{i,k} - \check{g}^*_{i,k} = \tilde{g}_{i,k} = \sum_r d_r v_i^r e^{\theta_r \log \frac{k}{k^o}} \tag{1.95}$$

Following this considerations we find that, in order to get the asymptotic behavior we need for our theory, we must impose the coupling constants to lie on the hypersurface generated from all the attractive directions, namely all the eigenvectors for which the correspondent eigenvector θ_i satisfies $\mathrm{Re}[\theta_i] < 0$. This represents a fine-tuning problem. In fact, if we slightly perturb our flow in any repulsive direction, we loose our asymptotic finite behavior. Thus, if we request reality to be described from a meaningful theory at arbitrary high energy, we need an infinite precision tuning of the coupling constant at an arbitrary finite energy scale k. Usually the opposite of the real part of the eigenvalues θ_r are also called critical exponent

$$b_r = -\mathrm{Re}[\theta_r] \tag{1.96}$$

and if our coupling constants are chosen in such a way that $\mathcal{M}$ is naturally diagonal, as usually happens, we can identify the eigenvectors with the coupling themselves and we call relevant the ones with positive critical exponent and irrelevant those for which the critical exponent is negative. Finally we call UV critical surface the hypersurface spanned by all the relevant eigenvectors, i.e. a surface parametrized by all the relevant couplings and defined by the condition $\tilde{g}_i = 0 \, \forall$ i irrelevant. It is interesting to note that the permitted trajectories are not asked to lie on the UV critical surface, but only to asymptotically approach the FP through it, as the linear approximation we used is valid only in the neighbourhood of the FP.

We can now come back to our initial problem. We have shown how we can guarantee that our theory remain "finite" when $k \to \infty$, thanks to the presence of a FP and to

the fine tuning of our trajectory in the theory space. But we want our theory to be predictive, that is the bare action to be fixed through a finite number of experiments. In the perturbative approach to QFT this problem is solved by the prescription of renormalizability. When we evaluate the vacuum-vacuum graphs contributing to the effective action, we find that an infinite number of divergences arises, unless all the dimensional coupling with negative mass dimensions are set exactly to 0. In this way, we reduces the number of relevant diagonal interactions to a finite one, and our theory become predictive. In an analogous way we can now use our prescription of finite high energy limit of our theory for reducing the number of the degrees of freedom in our model. Obviously we will obtain a predictive theory only if the UV critical surface is finite-dimensional. We will call "asymptotically safe" (AS) a QFT for which exists a non-Gaussian FP with a finite number of attractive directions. In an AS scenario it is always possible to achieve a fine tuning of the couplings making our theory finite also in the high energy limit, and this fine tuning is sufficient to make our theory also predictive.

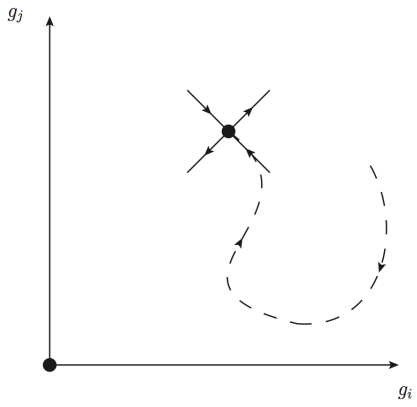

Figure 1.5: Graphic 2-dimensional representation of an AS scenario. The dashed line represent a safe trajectory, approaching the FP through the UV critical surface.

1.10 AS and Asymptotic Freedom

The perturbative expansion holds appropriate only when dealing with small couplings and consequently it allows a good approximation of our system only if we are in presence of a Gaussian FP. In such a situation we expect the non perturbative and perturbative approach to give consistent qualitative predictions about the allowed degrees of freedom in our theory. Starting from a representation of the Effective Action as the sum over all the 1PI graphs with external lines connected to the external sources J, we may employ a perturbative approach. In such a case, adopting the power counting criterion and assuming for shortness we are dealing with scalar fields, it is easy to show that we can express the superficial degree of divergence of a graph $\mathcal{G}$ in term of the number of external lines $\mathcal{E}$, the number of vertices with n legs $\mathcal{V}_n$ and the number of spacetime dimensions $\mathcal{D}$ [19] .

$$\omega(\mathcal{G}) = \mathcal{D} - \frac{(\mathcal{D}-2)\mathcal{E}}{2} + \sum_n \mathcal{V}_n \left(\frac{n(\mathcal{D}-2)}{2} - \mathcal{D} \right) \tag{1.97}$$

As a graph introduce a new primitive divergence whenever $\omega(\mathcal{G}) \geqslant 0$, we find that infinite many kind of primitive divergences are present in the graph sum unless

$$\mathcal{D} - n(\mathcal{D}-2) \geq 0 \tag{1.98}$$

As $\mathcal{D} - n(\mathcal{D}-2)$ is also the dimension of the coupling corresponding to a vertex with n legs, it means that coupling with negative mass dimension are forced to be zero in the bare action $\mathcal{S}$ in order to make our theory renormalizable. Such negative mass dimension couplings are called perturbatively non-renormalizable. Contrarily all the positive mass dimension are clearly allowed, as they introduce a finite number of divergent diagrams, and therefore they are called super-renormalizable. A special care is needed when dealing with dimensionless coupling constants, because in such a case we deal with infinite many divergent graphs, but only a finite number of divergent graphs types are allowed, where a graph type mean a graph with a certain number of external lines. In such a case it is still possible to renormalize our theory and we call such coupling constants renormalizable. We can now analyse the same situation of a GFP in a AS framework focusing on the dimensionless beta functions 1.88

$$\check{\beta}_i = -d_i \check{g}_i + k^{-d_i} \beta_i \tag{1.99}$$

As $g_i = 0$ also mean $\beta_i = 0$ because of the internal structure of the ERGE, the characteristic exponent of the couplings turn out to coincide with their canonical dimensions. In order to get an AS theory we must set all the couplings with negative critical exponent exactly to their FP value, and in our case this means all the non-renormalizable couplings with negative mass dimension must be set to zero while all the positive mass dimension super-renormalizable couplings represent allowed interactions in our model. Some more care is needed when studying the behavior of the dimensionless couplings, in the same way as happens when using the perturbative expansion.

The fact that the renormalizability and the AS prescriptions lead to the same predictive theory when a loop expansion approach is viable thanks to the presence of a GFP, lead us to interpret the AS as a generalization of renormalizability for non AF theories. There are many situations non-renormalizable in the perturbative sense which may be included by this new definition of renormalizability, such as for example the quantization of the gravitational tensor field using the Einstein-Hilbert truncation[16] [17] [8] [9] [27] [15] [25]. In this case we find that a NGFP exist with two non null couplings g^0 and g^2, where the first coupling is proportional to the vacuum energy Λ and the second coupling is proportional to the inverse of the gravitational constant G. The critical exponent are invariant under regular coordinate transformations in the space of all couplings, but the transformation $G \sim (g^2)^{-1}$ is singular at the GFP while it is obviously regular at the NGFP. Because of this, the model result to be non-renormalizable with perturbation theory but nevertheless asymptotically safe.

We have seen as the AS prescription could be a powerful criterion to construct a fundamental and predictive theory, i.e. a theory effective at every energy scale and capable to make quantitative predictions after a process of calibration has been achieved through a finite number of experiments.

In order to get this, we are forced to introduce a fictitious fine-tuning of the coupling constants, which are forced to lie on the finite-dimensional hypersurface comprising all the points in the couplings space asymptotically approaching the FP through the UV critical surface for high k in their flow. This infinite precision ad-hoc tuning of nature can move to many philosophical interpretations. Furthermore there is no experimental way to check if our theory really lies on the safe hypersurface or if it is not the case, as an arbitrarily small distance from it, also if smaller than every observable experimental

accuracy, would lead to an asymptotically divergent and so intrinsically effective theory.

Therefore, the AS approach is a very powerful tool for studying the UV asymptotic behavior of our theories and represent an interesting direction in the attempt to get a fundamental theory describing nature, but till now it remain a theoretical hypothesis far from being proved and has some almost philosophical connotations.

Chapter 2

ERGE at work in LPA

We will now implement the formalism we developed in the previous chapter focusing on a d-dimensional real scalar field theory and working with the balanced version of the Wetterich equation. We will introduce a quite simple truncation often used in the literature called "Local Potential Approximation" and we will achieve the RG flow equations for the dimensional and dimensionless couplings adopting the optimized cutoff term, which strongly simplifies our calculations.

2.1 Local Potential Approximation

As we saw, the ERGE is an exact integro-differential equation involving the functional $\Gamma[\phi]$ and we could hope to completely solve this equation with appropriate boundary conditions, without exploiting any particular approximation. Unfortunately, one can hope to achieve this only numerically, due to the intrinsic non-linearity of the flow, and it is in practice impossible also numerically, for general $\Gamma[\phi]$. Therefore, if we are interested in analytical results we are forced to introduce a truncation in our model. The space of allowed functionals for a standard D-dimensional QFT belonging to a single real scalar field admits all the functionals satisfying the required symmetries, such as a $\phi \to -\phi$ invariance in the case of a Z_2 invariant theory. It is the case of all the local potential terms

$$\int d^d x V[\phi(x)] \tag{2.1}$$

the n order derivative terms

$$\int d^d x H[\phi(x)](\partial^2)^{n_1}\phi(x)(\partial^2)^{n_2}\phi(x) \tag{2.2}$$

and the non-local terms

$$\int d^d x \phi(x)\log(-\partial^2)\phi \qquad \int d^d x \phi(x)(\partial^2)^{-n}\phi(x) \tag{2.3}$$

and therefore all these terms represent admissible candidates to be inserted in our truncation. We will now restrict to a simple and often used approximation which consists in introducing an arbitrary local potential term together with the simplest 1-order derivative term representing the standard kinetic operator

$$\Gamma_k[\phi] = \int d^d x \left(\frac{z_\phi}{2}\partial_\mu\phi(x)\partial^\mu\phi(x) + V[\phi(x)]\right) \tag{2.4}$$

Moreover, it is sometime useful to expand the effective potential $V[\phi]$ in a power expansion

$$V[\phi] = \sum_{n=0}^{\infty} g_n \phi^n \tag{2.5}$$

where, in the case of a Z_2 invariant theory, we will only consider the $n = 2m$ with m integer terms.

As we remember from 1.8, there are some invariance properties we can exploit to simplify our model. We know that the physical meaning of our theory is invariant under appropriate field redefinitions, as for example it is evidently the case for a field rescaling $\phi'(x) = c^{-1}\phi(x)$. This can be exported to our functional introducing an adapted allowed functional transformation leaving unchanged the corresponding physical theory

$$\Gamma_k(c^{-1}\phi, c^2 z_\phi, c^n g_n) = \Gamma_k(\phi, z_\phi, g_{2n}) \tag{2.6}$$

We can use this invariance property to fix one and for all the wave function renormalization parameter $z_\phi = 1$ by introducing the renormalized field, representing the actual field whose correlations we measure

$$\phi_R = \sqrt{z_\phi}\phi \tag{2.7}$$

The other invariance we deal with belongs to the dimensional analysis and, as we saw, the most well-advised choice consists in setting the scale parameter k as the

fundamental unit. In such a way, we can introduce the dimensionless renormalized field and potential

$$\check{\phi} = \quad k^{-\left(\frac{d-2}{2}\right)}\sqrt{z_\phi}\phi \tag{2.8}$$

$$\check{v}[\check{\phi}] = \quad \sum_{n=0}^{\infty} \check{g}_n \check{\phi}^n = k^{-d} V[k^{-\left(\frac{d-2}{2}\right)}\sqrt{z_\phi}\phi] \tag{2.9}$$

which will flow as follow

$$\partial_t \check{\phi} \quad = -\left(\frac{d-2}{2} + \frac{\eta_\phi}{2}\right)\check{\phi} \tag{2.10}$$

$$\partial_t \check{v}[\check{\phi}] \quad = -d\check{v}[\check{\phi}] + \frac{(d-2+\eta_\phi)}{2}\check{\phi}\frac{\partial \check{v}}{\partial \check{\phi}}[\check{\phi}] + k^{-d}\partial_t V[\phi] \tag{2.11}$$

$$\check{\beta}_n \quad = -\left(d - \frac{n}{2}(d-2+\eta_\phi)\right)\check{g}_n + k^{-\left(d-\frac{n}{2}(d-2)\right)} z_\phi^{-\frac{n}{2}} \beta_n \tag{2.12}$$

where η_ϕ is defined by $\eta_\phi = -\dfrac{\dot{z_\phi}}{z_\phi}$ and is called anomalous dimension because it affords a modification to the canonical dimension $\frac{d-2}{2}$ in the scaling properties of the field ϕ and the reason of its existence is that the t-derivatives are performed at fixed dimensional ϕ.

The terms introduced in the flow of $\check{\phi}$ and $\check{v}[\check{\phi}]$ by the rescaling can be interpreted as a consequence of performing, in every iteration of the RG process, an infinitesimal field rescaling transformation 2.6 with $c = 1 - \dfrac{1}{2}\eta_\phi \partial t$ and a dimensional rescaling transformation 1.85 with $b = 1 - \partial t$. In the following we will show how to obtain $\partial_t V[\phi]$ and η_ϕ using the ERGE, in order to achieve all the necessary elements for the evaluation of the flow of the dimensionless renormalized couplings we are interested in.

2.2 Constant field approximation and effective potential

The ERGE (1.67) equates two functionals of ϕ and must be satisfied for every field configuration. Therefore, we can consider the simple situation of constant field $\phi(x) = \phi$ and, under the assumption 2.4, the flow equation reduces to

$$\begin{aligned} \partial_t V[\phi] \int d^d x \quad = \quad & \frac{1}{2}\mathrm{Tr}\left[\left(-z_\phi\,\partial^2 + V^{(2)}[\phi] + \mathbb{R}_k(-\partial^2)\right)^{-1}\partial_t \mathbb{R}_k(-\partial^2)\right] \\ & -\frac{1}{2}\mathrm{Tr}\left[\partial_t \mathbb{R}_k\left(-z_\phi\,\partial^2 + \mathbb{R}_k\right)^{-1}\right] \end{aligned} \tag{2.13}$$

where, in this case, we can obtain the trace performing a Fourier Transform

$$\mathrm{Tr}\left[f(-\partial^2)\right] = \int \frac{d^dq}{(2\pi)^d} f(q^2) \int d^dx = \frac{Vol(S^{d-1})}{(2\pi)^d} \int dq q^{d-1} f(q^2) \int d^dx \tag{2.14}$$

If we want to proceed in the calculation we are forced to choose a particular cutoff term to work with, and in order to get simple analytical results we will now use the optimized cutoff 1.41. Substituting, we get

$$\frac{1}{z_\phi\, q^2 + V^{(2)}[\phi] + \mathbb{R}_k(q^2)} = \frac{\theta(q^2-k^2)}{z_\phi q^2 + V^{(2)}[\phi]} + \frac{\theta(k^2-q^2)}{z_\phi k^2 + V^{(2)}[\phi]} \tag{2.15}$$

and

$$\partial_t \mathbb{R}_k(q^2) = z_\phi(2k^2 - \eta_\phi(k^2-q^2)\theta(k^2-q^2) \tag{2.16}$$

finally, substituting and integrating, we get

$$\begin{aligned}
\partial_t V[\phi] &= \frac{Vol(S^{d-1})}{2(2\pi)^d}\left(\frac{1}{z_\phi k^2 + V^{(2)}[\phi]} - \frac{1}{z_\phi k^2}\right)\int_0^k dq q^{d-1} z_\phi \left((2-\eta_\phi)\, k^2 + \eta_\phi q^2\right) \\
&= \frac{k^d Vol(S^{d-1})}{d(2\pi)^d}\left(1 - \frac{\eta_\phi}{d+2}\right)\left(\frac{1}{1+\frac{V^{(2)}[\phi]}{z_\phi k^2}} - 1\right) \\
&= \frac{k^d 2^{1-d}\left(1-\frac{\eta_\phi}{d+2}\right)}{d\Gamma\left[\frac{d}{2}\right]\pi^{d/2}}\left(\frac{1}{1+\frac{V^{(2)}[\phi]}{z_\phi k^2}} - 1\right)
\end{aligned} \tag{2.17}$$

and we can now write the flow equation for the dimensionless renormalized potential

$$\partial_t \check{v}[\check{\phi}] = -d\check{v}[\check{\phi}] + \frac{(d-2+\eta_\phi)}{2}\check{\phi}\frac{\partial \check{v}}{\partial \check{\phi}}[\check{\phi}] + \frac{2^{1-d}\left(1-\frac{\eta_\phi}{d+2}\right)}{d\,\Gamma\left[\frac{d}{2}\right]\pi^{d/2}}\left(\frac{1}{1+\check{v}^{(2)}[\check{\phi}]} - 1\right) \tag{2.18}$$

This is a partial differential equation for the dimensionless potential $\check{v}[\check{\phi}]$. A possible way to analyse the flow of the dimensional potential is to assume reliable a power series representation for $V[\phi]$. Expanding in series the rhs denominator of equation 2.17 and equating the corresponding field operators assuming the power expansion 2.5, we can write the explicit flow equations for the dimensional couplings

$$\beta_o = \frac{k^d 2^{1-d}\left(1-\frac{\eta_\phi}{d+2}\right)}{d\,\Gamma\left[\frac{d}{2}\right]\pi^{d/2}}\left(\frac{1}{1+\frac{2g_2}{z_\phi k^2}} - 1\right) \tag{2.19}$$

$$\beta_{n^*>0} = \frac{k^d 2^{1-d}\left(1-\frac{\eta_\phi}{d+2}\right)}{d\,\Gamma\left[\frac{d}{2}\right]\pi^{d/2}\left(1+\frac{2g_2}{z_\phi k^2}\right)} \sum_{n_1+..+n_m=n^*}^{n_i>0}\left[\frac{(-1)^m B_{[\bar{n}]}}{\left(z_\phi k^2 + 2g_2\right)^m}\prod_{i=1}^{m} g_{n_i+2}(n_i+1)(n_i+2)\right]$$

where

$$B_{[\bar{n}]} = \frac{m!}{h_1!..h_r!} \tag{2.20}$$

with $n_1..n_m$ divided in r groups everyone containing h_j identical valued n_i

$$\sum_{j=1}^{r} h_j = m \qquad n_{i_1^j} = n_{i_2^j} = ... = n_{i_{h_j}^j} \tag{2.21}$$

and the derivation of the flow for the dimensionless couplings is straightforward. The last ingredient we need in order to achieve a complete differential system is the anomalous dimension η_ϕ. It is possible to show that, if we work with a Z_2 invariant theory and we study the ground state $\phi = 0$ using the simple truncation in 2.4, the integration over the field fluctuations generates no contribution to the field strength z_ϕ and the anomalous dimension η_ϕ is identically zero. This is similar to what happens in perturbation theory when we analyse the field anomalous dimension of a Z-2 invariant system at one loop. Generally this is not true but, as we will see next, setting $\eta_\phi = 0$ is however a good approximation in many situations. Under this hypothesis, we dispose of a complete differential system describing the flow of infinite many couplings and we can try to solve it. The t-derivatives of an arbitrary coupling g_n depends on all the couplings up to the order $n + 2$, therefore the only chance to get a solution for some couplings is that of fixing a maximal allowed order n_{max} in our truncation, setting all the remaining couplings to zero, and try to solve the finite differential system for the remaining couplings. As a further approximation, we could decide to solve our system setting all the couplings on the rhs of our equation fixed to their original value. We can repeat this procedure n-times, always using on the rhs the couplings achieved solving the previous iteration. If we use the vacuum configuration field $\phi = 0$ as reference and we deal with couplings close to their GFP value, this procedure allows us to achieve n-loop results, but It is important to stress that, as we are working with a differential system for the couplings achieved using a truncation for the EAA, all the $n > 1$ loop results will only be an approximation of the ones obtained in perturbation theory.

2.3 Anomalous dimension

We will now show how it is possible to exploit the ERGE to achieve a closed formula for the anomalous dimensions in the LPA truncation. Firstly we can use the definition

$$(2\pi)^d \delta^d \left(p_1 + .. + p_n\right) \Gamma_k^{(n)}(p_1, .., p_n) = \int d^d x_1 ... \int d^d x_n e^{i \sum_j p_j x_j} \frac{\delta^n \Gamma_k}{\delta\phi(x_1)...\delta\phi(x_n)} \tag{2.22}$$

to get the 2-point vertex according to the truncation 2.4

$$\Gamma_{k,p}^{(2)} = z_\phi p^2 + V''[\phi] \tag{2.23}$$

Such a 2-point vertex approximation is accurate in a small p regime. Luckily, the presence of the regulator in the ERGE trace causes only low momentum fluctuations to be relevant in the integration, making such a truncation adapted for a good evaluation of the flow. We can now exploit the same relation to get a formula for the flow of $\Gamma_{k,p}^{(2)}$

$$(2\pi)^d \, \delta(p_1 + p_2) \, \dot{\Gamma}_{k,p_1}^{(2)} = \frac{\delta^2 \dot{\Gamma}_k}{\delta\phi(p_1)\delta\phi(p_2)} \tag{2.24}$$

and, substituting 1.51, we can use the relations

$$\frac{\delta}{\delta\phi_p} G_{k;q} = -G_{k;q} \Gamma_{k;p,q,-p-q}^{(3)} G_{k;q+p} \tag{2.25}$$

and

$$\begin{aligned} \frac{\delta}{\delta\phi_{-p}} \left(-G_{k;q} \Gamma_{k;p,q,-p-q}^{(3)} G_{k;q+p} \right) \quad = \quad & 2 G_{k;q} \Gamma_{k;p,q,-p-q}^{(3)} G_{k;q+p} \Gamma_{k;p+q,-p,-q}^{(3)} G_{k;q} \\ & - G_{k;q} \Gamma_{k;p,q,-p,-q}^{(4)} G_{k;q} \end{aligned} \tag{2.26}$$

where

$$G_{k;q} = \left(\Gamma_{k;q}^{(2)} + \mathbb{R}_{k;q} \right)^{-1} \tag{2.27}$$

to get a closed formula for the flow of the 2-point vertex

$$\begin{aligned} \dot{\Gamma}_{k,p}^{(2)} = \quad & \int \frac{d^d q}{(2\pi)^d} G_{k;q} \Gamma_{k;p,q,-p-q}^{(3)} G_{k;q+p} \Gamma_{k;p+q,-p,-q}^{(3)} G_{k;q} \dot{\mathbb{R}}_{k;q} \\ & - \frac{1}{2} \int \frac{d^d q}{(2\pi)^d} G_{k;q} \Gamma_{k;p,q,-p,-q}^{(4)} G_{k;q} \dot{\mathbb{R}}_{k;q} \end{aligned} \tag{2.28}$$

where the two contributions on the rhs correspond to the vertices showed in figure 2.1. We note that this equation is valid for every QFT and for every truncation we adopted.

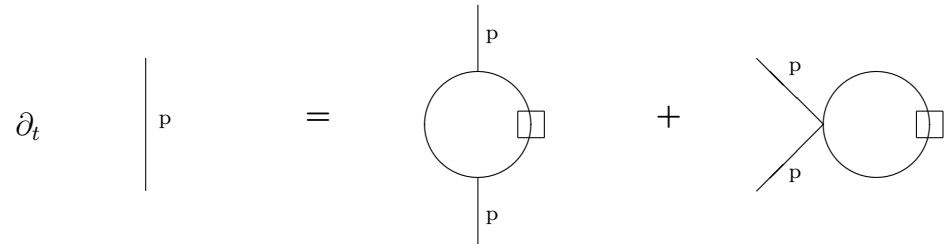

Figure 2.1: Diagrammatic representation of the graphs contributing to the flow of the 2-point vertex.

In our situation of a scalar field in LPA approximation, we find the n-point vertex with $n > 2$ to be independent of the momentum incoming p_i

$$\Gamma^{(n)}_{k;Pq_1\ldots q_n} = V^{(n)}[\phi] \tag{2.29}$$

and, therefore, our equation strongly simplifies.

$$\dot{\Gamma}^{(2)}_{k,p} = \left(V^{(3)}[\phi]\right)^2 \int \frac{d^dq}{(2\pi)^d} G^2_{k;q} G_{k;q+p} \dot{\mathbb{R}}_{k;q} - \frac{V^{(4)}[\phi]}{2} \int \frac{d^dq}{(2\pi)^d} G^2_{k;q} \dot{\mathbb{R}}_{k;q} \tag{2.30}$$

It is easy to show that the only momentum dependent contribution to the 2-point function flow comes from the first term of the rhs of equation 2.30, and we can write

$$\partial_t V^{(2)}[\phi] = \left(V^{(3)}[\phi]\right)^2 \int \frac{d^dq}{(2\pi)^d} G^3_{k;q} \dot{\mathbb{R}}_{k;q} - \frac{V^{(4)}[\phi]}{2} \int \frac{d^dq}{(2\pi)^d} G_{k;q} G_{k;q} \dot{\mathbb{R}}_{k;q} \tag{2.31}$$

$$\partial_t z_\phi = \left(V^{(3)}[\phi]\right)^2 \int \frac{d^dq}{(2\pi)^d} \left.\frac{\partial G_{k;q+p}}{\partial p^2}\right|_{p=0} G^2_{k;q} \dot{\mathbb{R}}_{k;q} \tag{2.32}$$

The choice of using the p^2 derivatives of $\dot{\Gamma}^{(2)}_{k,p}$ calculated in $p = 0$ to fix the field strength variation will reveal to be a good choice, as we are interested in the small-p behavior of $\Gamma^{(2)}_{k,p}$ and our truncation $\Gamma^{(2)}_{k,p} = z_\phi p^2 + V''[\phi]$ is accurate only in this regime. It is also possible to construct an equation for the flow of the entire self energy $\Sigma(p^2)$

$$\partial_t \Sigma(p^2) = \left(V^{(3)}[\phi]\right)^2 \int \frac{d^dq}{(2\pi)^d} G^2_{k;q} (G_{k;q+p} - G_{k;q}) \dot{\mathbb{R}}_{k;q} \tag{2.33}$$

but this goes beyond our truncation and it is not a consistent result because it has been obtained under the truncation hypothesis. Moreover, with this approach it is possible to find the flow of $\Gamma^{(n)}_{k;p_1,..,p_n}$ conserving the entire derivative dependence also when it

is evaluated at constant ϕ and in a general truncation and cutoff scheme. This can be achieved for every n and, therefore, we can expand the ERGE in function of the n-point vertices.

$$\dot{\Gamma}^{(n)}_{k;p_1,..,p_n} = B_n\left[\Gamma^{(2)}_k,..,\Gamma^{(n+2)}_k;p_1,..,p_n)\right] \tag{2.34}$$

But, again, such a system can be solved only numerically. It is finally interesting to use equation 2.31 to test the validity of our previous results.

2.4 Anomalous dimension with optimized cutoff

If we consider an optimized cutoff, we can still use the relations 2.15 and 2.16 and we can try to make explicit the field strength variation by evaluating

$$\begin{aligned}
\frac{\delta}{\delta p^2}G_{k;p+q}\Big|_{p=0} &\cong \frac{1}{2d}\,\frac{\delta^2}{\delta p^\mu \delta p_\mu}G_{k;p+q}\Big|_{p=0} \\
&= \frac{1}{2d}\frac{\delta^2}{\delta q^\mu \delta q_\mu}G_{k;q} \\
&= -\frac{1}{2d}\frac{\delta}{\delta q^\mu}\frac{2z_\phi q^\mu}{(z_\phi q^2+V^{(2)}[\phi])^2}\theta(q^2-k^2) \\
&= -\frac{1}{2d}\frac{4z_\phi q^2}{(z_\phi q^2+V^{(2)}[\phi])^2}\delta(q^2-k^2)+\theta(q^2-k^2)F_{q,z_\phi,k^2,V^{(2)}} \\
&= -\frac{2}{d}\frac{z_\phi k^2}{(z_\phi k^2+V^{(2)}[\phi])^2}\delta(q^2-k^2)
\end{aligned} \tag{2.35}$$

as the term proportional to $\theta(q^2-k^2)$ will not contribute to the integration thanks to the presence of a complementary theta coming from the regulator's t-derivative. Moreover, we find that in the presence of the $\delta(p^2-k^2)$ term forcing q to acquire k value, the regulator derivatives term reduces to

$$\partial_t \mathbb{R}_k(q^2) = z_\phi(2k^2)\theta(k^2-q^2) \tag{2.36}$$

Finally we note that actually in the integration there is only one $\theta(k^2-q^2)$ term coming from the correlation functions, as in the ϕ expansion no more theta term is generated

$$\begin{aligned}
\frac{\delta}{\delta\phi}\frac{1}{z_\phi k^2+V^{(2)}[\phi]}\theta(k^2-q^2) &= \frac{V^{(3)}[\phi]}{(z_\phi k^2+V^{(2)[\phi]})^2}\theta(k^2-q^2) \\
&\ldots
\end{aligned} \tag{2.37}$$

Therefore, we can now calculate the flow of the field strength

$$\begin{aligned}
\partial_t z_\phi &= -\frac{4V^{(3)}[\phi]^2}{d}\int \frac{d^dq}{(2\pi)^d}\frac{z_\phi^2 k^4}{(z_\phi k^2+V^{(2)}[\phi])^4}\theta(k^2-q^2)\delta(k^2-q^2) \\
&= -\frac{4Vol(S^{d-1})}{d\,(2\pi)^d}\frac{V^{(3)}[\phi]^2 z_\phi^2 k^4}{(z_\phi k^2+V^{(2)}[\phi])^4}\int dq q^{d-1}\theta(k^2-q^2)\delta(k^2-q^2) \\
&= -\frac{4Vol(S^{d-1})}{d\,(2\pi)^d}\frac{V^{(3)}[\phi]^2 z_\phi^2 k^{2+d}}{(z_\phi k^2+V^{(2)}[\phi])^4}\int \frac{dz}{2}\theta(k^2-z)\delta(k^2-z) \\
&= -\frac{Vol(S^{d-1})}{d\,(2\pi)^d}\frac{V^{(3)}[\phi]^2 z_\phi^2 k^{2+d}}{(z_\phi k^2+V^{(2)}[\phi])^4} \\
&= -\frac{2^{1-d}V^{(3)}[\phi]^2}{d\,\Gamma[\frac{d}{2}]\pi^{\frac{d}{2}}}\frac{z_\phi^2 k^{2+d}}{(z_\phi k^2+V^{(2)}[\phi])^4}
\end{aligned} \tag{2.38}$$

and therefore, recalling relations 2.8 and 2.9, we can achieve the following transformation rules

$$\begin{aligned}
\check{v}^{(2)}[\check{\phi}] &= k^{-2}z_\phi^{-1}V^{(2)}[k^{-\left(\frac{d-2}{2}\right)}z_\phi^{\frac{1}{2}}\phi] \\
\check{v}^{(3)}[\check{\phi}] &= k^{\frac{d}{2}-3}z_\phi^{-\frac{3}{2}}V^{(3)}[k^{-\left(\frac{d-2}{2}\right)}z_\phi^{\frac{1}{2}}\phi]
\end{aligned} \tag{2.39}$$

and, substituting, we can write a relation for the anomalous dimension expressed as a function of the dimensionless renormalized couplings

$$\eta_\phi = \frac{2^{1-d}}{d\,\Gamma[\frac{d}{2}]\pi^{\frac{d}{2}}}\frac{\check{v}^{(3)}[\check{\phi}]^2}{(1+\check{v}^{(2)}[\check{\phi}])^4} \tag{2.40}$$

2.5 Z-rule and VEV

Since now we omitted a conceptual problem which arises in our calculations because of the approximation employed. In all our equations describing the flow of z_ϕ we find an implicit dependence on the field configuration ϕ through the effective potential terms $\check{v}^{(2)}[\check{\phi}]$and $\check{v}^{(3)}[\check{\phi}]$, while in our truncation the field strength is independent from any field configuration. Therefore, we are forced to introduce a preferential field value $\hat{\phi}_k$ under which the field strength flow has to be evaluated. These new scheme dependence is called "Z-rule" and is a natural consequence of our LPA truncation, as in a general effective action all the generated terms would be allowed and there would be no need for preferential field configuration in order to get a complete theory. The choice of $\hat{\phi}_k$ is

completely arbitrary, but the most natural thing we can do is to give a physical meaning to the preferred field configuration, such as for example the vacuum expectation value VEV, i.e. the minimum of the potential, as our reference field configuration for the evaluation of the anomalous dimension. This coincides with the choice of $\hat{\phi}_k = 0$ in the case of a symmetric potential without symmetry-breaking, otherwise we will be driven to introduce a non-trivial choice, as we will see further. We will now show how it is possible to implement the Z-rule in our flow, by focusing on the effective average action and the effective potential in the neighbourhood of the reference field configuration $\hat{\phi}_k$. As a first step we can introduce the shifted effective average action

$$\hat{\Gamma}_k[\phi] = \Gamma_k[\phi + \hat{\phi}_k] \tag{2.41}$$

and the shifted effective potential

$$\begin{aligned} \hat{V}_k[\phi] &= V_k[\phi + \hat{\phi}_k] && (2.42)\\ &= \sum_{n=0}^{\infty} \hat{g}_{k,n}\phi^n && (2.43) \end{aligned}$$

where

$$\hat{g}_{k,m} = g_{k,m} + \sum_{n=1}^{\infty} \binom{n+m}{n} g_{k,n+m}\hat{\phi}_k^n \tag{2.44}$$

We can now study the flow of the effective potential

$$\begin{aligned} \partial_t \hat{V}_k[\phi] &= \dot{V}_k[\phi + \hat{\phi}_k] + V_k'[\phi + \hat{\phi}_k]\partial_t\hat{\phi}_k && (2.45)\\ &= \sum_{n=0}^{\infty} \left(\beta_n(k, \hat{g}_1, ..\hat{g}_n, ...) + (n+1)\ \hat{g}_{k,n+1}\partial_t\hat{\phi}_k\right)\phi^n && (2.46)\\ &= \sum_{n=0}^{\infty} \hat{\beta}_n(k, \hat{g}_1, ..\hat{g}_n, ...)\phi^n && (2.47) \end{aligned}$$

Therefore, it is sufficient to add a shifting term $(n+1)\ \hat{g}_{n+1}\partial_t\hat{\phi}_k$ to our original beta functions β_n in order to get a flow for our effective potential expanded around the reference field $\hat{\phi}_k$. Under the hypothesis of the reference field to be the stationary point of the effective potential at the original momentum scale k^o

$$\hat{g}_{k^o,1} = 0 \tag{2.48}$$

it is sufficient to impose

$$\begin{aligned}\hat{\beta}_1(k, \hat{g}_1, ..\hat{g}_n, ...) &= 0 \\ \partial_t \hat{\phi}_k &= -\frac{\hat{\beta}_1(k, \hat{g}_1, ..\hat{g}_n, ...)}{2\hat{g}_{k,2}}\end{aligned} \tag{2.49}$$

in order fix the reference field to the stationary point value for every k. As we expect, this make sense only under the condition of $\hat{g}_{k,2} > 0$, that is a positive mass effective theory, and in such a situation, assuming our local minimum to be also a global minimum, the stationary point of the effective potential will coincide with the VEV. Finally, we find

$$\hat{\beta}_n(k, \hat{g}_1, ..\hat{g}_n, ...) = \beta_n(k, \hat{g}_1, ..\hat{g}_n, ...) - (n+1)\, \hat{g}_{k,n+1} \frac{\beta_1(k, \hat{g}_1, ..\hat{g}_n, ...)}{2\hat{g}_{k,2}} \tag{2.50}$$

and the generalization to the dimensionless renormalized beta functions and couplings is straightforward. Finally, as a consequence of this approach, the Z-rule comes natural simply imposing $\phi = 0$ in the evaluation of the anomalous dimension.

2.6 Euclidean anharmonic oscillator and vacuum energy

We will now explore the meaning of these results in the simple framework of a 0+1 dimensional real scalar field theory, corresponding to the QFT transposition of the quantum mechanical anharmonic oscillator. In the power expansion of the effective potential we will restrict to all the symmetric terms up to the 4-order, namely considering only the couplings $g_0 = \mathcal{E}$, $g_2 = \frac{m}{2}$ and $g_4 = \frac{\lambda}{4!}$ and we will work with dimensional couplings, as this fairly simplify our calculations and it is sufficient for the considerations we are interested in. As we restricted to a symmetric potential, from 2.40 we can realize that actually there is no flow for the field strength $z_\phi = 1$ because of the simple truncation choice and, from 2.19 we can get the equations

$$\beta_{k,\mathcal{E}} = \frac{k^3}{\pi(k^2 + m_k)} - \frac{k}{\pi} \tag{2.51}$$

$$\beta_{k,m} = -\frac{k^3}{\pi(k^2 + m_k)^2}\lambda_k \tag{2.52}$$

$$\beta_{k,\lambda} = \frac{6k^3}{\pi(k^2 + m_k)^3}\lambda_k^2 \tag{2.53}$$

We can now get an approximated evaluation for the mass term simply by integrating 2.52 neglecting the flow of $m_k = m$ and $\lambda_k = \lambda$ on the rhs: in such a way, we achieve the same 1-loop approximation for the mass flow we would get with perturbative expansion

$$m_k^{1-\text{loop}} = m + \frac{1}{4}\lambda\sqrt{\frac{1}{m}} + \frac{\lambda}{2\pi}\left(\frac{k}{k^2+m} - \frac{\tan^{-1}\left(\frac{k}{\sqrt{m}}\right)}{\sqrt{m}}\right) \tag{2.54}$$

With an analogous procedure we can obtain a λ expansion for the vacuum energy ϵ_0 simply solving eq 2.52 under the assumption of constant λ and inserting the result in the rhs of eq 2.51

$$\epsilon_o = \frac{1}{2}\sqrt{m} + \frac{3}{4}\sqrt{m}\left(\frac{\lambda}{24m^{\frac{3}{2}}}\right) - \frac{87+24\pi^2}{16\pi^2}\sqrt{m}\left(\frac{\lambda}{24m^{\frac{3}{2}}}\right)^2 + ... \tag{2.55}$$

Comparing our 2-order result with the one achieved in a standard perturbation theory framework,

$$\epsilon_o^{pt} = \frac{1}{2}\sqrt{m} + \frac{3}{4}\sqrt{m}\left(\frac{\lambda}{24m^{\frac{3}{2}}}\right) - \frac{105}{40}\sqrt{m}\left(\frac{\lambda}{24m^{\frac{3}{2}}}\right)^2 + ... \tag{2.56}$$

we find an exact agreement for the harmonic oscillator vacuum energy ($\lambda = 0$) and the first perturbative expansion term in λ, while for higher terms the correspondence is only approximated, as a consequence of the truncation we introduced. For example, the second expansion term in λ achieved using the differential system belonging to the LPA is approximatively $2.051\ 24^{-2}\, m^{-\frac{5}{2}}\, \lambda^2$, about a 20 percent inferior than the result achieved in perturbation theory, that is $2.625\ 24^{-2}\, m^{-\frac{5}{2}}\, \lambda^2$.

Moreover, it is interesting to note that the $-\frac{k}{\pi}$ term in equation 2.51 coming from the Balanced Coarse-Graining prescription is fundamental in order to achieve a finite result for the vacuum energy. Therefore, this is a comforting result both about the LPA approximation and the Balanced Coarse-Graining approach, and comforting results also comes from the strong-coupling regime analysis [10], where the ERGE approach through LPA reveals to be much more accurate than the perturbative expansion in order to get good quantitative results.

2.7 Some non perturbative results for scalar theories

We will now give a brief summary of the main asymptotic results about d-dimensional real scalar field theories under the LPA truncation, focusing on symmetric models

evaluated adopting $\phi = 0$ as reference field.

In d=2 space-time dimension, a numerical investigation has shown that it is possible to find a series of fixed points called "multicritical fixed points" CFP. Their existence was first discovered by Morris using a truncation that goes beyond the LPA introducing a field-dependent field strength z_ϕ. These fixed points correspond to some minimal models of CFT and their anomalous dimensions are known exactly. Therefore, we are able to compare our results with the exact ones and check the accuracy of our truncation. We find that LPA provides good qualitative results, but an increased truncation would lead to more accurate predictions and it is necessary in order to achieve many features of the theory.

In d=3, it has been shown that a non-Gaussian fixed point still exist, called Wilson-Fisher FP which, however, should be physically interpreted as an IR FP. It is nevertheless possible to compare the ERGE results about the W-F FP with the ones achieved using numerical tools, finding a good accuracy of the LPA truncation outcomes in many situations.

In d=4 the only FP is the Gaussian one, as we can see from 2.12. As the GFP reveals to be repulsive in all the directions, we find the UV critical surface to coincide with the FP itself, providing every fundamental theory to be trivial, non-interacting and scale independent.

Chapter 3

Non-Local Truncation

The Local Potential Approximation allows us to achieve accurate results in many situations, as that the presence of the cutoff derivative term $\dot{\mathbb{R}}_{k,q}$ in the ERGE restricts the field fluctuations contributing to the functional integration to the only ones with low momentum q, and therefore approximating the n-point vertices to their zero-momentum value introduces a small error in the flow of the couplings. But if we want to go beyond the LPA we are forced to consider a non-trivial momentum dependence for our n-point effective average vertices and above all for the 2-point one. Moreover, there are some physical situations in which the non-local behavior of the effective average action become fundamental in order to achieve meaningful results. This appears fundamental when analysing QCD at low energies in the regime close to the confinement. Erge with non-local truncations has been able to give, for example, for the gluon propagator results equivalent to the best available from Montecarlo analysis on lattice. Moreover, one needs to consider such less trivial truncations in order to compute the vacuum energy for theories exactly massless. There are many ways to realize this, the simplest one is the so called derivative expansion, consisting in the expansion of the 2-point vertex $\Gamma_p^{(2)}$ in powers of the momentum p. In this chapter, as our original work, we are going to introduce an alternative way to achieve this result introducing a non-local truncation and comparing the achieved results with the ones obtained using other asserted techniques.

3.1 1-loop 2-point vertex

In order to understand the structure of non localities in the effective action it is useful to derive the n-loop perturbative EAA starting from the ERGE. We will focus on the 2-loop expansion in a simple 1-dimensional real scalar QFT using the optimized cutoff, in order to investigate the 1-loop non-local structure of the 2-point vertex and it's influence on the flow of the vacuum energy. As we saw in section 1.5, perturbative loop expansion can be derived from ERGE expanding the average effective action in $\hbar$

$$\Gamma_k[\bar{\phi}] = \Gamma_k^{0-l}[\bar{\phi}] + \hbar\Gamma_k^{1-l}[\bar{\phi}] + \hbar^2\Gamma_k^{2-l}[\bar{\phi}] + \dots \tag{3.1}$$

In such a way, we can write the flow equation for the n-loop average effective action

$$\begin{aligned}
\partial_t\Gamma_k^{1-l}[\bar{\phi}] &= \frac{1}{2}\int_q G_{k;q}^{(2)0-l}\ \dot{\mathbb{R}}_{k;q} \\
\partial_t\Gamma_k^{2-l}[\bar{\phi}] &= -\frac{1}{2}\int_q \left(G_{k;q}^{(2)0-l}\right)^2\Gamma_{k;q}^{(2)1-l}\ \dot{\mathbb{R}}_{k;q} \\
\partial_t\Gamma_k^{3-l}[\bar{\phi}] &= \frac{1}{2}\int_q \left(G_{k;q}^{(2)0-l}\right)^3\left(\Gamma_{k;q}^{(2)1-l}\right)^2\ \dot{\mathbb{R}}_{k;q} - \frac{1}{2}\int_q \left(G_{k;q}^{(2)0-l}\right)^2\Gamma_{k;q}^{(2)2-l}\ \dot{\mathbb{R}}_{k;q} \\
\dots &\quad \dots
\end{aligned} \tag{3.2}$$

with

$$\begin{aligned}
\Gamma_{k;p}^{(2)1-l} &= \frac{1}{2}\int\limits_{s>k}\frac{ds}{s}\int_q \left(G_{s;q}^{(2)0-l}\right)^2\Gamma_{s;q,q,p,p}^{(4)0-l}\ \dot{\mathbb{R}}_{s;q} - \int\limits_{s>k}\frac{ds}{s}\int_q \left(G_{s;q}^{(2)0-l}\right)^2 G_{s;q+p}^{(2)0-l}\left(\Gamma_{s;q,q,p}^{(3)0-l}\right)^2\dot{\mathbb{R}}_{s;q} \\
\dots &\quad \dots
\end{aligned} \tag{3.3}$$

with a little work, it is possible to compute analytically the first terms in this expansion in the simple framework of a d-dimensional scalar field theory using the optimized cut-off. These calculations are given in appendix A, where the 1-loop momentum-dependent structure of the 2-point vertex is investigated together with the 2-loop vacuum energy term. In the appendix we find a quite complex analytical expression for $\Gamma_{k;p}^{(2)1-l}$, but the momentum shape of this 2-point function seems to be well-described by a regular monotonous-increasing limited function at every scale k. Moreover, the momentum shape of $\Gamma_{k;p}^{(2)1-l}$ for different scale k can be well-fitted by a rescaling and shifting of the same momentum-dependent function. Therefore, we can introduce a parameter-dependent function able to fit the momentum shape of the 1-loop 2-point vertex for an

opportune choice of the parameters and hope such a function to accurately fit also the exact 2-point vertex for appropriate values of the parameters, probably different from the former one. Such an assumption is evidently strong and objectionable, as there is no real reason suggesting such a behavior, but achieving the perturbative analytical n-loop 2-point vertex for $n > 2$ is quite an hard task and in any case we would like to go beyond perturbation theory in principle. Thus, at present the most reasonable way to test this assumption is to assume it first, and than compare the obtained results with the asserted ones. furthermore, in chapter 4 we will introduce a more rigorous test for this assumption, developing a non-perturbative tool able to investigate the momentum dependence of $\Gamma^{(2)1-l}_{k;p}$.

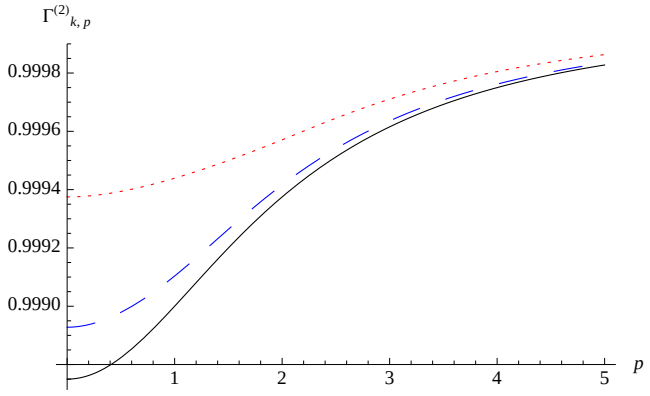

Figure 3.1: Graphical representation of the 1-loop 2-point effective average vertex structure $\Gamma^{(2)1-l}_{k;p}$ at different energy scales k for a 1-dimensional real scalar field theory described by the bare potential $V^{(2)} = 1$ and $V^{(3)} = 0.1$. Solid-black line: effective result at the energy scale k=0; dashed-blue line: effective average result at the energy scale k=0.5; dotted-red line: effective average result at the energy scale k=1.

3.2 Non-local 2-point vertex ansatz and 1-loop result in QM

The simplest analytical non-local ansatz for the 2-point vertex able to accurately fit the perturbative 1-loop result in d=1 is

$$\Gamma_{k;p}^{(2)1-l} \approx p^2 + m_k + \sigma_{\alpha_k,\beta_k;\,p} \tag{3.4}$$

with

$$\sigma_{\alpha,\beta;\,p} = \frac{\alpha\beta}{\alpha + \beta p^2} \tag{3.5}$$

It is interesting to stress that the m_k term in equation 3.4 is not a conventional mass term, as for zero momentum p the non-local function $\sigma_{\alpha_k,\beta_k;\,p}$ produce a non-zero contribution to the effective average potential. We can expand the behavior of our ansatz for small-momenta

$$\Gamma_{k;p}^{(2)1-l} \approx m_k + \beta_k + \left(1 - \frac{\beta_k^2}{\alpha_k}\right) p^2 + O\left(p^4\right) \tag{3.6}$$

and for high momenta

$$\Gamma_{k;p}^{(2)1-l} \approx m_k + \alpha_k \frac{1}{p^2} + O\left(\frac{1}{p^4}\right) \tag{3.7}$$

As the derivative 1-loop contribution to the 2-point vertex $\Gamma_{k;p}^{(2)p-dep}$ tend to 0 for high momenta, we can identify the m_k term in our truncation with the momentum-independent 1-loop 2-point vertex contribution A.8

$$m_k = m_o + \Gamma_{k;p}^{(2)p-ind} = m_o + \frac{V^{(4)}}{4\pi}\left(\frac{2k}{k^2 + V''} - \frac{2\tan^{-1}\left(\frac{k}{\sqrt{V''}}\right)}{\sqrt{V''}} + \pi\sqrt{\frac{1}{V''}}\right) \tag{3.8}$$

and, therefore

$$\sigma_{\alpha_k,\beta_k;\,p} \approx \Gamma_{k;p}^{(2)p-dep} \tag{3.9}$$

The most natural thing we can do in order to fit the 2-point vertex function is to use equation A.19 and set

$$\begin{aligned} \beta_k &= \Gamma_{k;0}^{(2)p-dep} \\ &= -\frac{V^2\left(\pi\left(k^2+m\right)^2 - 2k\sqrt{m}\left(k^2-m\right) - 2\left(k^2+m\right)^2\tan^{-1}\left(\frac{k}{\sqrt{m}}\right)\right)}{8\pi m^{3/2}\left(k^2+m\right)^2} \end{aligned} \tag{3.10}$$

The only remaining parameter of the ansatz to be fixed is α_k. We can try to set it's value both considering the high momentum behaviour of $\Gamma^{(2)p-dep}_{k;p}$

$$\begin{aligned}\alpha_k &= p^2 \lim_{p\to\infty} \Gamma^{(2)p-dep}_{k;p} \\ &= -\frac{V^2\left(\pi\left(k^2+m\right)-2\left(k^2+m\right)\tan^{-1}\left(\frac{k}{\sqrt{m}}\right)+2k\sqrt{m}\right)}{2\pi\sqrt{m}\left(k^2+m\right)}\end{aligned} \tag{3.11}$$

or the small momentum behaviour

$$\begin{aligned}-\frac{\beta_k^2}{\alpha_k} &= \frac{1}{p^2}\left(\lim_{p\to 0}\Gamma^{(2)p-dep}_{k;p}-\beta_k\right) \\ &= \frac{V^2\left(3\pi\left(k^2+m\right)^3-2k\sqrt{m}\left(3k^2-m\right)\left(k^2+3m\right)-6\left(k^2+m\right)^3\tan^{-1}\left(\frac{k}{\sqrt{m}}\right)\right)}{96\pi m^{5/2}\left(k^2+m\right)^3}\end{aligned} \tag{3.12}$$

We find that both the choices are possible in order to accurately fit $\Gamma^{(2)p-dep}_{k;p}$ and they bring to very similar results, as we can see in fig. 3.2. In the following, we will use the high momentum behavior of the 2 point vertex for the calibration of the parameters, as it will bring to simpler analytical results in the evaluation of the ERGE. It is interesting to investigate how our approximation modify the 1-loop 2-point Green function in the momentum range $p < k$ contributing to the functional integration of the ERGE for zero external momenta, and we find that in the 1-loop calculations the non-local ansatz introduces, for $p \simeq k$, a small improvement of the results achieved using LPA with non-trivial anomalous dimension, as we see in Fig. 3.3.

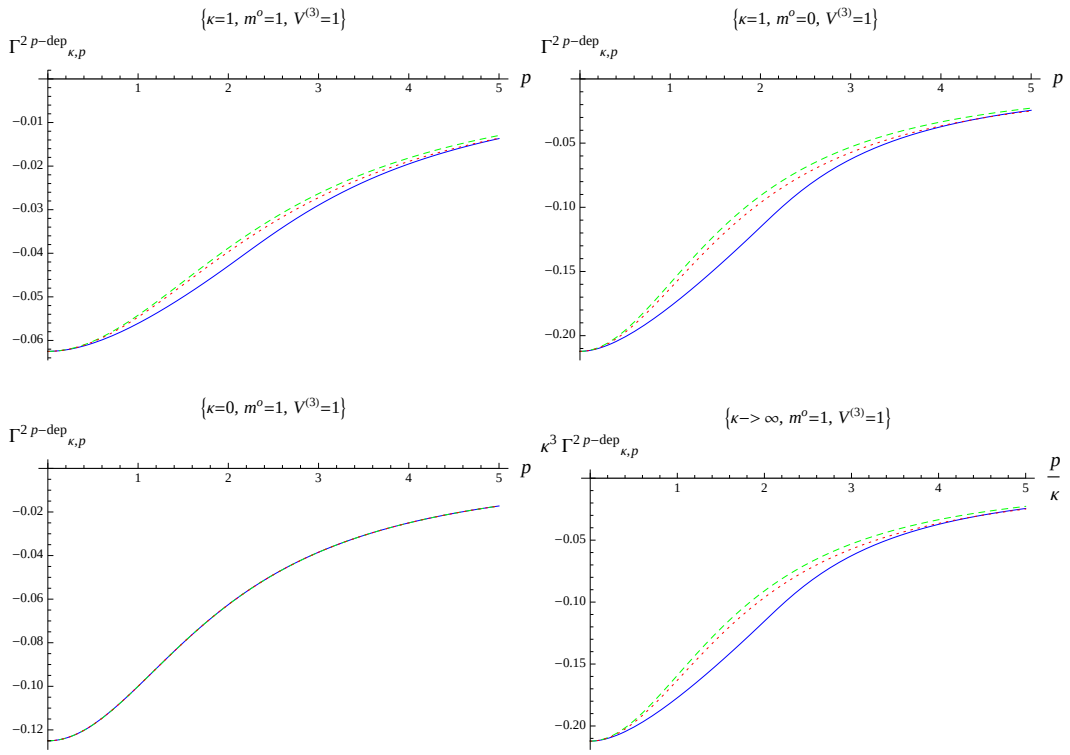

Figure 3.2: In this figure, the momentum dependent contribution to the 1-dimensional perturbative 1-loop 2-point vertex A.19 is represented (solid-blue line) together with the non-local ansatz of 3.9 calibrated in order to fit the high momenta behavior, using 3.10 and 3.11 (dashed-green line) or the low momenta behavior, using 3.10 and 3.12 (dotted-red line). The results for different bare actions and evaluated at different scales k are shown in the figures.

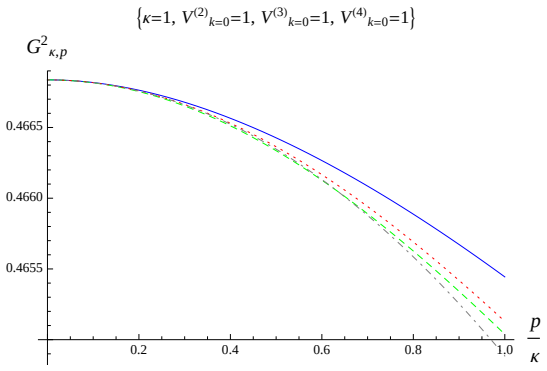

Figure 3.3: Here the results of the 1-loop 2-point Green's function achieved using different approximations are shown: 1-dimensional perturbative 1-loop 2-point Green Function (solid-blue line), result achieved by fitting the high momenta 2-point vertex behavior using 3.9, 3.10 and 3.11 (dashed-green line), result achieved by fitting the low momenta 2-point vertex behavior using 3.9, 3.10 and 3.12 (dotted-red line), Local Power Approximation with non-trivial anomalous dimension evaluated at 1-loop (dot/dashed-gray line).

3.3 Non-local 2-point vertex truncation and ERGE

We will now use the ERGE in order to evaluate the RG flow of the couplings of a truncation containing the LPA together with the non-local ansatz for the 2-point function we introduced in 3.4

$$\Gamma_k[\phi] = \int dx \left(\frac{1}{2}\partial_\mu \phi(x) \partial^\mu \phi(x) + \frac{1}{2}\phi(x) \sigma_{\alpha_k,\beta_k;\partial}\ \phi(x) + V[\phi(x)] \right) \tag{3.13}$$

with

$$\sigma_{\alpha,\beta;\,p} = \frac{\alpha\beta}{\alpha + \beta p^2} \tag{3.14}$$

We will consider a potential containing all the terms up to the 4-order in ϕ

$$V_k[\phi] \quad = \quad \sum_{n=0}^{4} g_n \phi^n \tag{3.15}$$

and we will introduce the shifted potential $\hat{V}$, as shown in section 2.5, in order to follow the reference field configuration $\hat{\phi}_k = VEV$ during our flow

$$\begin{aligned} \hat{V}_k[\phi] &= V_k[\phi + \hat{\phi}_k] \\ &= \epsilon_k + \frac{m_k}{2}\phi^2 + \frac{\rho_k}{3}\phi^3 + \frac{\lambda_k}{4}\phi^4 \end{aligned} \tag{3.16}$$

It is useful to investigate the dimension of the couplings in our truncation using natural units

$$[\epsilon_k] = \mathrm{m}^d; \quad [m_k] = [\beta_k] = \mathrm{m}^2; \quad [\alpha_k] = \mathrm{m}^4; \quad [\rho_k] = \mathrm{m}^{3-\frac{d}{2}}; \quad [\lambda_k] = \mathrm{m}^{4-d} \tag{3.17}$$

Finally we will adopt the optimized cutoff term

$$R_{k;q} = (k^2 - q^2)\theta(k^2 - q^2) \qquad \dot{R}_{k;q} = 2k^2\theta(k^2 - q^2) \tag{3.18}$$

providing the propagator

$$\begin{aligned} G_{k;q} &= \frac{1}{(q^2 + m_k) + R_{k;q}} \\ &= \frac{1}{(q^2 + m_k + \sigma_{\alpha_k,\beta_k;q})}\theta(q^2 - k^2) + \frac{1}{(k^2 + m_k + \sigma_{\alpha_k,\beta_k;q})}\theta(k^2 - q^2) \end{aligned} \tag{3.19}$$

and, using the ERGE, we can achieve the flow of the coupling in d=1

$$\begin{aligned}
\partial_t\hat{\phi}_k &= \frac{\rho_k}{2(m_k+\beta_k)}\int\frac{dq}{2\pi}(G_{k;q})^2\,\dot{\mathbb{R}}_{k;q}\\
&= \frac{k^2\rho_k}{2\pi\left(\beta_k+m_k\right)}\left(\frac{k\left(\frac{\alpha_k\beta_k^2}{(k^2+\beta_k+m_k)(k^4\beta_k+k^2(\alpha_k+\beta_k m_k)+\alpha_k(\beta_k+m_k))}+2\right)}{\left(k^2+m_k\right)^2}\right.\\
&\left.-\frac{\sqrt{\alpha_k}\sqrt{\beta_k}\left(4k^2+3\beta_k+4m_k\right)\tan^{-1}\left(\frac{k\sqrt{\beta_k}\sqrt{k^2+m_k}}{\sqrt{\alpha_k}\sqrt{k^2+\beta_k+m_k}}\right)}{\left(k^2+m_k\right)^{5/2}\left(k^2+\beta_k+m_k\right)^{3/2}}\right)
\end{aligned}\tag{3.20}$$

$$\begin{aligned}
\partial_t\epsilon_k &= \frac{1}{2}\int\frac{dq}{2\pi}G_{k;q}\dot{\mathbb{R}}_{k;q}-\frac{1}{2}\int\frac{dq}{2\pi}(q^2+\mathbb{R}_{k;q})^{-1}\dot{\mathbb{R}}_{k;q}\\
&= -\frac{k}{\pi}\left(\frac{k\sqrt{b_k}\sqrt{\alpha_k}\tan^{-1}\left(\frac{k\sqrt{b_k}\sqrt{k^2+m_k}}{\sqrt{\alpha_k}\sqrt{b_k+k^2+m_k}}\right)}{\left(k^2+m_k\right)^{3/2}\sqrt{b_k+k^2+m_k}}+\frac{m_k}{k^2+m_k}\right)
\end{aligned}\tag{3.21}$$

$$\begin{aligned}
\partial_t m_k &= -\frac{1}{2}\lambda_k\int\frac{dq}{2\pi}(G_{k;q})^2\,\dot{\mathbb{R}}_{k;q}+\rho_k\,\partial_t\hat{\phi}_k\\
&= \frac{k^2}{2\pi}\left(\frac{\rho_k^2}{\beta_k+m_k}-\lambda_k\right)\left(\frac{k\left(\frac{\alpha_k\beta_k^2}{(k^2+\beta_k+m_k)(k^4\beta_k+k^2(\alpha_k+\beta_k m_k)+\alpha_k(\beta_k+m_k))}+2\right)}{\left(k^2+m_k\right)^2}\right.\\
&\left.-\frac{\sqrt{\alpha_k}\sqrt{\beta_k}\left(4k^2+3\beta_k+4m_k\right)\tan^{-1}\left(\frac{k\sqrt{\beta_k}\sqrt{k^2+m_k}}{\sqrt{\alpha_k}\sqrt{k^2+\beta_k+m_k}}\right)}{\left(k^2+m_k\right)^{5/2}\left(k^2+\beta_k+m_k\right)^{3/2}}\right)
\end{aligned}\tag{3.22}$$

$$\begin{aligned}
\partial_t\alpha_k &= \rho_k^2\int\frac{dq}{2\pi}(G_{k;q})^2\,\dot{\mathbb{R}}_{k;q}\\
&= \frac{k^2\rho_k^2}{\pi}\left(\frac{k\left(\frac{\alpha_k\beta_k^2}{(k^2+\beta_k+m_k)(k^4\beta_k+k^2(\alpha_k+\beta_k m_k)+\alpha_k(\beta_k+m_k))}+2\right)}{\left(k^2+m_k\right)^2}\right.\\
&\left.-\frac{\sqrt{\alpha_k}\sqrt{\beta_k}\left(4k^2+3\beta_k+4m_k\right)\tan^{-1}\left(\frac{k\sqrt{\beta_k}\sqrt{k^2+m_k}}{\sqrt{\alpha_k}\sqrt{k^2+\beta_k+m_k}}\right)}{\left(k^2+m_k\right)^{5/2}\left(k^2+\beta_k+m_k\right)^{3/2}}\right)
\end{aligned}\tag{3.23}$$

$$\begin{aligned}
\partial_t\beta_k &= \rho_k^2\int\frac{dq}{2\pi}(G_{k;q})^3\,\dot{\mathbb{R}}_{k;q}\\
&= \frac{k^2\rho_k^2}{4\pi}\left(-\frac{2k\alpha_k^2\beta_k^3}{\left(k^2+m_k\right)^3\left(k^2+\beta_k+m_k\right)\left(\alpha_k\left(k^2+\beta_k+m_k\right)+k^2\beta_k\left(k^2+m_k\right)\right)^2}\right.\\
&+\frac{3k\alpha_k\beta_k^2\left(4\left(k^2+m_k\right)+3\beta_k\right)}{\left(k^2+m_k\right)^3\left(k^2+\beta_k+m_k\right)^2\left(\alpha_k\left(k^2+\beta_k+m_k\right)+k^2\beta_k\left(k^2+m_k\right)\right)}\\
&-\frac{3\sqrt{\alpha_k}\sqrt{\beta_k}\left(12\beta_k\left(k^2+m_k\right)+8\left(k^2+m_k\right)^2+5\beta_k^2\right)\tan^{-1}\left(\frac{k\sqrt{\beta_k}\sqrt{k^2+m_k}}{\sqrt{\alpha_k}\sqrt{k^2+\beta_k+m_k}}\right)}{\left(k^2+m_k\right)^{7/2}\left(k^2+\beta_k+m_k\right)^{5/2}}\\
&\left.+\frac{8k}{\left(k^2+m_k\right)^3}\right)
\end{aligned}\tag{3.24}$$

$$
\begin{aligned}
\partial_t \rho_k &= 3\lambda_k \rho_k \int \frac{dq}{2\pi} (G_{k;q})^3 \, \dot{\mathbb{R}}_{k;q} - 3\rho^3 \int \frac{dq}{2\pi} (G_{k;q})^4 \, \dot{\mathbb{R}}_{k;q} + \lambda_k \, \partial_t \hat{\phi}_k \\
&= \frac{3k^2 \lambda_k \rho_k}{4\pi} \times \left(\frac{8k}{\left(k^2+m_k\right)^3} \right. \\
&- \frac{2kb_k^3 \alpha_k^2}{\left(k^2+m_k\right)^3 \left(b_k+k^2+m_k\right) \left(b_k \left(k^4+k^2 m_k+\alpha_k\right)+\alpha_k \left(k^2+m_k\right)\right)^2} \\
&+ \frac{3kb_k^2 \alpha_k \left(3b_k+4\left(k^2+m_k\right)\right)}{\left(k^2+m_k\right)^3 \left(b_k+k^2+m_k\right)^2 \left(b_k \left(k^4+k^2 m_k+\alpha_k\right)+\alpha_k \left(k^2+m_k\right)\right)} \\
&\left. - \frac{3\sqrt{b_k}\sqrt{\alpha_k} \left(12b_k \left(k^2+m_k\right)+5b_k^2+8\left(k^2+m_k\right)^2\right) \tan^{-1}\left(\frac{k\sqrt{b_k}\sqrt{k^2+m_k}}{\sqrt{\alpha_k}\sqrt{b_k+k^2+m_k}}\right)}{\left(k^2+m_k\right)^{7/2} \left(b_k+k^2+m_k\right)^{5/2}} \right) \\
&+ \frac{k^2 \lambda_k \rho_k}{2\pi \left(b_k+m_k\right)} \times \\
&\left(\frac{k\left(\frac{b_k^2 \alpha_k}{\left(b_k+k^2+m_k\right)\left(b_k\left(k^4+k^2 m_k+\alpha_k\right)+\alpha_k\left(k^2+m_k\right)\right)}+2\right)}{\left(k^2+m_k\right)^2} \right. \\
&\left. - \frac{\sqrt{b_k}\sqrt{\alpha_k} \left(3b_k+4\left(k^2+m_k\right)\right) \tan^{-1}\left(\frac{k\sqrt{b_k}\sqrt{k^2+m_k}}{\sqrt{\alpha_k}\sqrt{b_k+k^2+m_k}}\right)}{\left(k^2+m_k\right)^{5/2} \left(b_k+k^2+m_k\right)^{3/2}} \right) \\
&- \frac{k^2 \rho_k^3}{8\pi} \times \left(\frac{48k}{\left(k^2+m_k\right)^4} \right. \\
&- \frac{3\sqrt{b_k}\sqrt{\alpha_k} \left(120b_k^2 \left(k^2+m_k\right)+144b_k \left(k^2+m_k\right)^2+35b_k^3+64\left(k^2+m_k\right)^3\right) \tan^{-1}\left(\frac{k\sqrt{b_k}\sqrt{k^2+m_k}}{\sqrt{\alpha_k}\sqrt{b_k+k^2+m_k}}\right)}{\left(k^2+m_k\right)^{9/2} \left(b_k+k^2+m_k\right)^{7/2}} \\
&+ \frac{8kb_k^4 \alpha_k^3}{\left(k^2+m_k\right)^4 \left(b_k+k^2+m_k\right) \left(b_k \left(k^4+k^2 m_k+\alpha_k\right)+\alpha_k \left(k^2+m_k\right)\right)^3} \\
&- \frac{2kb_k^3 \alpha_k^2 \left(19b_k+24\left(k^2+m_k\right)\right)}{\left(k^2+m_k\right)^4 \left(b_k+k^2+m_k\right)^2 \left(b_k \left(k^4+k^2 m_k+\alpha_k\right)+\alpha_k \left(k^2+m_k\right)\right)^2} \\
&\left. + \frac{3kb_k^2 \alpha_k \left(72b_k \left(k^2+m_k\right)+29b_k^2+48\left(k^2+m_k\right)^2\right)}{\left(k^2+m_k\right)^4 \left(b_k+k^2+m_k\right)^3 \left(b_k \left(k^4+k^2 m_k+\alpha_k\right)+\alpha_k \left(k^2+m_k\right)\right)} \right)
\end{aligned}
\tag{3.25}
$$

$$
\begin{aligned}
\partial_t \lambda_k &= 3\lambda_k^2 \int \frac{dq}{2\pi} (G_{k;q})^3 \, \dot{\mathbb{R}}_{k;q} - 18\rho_k^2 \lambda_k \int \frac{dq}{2\pi} (G_{k;q})^4 \, \dot{\mathbb{R}}_{k;q} + 12\rho_k^4 \int \frac{dq}{2\pi} (G_{k;q})^5 \, \dot{\mathbb{R}}_{k;q} \\
&= \frac{3k^2\lambda_k^2}{4\pi} \times \left(\frac{8k}{(k^2+m_k)^3} \right. \\
&- \frac{2k\alpha_k^2\beta_k^3}{(k^2+m_k)^3 (k^2+\beta_k+m_k) (\alpha_k (k^2+\beta_k+m_k) + k^2\beta_k (k^2+m_k))^2} \\
&+ \frac{3k\alpha_k\beta_k^2 \left(4k^2+3\beta_k+4m_k\right)}{(k^2+m_k)^3 (k^2+\beta_k+m_k)^2 (\alpha_k (k^2+\beta_k+m_k) + k^2\beta_k (k^2+m_k))} \\
&\left. - \frac{3\sqrt{\alpha_k}\sqrt{\beta_k} \left(12\beta_k \left(k^2+m_k\right) + 8\left(k^2+m_k\right)^2 + 5\beta_k^2\right) \tan^{-1}\left(\frac{k\sqrt{\beta_k}\sqrt{k^2+m_k}}{\sqrt{\alpha_k}\sqrt{k^2+\beta_k+m_k}} \right)}{(k^2+m_k)^{7/2} (k^2+\beta_k+m_k)^{5/2}} \right) \\
&- \frac{3k^2\lambda_k\rho_k^2}{4\pi} \times \left(\frac{48k}{(k^2+m_k)^4} \right. \\
&+ \frac{8k\alpha_k^3\beta_k^4}{(k^2+m_k)^4 (k^2+\beta_k+m_k) (\alpha_k (k^2+\beta_k+m_k) + k^2\beta_k (k^2+m_k))^3} \\
&- \frac{2k\alpha_k^2\beta_k^3 \left(24k^2+19\beta_k+24m_k\right)}{(k^2+m_k)^4 (k^2+\beta_k+m_k)^2 (\alpha_k (k^2+\beta_k+m_k) + k^2\beta_k (k^2+m_k))^2} \\
&+ \frac{3k\alpha_k\beta_k^2 \left(48k^4+72k^2\beta_k+24\left(4k^2+3\beta_k\right)m_k+29\beta_k^2+48m_k^2\right)}{(k^2+m_k)^4 (k^2+\beta_k+m_k)^3 (\alpha_k (k^2+\beta_k+m_k) + k^2\beta_k (k^2+m_k))} \\
&- \left(144\beta_k \left(k^2+m_k\right)^2 + 120\beta_k^2 \left(k^2+m_k\right) + 64\left(k^2+m_k\right)^3 + 35\beta_k^3\right) \times \\
&\left. \frac{3\sqrt{\alpha_k}\sqrt{\beta_k} \tan^{-1}\left(\frac{k\sqrt{\beta_k}\sqrt{k^2+m_k}}{\sqrt{\alpha_k}\sqrt{k^2+\beta_k+m_k}} \right)}{(k^2+m_k)^{9/2} (k^2+\beta_k+m_k)^{7/2}} \right) \\
&+ \frac{k^2\rho_k^4}{16\pi} \times \left(\frac{384k}{(k^2+m_k)^5} \right. \\
&- \frac{48k\alpha_k^4\beta_k^5}{(k^2+m_k)^5 (k^2+\beta_k+m_k) (\alpha_k (k^2+\beta_k+m_k) + k^2\beta_k (k^2+m_k))^4} \\
&+ \frac{8k\alpha_k^3\beta_k^4 \left(40k^2+33\beta_k+40m_k\right)}{(k^2+m_k)^5 (k^2+\beta_k+m_k)^2 (\alpha_k (k^2+\beta_k+m_k) + k^2\beta_k (k^2+m_k))^3} \\
&- \frac{10k\alpha_k^2\beta_k^3 \left(96k^4+152k^2\beta_k+8\left(24k^2+19\beta_k\right)m_k+63\beta_k^2+96m_k^2\right)}{(k^2+m_k)^5 (k^2+\beta_k+m_k)^3 (\alpha_k (k^2+\beta_k+m_k) + k^2\beta_k (k^2+m_k))^2} \\
&+ \frac{15k\alpha_k\beta_k^2 \left(128k^6+288k^4\beta_k+232k^2\beta_k^2+65\beta_k^3+128m_k^3\right)}{(k^2+m_k)^5 (k^2+\beta_k+m_k)^4 (\alpha_k (k^2+\beta_k+m_k) + k^2\beta_k (k^2+m_k))} \\
&+ \frac{15k\alpha_k\beta_k^2 \left(96\left(4k^2+3\beta_k\right)m_k^2+8\left(48k^4+72k^2\beta_k+29\beta_k^2\right)m_k\right)}{(k^2+m_k)^5 (k^2+\beta_k+m_k)^4 (\alpha_k (k^2+\beta_k+m_k) + k^2\beta_k (k^2+m_k))} \\
&- \left(384\beta_k \left(k^2+m_k\right)^3 + 480\beta_k^2 \left(k^2+m_k\right)^2 + 280\beta_k^3 \left(k^2+m_k\right) + 128\left(k^2+m_k\right)^4 + 63\beta_k^4\right) \times \\
&\left. \frac{15\sqrt{\alpha_k}\sqrt{\beta_k} \tan^{-1}\left(\frac{k\sqrt{\beta_k}\sqrt{k^2+m_k}}{\sqrt{\alpha_k}\sqrt{k^2+\beta_k+m_k}} \right)}{(k^2+m_k)^{11/2} (k^2+\beta_k+m_k)^{9/2}} \right)
\end{aligned}
\tag{3.26}
$$

Finally, we can numerically solve the differential system of the coupled equations for arbitrary initial conditions. An example is given in figure 3.4.

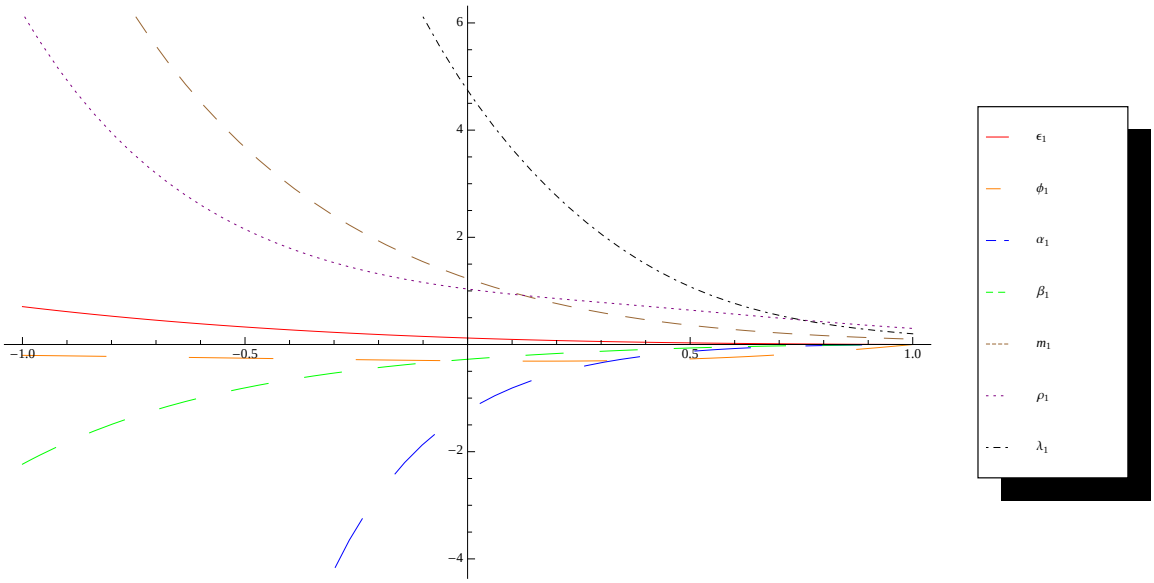

Figure 3.4: RG Flow of the dimensionless couplings $\check{g}_{i,k} = g_{i,k}k^{-d_i}$ from t=1 to t=-1 achieved using the non-local truncation defined in 3.13, 3.16 for the initial conditions $\epsilon_1 = \hat{\phi}_1 = \alpha_1 = \beta_1 = 0,\ m_1 = 0.1,\ \rho_1 = 0.3,\ \lambda_1 = 0.2$ in d=1.

3.4 Approximation scheme for non-local 4-point vertex ansatz

If we work with a Z_2 invariant QFT with a momentum-independent 4-point vertex, no momentum-dependent contribution to the 2-point vertex is generated, as we can see from 2.28. Therefore, if we want to go beyond the LPA in a Z_2 invariant framework, we are forced to introduce a non-trivial momentum dependence of the 4-point vertex. In order to do this, it is useful to introduce some approximations about the 4-point vertex structure and it's RG flow in d-dimension.

First of all, using symmetry considerations it is possible to show that we can write the 4-point scalar vertex as a function of the variables a, b and c defined as follow

$$\Gamma^{(4)}_{k;p_1,p_2,p_3,p_4} = \Gamma^{(4)}_{k;a,b,c} \qquad \begin{cases} a = p_1 + p_2 \\ b = p_1 + p_3 \\ c = p_2 + p_3 \end{cases} \tag{3.27}$$

and, inverting,

$$p_1 = \frac{a+b-c}{2}; \quad p_2 = \frac{a-b+c}{2}; \quad p_3 = \frac{-a+b+c}{2}; \quad p_4 = \frac{-a-b-c}{2} \tag{3.28}$$

Using the ERGE, we can evaluate the complete flow for the 4-point vertex:

$$\begin{aligned} \dot{\Gamma}^{(4)}_{k;a,b,c} &= \frac{1}{2}\int \frac{d^dq}{(2\pi)^d} G_{k;q}\Gamma^{(4)}_{k;a,\,p_1+q,\,p_2+q} G_{k;q+a}\Gamma^{(4)}_{k;a,\,p_3-q,\,p_1+p_2+p_3+q} G_{k;q}\dot{\mathbb{R}}_{k;q} \\ &\quad + \text{permutations}[a,b,c] - \frac{1\!\!1}{2}\int \frac{d^dq}{(2\pi)^d} G_{k;q}\Gamma^{(6)}_{k;p_1,p_2,p_3,p_4,q,-q} G_{k;q}\dot{\mathbb{R}}_{k;q} \end{aligned} \tag{3.29}$$

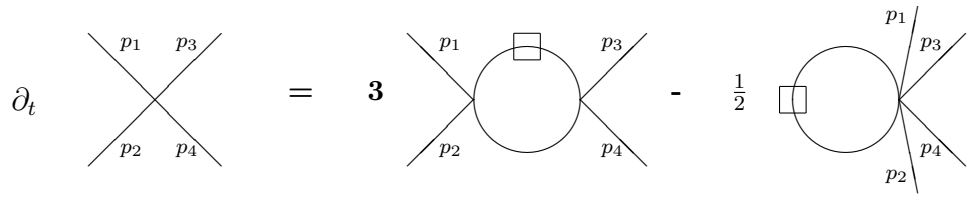

Figure 3.5: Graphical representation of the flow of the 4-point vertex $\partial_t\Gamma^{(4)}_{k;p_1,p_2,p_3,p_4}$.

If we work with the optimized cutoff scheme the integration over the field fluctuations, which contribute to the k derivative of $\partial_t\Gamma^{(4)}_{k;a,b,c}$, is restricted to all momenta lower than the scale k thanks to the presence of the cutoff term $\dot{\mathbb{R}}_{k;q}$ in the ERGE trace. Therefore, it is possible to evaluate equation 3.29 under the hypothesis of high external momenta $p_i \gg k$ and approximate the fluctuation momenta q to zero in the n-point vertex terms, reducing to

$$\begin{aligned} \dot{\Gamma}^{(4)}_{k;a,b,c} &= \frac{1}{2}\,\Gamma^{(4)}_{k;a,\frac{a+b-c}{2},\frac{a-b+c}{2}}\Gamma^{(4)}_{k;a,\frac{b+c-a}{2},\frac{a+b+c}{2}}\mathcal{J}^3_{k;a} + \text{permutations}[a,b,c] \\ &\quad -\frac{1}{2}\Gamma^{(6)}_{k;p_1,p_2,p_3,p_4,0,0}\mathcal{I}^2_k \end{aligned} \tag{3.30}$$

with

$$\mathcal{J}^n_{k;a} = \int \frac{d^dq}{(2\pi)^d} G^{n-1}_{k;q} G_{k;q+a} \dot{\mathbb{R}}_{k;q} \tag{3.31}$$

$$\mathcal{I}^n_k = \int \frac{d^dq}{(2\pi)^d} G^n_{k;q} \dot{\mathbb{R}}_{k;q} \tag{3.32}$$

Such an approximation has been already tested by Blaizot, Mendez and Wschebor [6] with good results.

It is now useful to construct a 1-loop perturbative expansion for the 4-point vertex $\Gamma^{(4)}_{k;a,b,c}$

$$\dot{\Gamma}^{(4)1-loop}_{k;a,b,c} = (\Gamma^{(4)0-loop})^2 \left(\mathcal{J}_a^{3\ 0-loop} + \mathcal{J}_b^{3\ 0-loop} + \mathcal{J}_c^{3\ 0-loop}\right) - \frac{1}{2}\Gamma^{(6)0-loop}\mathcal{I}^{2\ 0-loop} \tag{3.33}$$

and, without loosing generality, we can write

$$\Gamma^{(4)1-loop}_{k;a,b,c} = \frac{1}{3}\left(\gamma^{1-loop}_{k;a} + \gamma^{1-loop}_{k;b} + \gamma^{1-loop}_{k;c}\right) \tag{3.34}$$

with

$$\dot{\gamma}^{1-loop}_{k;a} = 3(\Gamma^{(4)0-loop})^2 \mathcal{J}_a^{3\ 0-loop} - \frac{1}{2}\Gamma^{(6)0-loop}\mathcal{I}^{2\ 0-loop} \tag{3.35}$$

If we force $\Gamma^{(4)}_{k;a,b,c}$ to be of the form 3.34 at every perturbative order and we assume $\gamma_{k;a} = \gamma_{k;-a}$ for every a, equation 3.30 reduces to

$$\begin{aligned}\dot{\Gamma}^{(4)}_{k;a,b,c} &= \frac{1}{18}\left(\gamma_{k;a} + \gamma_{k;\frac{a+b-c}{2}} + \gamma_{k;\frac{a-b+c}{2}}\right)\left(\gamma_{k;a} + \gamma_{k;\frac{a+b+c}{2}} + \gamma_{k;\frac{a-b-c}{2}}\right)\mathcal{J}^3_{k;a} \\ &\quad + \text{permutations}[a,b,c] - \frac{1}{2}\Gamma^{(6)}_{k;p_1,p_2,p_3,p_4,0,0}\mathcal{I}^2_k\end{aligned} \tag{3.36}$$

Let us now consider another approximation in order to strongly simplify this relation. We can consider a truncation with a local 6-point vertex and approximate

$$\gamma_{k;\frac{a}{2}+\frac{b-c}{2}} + \gamma_{k;\frac{a}{2}-\frac{b-c}{2}} \approx \gamma_{k;\frac{a}{2}+\frac{b+c}{2}} + \gamma_{k;\frac{a}{2}-\frac{b+c}{2}} \approx 2\gamma_{k;\frac{a}{2}} \tag{3.37}$$

Such an approximation, that we will call "collinear simplification" in the following, is not a priori justified from analytical considerations, as neither $(b-c)$, $(b+c)$ or $\gamma''_{k;a}$

are supposed to be small. Nevertheless this approximation is fundamental in order to conserve the structure 3.34 we assumed for $\Gamma^{(4)}_{k;a,b,c}$ during the RG flow, as it allows us to consistently write

$$\Gamma^{(4)}_{k;a,b,c} = \frac{1}{3}\left(\gamma_{k;a}+\gamma_{k;b}+\gamma_{k;c}\right) \tag{3.38}$$

$$\dot{\gamma}_{k;a} = \frac{1}{3}\left(\gamma_{k;a}+2\gamma_{k;\frac{a}{2}}\right)^2 \mathcal{J}^3_{k;a} - \frac{1}{2}\Gamma^{(6)}_k \mathcal{I}^2_k \tag{3.39}$$

It is possible to improve such an equation evaluating separately the flow of $\gamma_{k;a}$ for zero momentum $a = 0$. In such a situation, the approximation we made of high momenta is obviously inaccurate, and we should use the exact relation

$$\dot{\gamma}_{k;a=0} = 3\int \frac{d^dq}{(2\pi)^d} G_{k;q}\Gamma^{(4)}_{k;0,q,-q} G_{k;q}\Gamma^{(4)}_{k;0,-q,q} G_{k;q}\dot{\mathbb{R}}_{k;q} - \frac{1}{2}\Gamma^{(6)}_k \mathcal{I}^2_k \tag{3.40}$$

$$= \frac{1}{3}\int \frac{d^dq}{(2\pi)^d}\left(\gamma_{k;0}+2\gamma_{k;q}\right)^2 \left(G_{k;q}\right)^3 \dot{\mathbb{R}}_{k;q} - \frac{1}{2}\Gamma^{(6)}_k \mathcal{I}^2_k \tag{3.41}$$

We can now use a similar approach in order to get an approximated equation for the flow of the 2-point vertex. Starting from the ERGE we consider the exact flow equation

$$\dot{\Gamma}^{(2)}_{k;p} = -\frac{1}{2}\int \frac{d^dq}{(2\pi)^d} G_{k;q}\Gamma^{(4)}_{k;p+q,p-q,0} G_{k;q}\dot{\mathbb{R}}_{k;q} \tag{3.42}$$

and use the assumption of $\Gamma^{(4)}_{k;a,b,c}$ to be of the form 3.38. Taking the BMW high external momenta approximation, we can then write

$$\dot{\Gamma}^{(2)}_{k;p} = -\frac{1}{6}\left(2\gamma_{k;p}+\gamma_{k;0}\right)\mathcal{I}^2_k \tag{3.43}$$

and, as we did for the flow of the 4-point vertex, it is possible to improve the flow equation evaluating separately the flow for zero momentum $p = 0$.

$$\dot{\Gamma}^{(2)}_{k;p=0} = -\frac{1}{6}\int \frac{d^dq}{(2\pi)^d}\left(2\gamma_{k;q}+\gamma_{k;0}\right)\left(G_{k;q}\right)^2 \dot{\mathbb{R}}_{k;q} \tag{3.44}$$

and, finally, if we want to achieve a momentum dependent function with the right 0-momentum behavior, we can write

$$\dot{\Gamma}^{(2)}_{k;p} = -\frac{1}{3}\left(\gamma_{k;p}-\gamma_{k;0}\right)\mathcal{I}^2_k + \dot{\Gamma}^{(2)}_{k;p=0} \tag{3.45}$$

3.5 Non-local Z-2 invariant truncation and ERGE

Using the BMW approximation of small internal momenta and the collinear simplification, we achieved a system of flow equations compatible with the simplification of equation 3.38. In such a way, the momentum dependent structure of the 4-point vertex strongly simplify and we can investigate such a structure in order to introduce a suitable ansatz describing $\gamma_{k;p}$ in a 1-dimensional theory. Comparing 3.35 with 3.3 we find that the 1-loop contribution to the flow of $\gamma_{k;p}$ has a very similar momentum-dependent structure to the 1-loop contribution of the flow for the 2-point vertex. Therefore, we can introduce an ansatz for $\gamma_{k;p}$ with the same structure of the one we already used for the 2-point effective average function

$$\gamma_{k;p} = \lambda_k + \sigma_{\mu_k,\nu_k;\,p} \tag{3.46}$$

with, again,

$$\sigma_{\mu,\nu;\,p} = \frac{\mu\nu}{\mu + \nu p^2} \tag{3.47}$$

Moreover, from equation 3.43 we find that, under the BMW approximation, the momentum dependent structure of the 2-point vertex flow reproduces the momentum dependent structure of $\gamma_{k;p}$. It is possible to show that the function $\sigma_{\mu,\nu;\,p}$ verify the property

$$\int_{k_o}^{k_1} dk \sigma_{\mu_k,\nu_k;\,p} \approx \sigma_{\bar{\mu},\bar{\nu};\,p} \tag{3.48}$$

with

$$\begin{aligned} \bar{\mu} &= \int_{k_o}^{k_1} dk \mu_k \\ \bar{\nu} &= \int_{k_o}^{k_1} dk \nu_k \end{aligned} \tag{3.49}$$

whenever μ_k and ν_k are regular monotonous positive (or negative) functions. Therefore, as $\gamma_{k;p}$ is supposed to verify these requests, it is reasonable to introduce again a similar

ansatz for the 2-point vertex even in this more general truncation for Γ_k

$$\Gamma^{(2)}_{k;p} = p^2 + m_k + \sigma_{\alpha_k,\beta_k;\,p} \tag{3.50}$$

and we finally get

$$\Gamma_k[\phi] = \int dx \left(\frac{1}{2}\partial_\mu\phi(x)\partial^\mu\phi(x) + \frac{1}{2}\phi(x)\sigma_{\alpha_k,\beta_k;\partial}\ \phi(x) + \frac{1}{4!}\Sigma_{\mu_k,\nu_k}[\phi,x] + V[\phi(x)] \right) \tag{3.51}$$

with

$$\Sigma_{\mu_k,\nu_k}[\phi,x] = \frac{1}{3}\sum_{s=a,b,c}\int\prod_{i=1}^{4}\left(\frac{dp_i}{(2\pi)^d}\ \tilde{\phi}(p_i)\right) e^{-ix\sum p_i}\ \sigma_{\mu_k,\nu_k;s} \qquad \begin{cases} a = p_1 + p_2 \\ b = p_1 + p_3 \\ c = p_2 + p_3 \end{cases} \tag{3.52}$$

and

$$\begin{aligned} V_k[\phi] &= \sum_{n=0}^{2} g_{2n}\phi^{2n} \\ &= \epsilon_k + \frac{m_k}{2}\phi^2 + \frac{\lambda_k}{4!}\phi^4 \end{aligned} \tag{3.53}$$

Adopting the optimized cutoff term 3.18 and using the ERGE, we can obtain

$$\begin{aligned} \partial_t\epsilon_k =& \frac{1}{2}\int\frac{dq}{2\pi}G_{k;q}\dot{\mathbb{R}}_{k;q} - \frac{1}{2}\int\frac{dq}{2\pi}(q^2+\mathbb{R}_{k;q})^{-1}\dot{\mathbb{R}}_{k;q} \\ =& -\frac{k}{\pi}\left(\frac{k\sqrt{b_k}\sqrt{\alpha_k}\tan^{-1}\left(\frac{k\sqrt{b_k}\sqrt{k^2+m_k}}{\sqrt{\alpha_k}\sqrt{b_k+k^2+m_k}}\right)}{(k^2+m_k)^{\,3/2}\sqrt{b_k+k^2+m_k}} + \frac{m_k}{k^2+m_k} \right) \end{aligned} \tag{3.54}$$

Form equation 3.43 we can calculate the RG flow for m_k

$$\begin{aligned}\partial_t m_k &= \lim_{p\to\infty} \partial_t \Gamma^{(2)}_{k;p} \\ &= -\frac{1}{6}\left(3\lambda_k+\nu_k\right)\int \frac{dq}{2\pi}(G_{k;q})^2\,\dot{\mathbb{R}}_{k;q} \\ &= -\frac{k^2\left(3\lambda_k+\nu_k\right)}{6\pi}\left(\frac{k\left(\frac{\alpha_k\beta_k^2}{(k^2+\beta_k+m_k)(k^4\beta_k+k^2(\alpha_k+\beta_k m_k)+\alpha_k(\beta_k+m_k))}+2\right)}{\left(k^2+m_k\right)^2}\right. \\ &\quad \left. -\frac{\sqrt{\alpha_k}\sqrt{\beta_k}\left(4k^2+3\beta_k+4m_k\right)\tan^{-1}\left(\frac{k\sqrt{\beta_k}\sqrt{k^2+m_k}}{\sqrt{\alpha_k}\sqrt{k^2+\beta_k+m_k}}\right)}{\left(k^2+m_k\right)^{5/2}\left(k^2+\beta_k+m_k\right)^{3/2}}\right)\end{aligned} \tag{3.55}$$

and, from 3.43 and 3.44, we can achieve the flow of α_k and β_k

$$\begin{aligned}\partial_t \alpha_k &= \lim_{p\to\infty} p^2\partial_t\left(\Gamma^{(2)}_{k;p} - \lim_{p\to\infty}\Gamma^{(2)}_{k;p}\right) \\ &= -\frac{1}{3}\mu_k\int \frac{dq}{2\pi}(G_{k;q})^2\,\dot{\mathbb{R}}_{k;q} \\ &= -\frac{k^2\mu_k}{3\pi}\times\left(\frac{k\left(\frac{\alpha_k\beta_k^2}{(k^2+\beta_k+m_k)(\alpha_k(k^2+\beta_k+m_k)+k^2\beta_k(k^2+m_k))}+2\right)}{\left(k^2+m_k\right)^2}\right. \\ &\quad \left. -\frac{\sqrt{\alpha_k}\sqrt{\beta_k}\left(4\left(k^2+m_k\right)+3\beta_k\right)\tan^{-1}\left(\frac{k\sqrt{\beta_k}\sqrt{k^2+m_k}}{\sqrt{\alpha_k}\sqrt{k^2+\beta_k+m_k}}\right)}{\left(k^2+m_k\right)^{5/2}\left(k^2+\beta_k+m_k\right)^{3/2}}\right)\end{aligned} \tag{3.56}$$

$$
\begin{aligned}
\partial_t\beta_k =&\partial_t\left(\Gamma^{(2)}_{k;0}-\lim_{p\to\infty}\Gamma^{(2)}_{k;p}\right)\\
=&-\frac{1}{3}\int\frac{dq}{2\pi}\left(\gamma_{k;q}-\lambda_k\right)\left(G_{k;q}\right)^2\dot{\mathbb{R}}_{k;q}\\
=&-\frac{k^2\mu_k\nu_k}{3\pi\left(\beta_k\mu_k\left(k^2+m_k\right)-\alpha_k\nu_k\left(k^2+\beta_k+m_k\right)\right)^2}\times\\
&\left(\frac{2\tan^{-1}\left(\frac{k\sqrt{\nu_k}}{\sqrt{\mu_k}}\right)\left(\beta_k\mu_k-\alpha_k\nu_k\right)^2}{\sqrt{\mu_k}\sqrt{\nu_k}}\right.\\
&+\frac{k\alpha_k\beta_k^3\left(\beta_k\mu_k\left(k^2+m_k\right)-\alpha_k\nu_k\left(k^2+\beta_k+m_k\right)\right)}{\left(k^2+m_k\right)\left(k^2+\beta_k+m_k\right)\left(\alpha_k\left(k^2+\beta_k+m_k\right)+k^2\beta_k\left(k^2+m_k\right)\right)}\\
&+\left(\alpha_k\nu_k\left(k^2+\beta_k+m_k\right)\left(4\left(k^2+m_k\right)+\beta_k\right)+\beta_k\mu_k\left(-k^2-m_k\right)\left(4\left(k^2+m_k\right)+3\beta_k\right)\right)\times\\
&\left.\frac{\sqrt{\alpha_k}\beta_k^{3/2}\tan^{-1}\left(\frac{k\sqrt{\beta_k}\sqrt{k^2+m_k}}{\sqrt{\alpha_k}\sqrt{k^2+\beta_k+m_k}}\right)}{\left(k^2+m_k\right)^{3/2}\left(k^2+\beta_k+m_k\right)^{3/2}}\right)
\end{aligned}
\tag{3.57}
$$

using equation 3.39 we can achieve the flow equation for λ_k, that for the maximum potential order in our truncation $2m=12$ is null

$$
\begin{aligned}
\partial_t\lambda_k=&\lim_{p\to\infty}\partial_t\gamma_{k;p}\\
=&-\frac{1}{2}\omega_k\int\frac{dq}{2\pi}(G_{k;q})^2\,\dot{\mathbb{R}}_{k;q}\\
=&0
\end{aligned}
\tag{3.58}
$$

and, using equations 3.39 and 3.41, we can achieve the flow equation for μ_k and ν_k

$$
\begin{aligned}
\partial_t\mu_k=&\lim_{p\to\infty}p^2\partial_t\left(\gamma_{k;p}-\lim_{p\to\infty}\gamma_{k;p}\right)\\
=&3\lambda_k^2\int\frac{dq}{2\pi}(G_{k;q})^2\,\dot{\mathbb{R}}_{k;q}\\
=&\frac{3k^2\lambda_k^2}{\pi}\times\left(\frac{k\left(\frac{\alpha_k\beta_k^2}{\left(k^2+\beta_k+m_k\right)\left(\alpha_k\left(k^2+\beta_k+m_k\right)+k^2\beta_k\left(k^2+m_k\right)\right)}+2\right)}{\left(k^2+m_k\right)^2}\right.\\
&\left.-\frac{\sqrt{\alpha_k}\sqrt{\beta_k}\left(4\left(k^2+m_k\right)+3\beta_k\right)\tan^{-1}\left(\frac{k\sqrt{\beta_k}\sqrt{k^2+m_k}}{\sqrt{\alpha_k}\sqrt{k^2+\beta_k+m_k}}\right)}{\left(k^2+m_k\right)^{5/2}\left(k^2+\beta_k+m_k\right)^{3/2}}\right)
\end{aligned}
\tag{3.59}
$$

$$
\begin{aligned}
\partial_t \nu_k =& \partial_t \left(\gamma_{k;0} - \lim_{p\to\infty} \gamma_{k;p} \right) \\
=& 3 \int \frac{dq}{2\pi} \left(\frac{\gamma_{k;0} + 2\gamma_{k;q}}{3} \right)^2 (G_{k;q})^3 \, \dot{\mathbb{R}}_{k;q} \\
\simeq& 3 \int \frac{dq}{2\pi} \left(\gamma_{k;0}\right)^2 (G_{k;q})^3 \, \dot{\mathbb{R}}_{k;q} \\
=& \frac{3k^2 \left(\lambda_k + \nu_k\right)^2}{4\pi} \Bigg(\frac{8k}{\left(k^2 + m_k\right)^3} \\
&+ \frac{3k\alpha_k \beta_k^2 \left(4\left(k^2 + m_k\right) + 3\beta_k\right)}{\left(k^2 + m_k\right)^3 \left(k^2 + \beta_k + m_k\right)^2 \left(\alpha_k \left(k^2 + \beta_k + m_k\right) + k^2 \beta_k \left(k^2 + m_k\right)\right)} \\
&- \frac{3\sqrt{\alpha_k}\sqrt{\beta_k} \left(12\beta_k \left(k^2 + m_k\right) + 8\left(k^2 + m_k\right)^2 + 5\beta_k^2\right) \tan^{-1}\left(\frac{k\sqrt{\beta_k}\sqrt{k^2 + m_k}}{\sqrt{\alpha_k}\sqrt{k^2 + \beta_k + m_k}} \right)}{\left(k^2 + m_k\right)^{7/2} \left(k^2 + \beta_k + m_k\right)^{5/2}} \\
&- \frac{2k\alpha_k^2 \beta_k^3}{\left(k^2 + m_k\right)^3 \left(k^2 + \beta_k + m_k\right) \left(\alpha_k \left(k^2 + \beta_k + m_k\right) + k^2 \beta_k \left(k^2 + m_k\right)\right)^2} \qquad (3.60)
\end{aligned}
$$

In equation 3.60 we used a zero internal momenta approximation for the term $\gamma_{k;q}$, in order to achieve a reasonable analytical expression to write in the text. However, it is possible to achieve an analytical expression also evaluating the exact integral without any approximation, and the numerical results achieved solving the system with the exact equation are very similar to the ones achieved using it's approximated version.

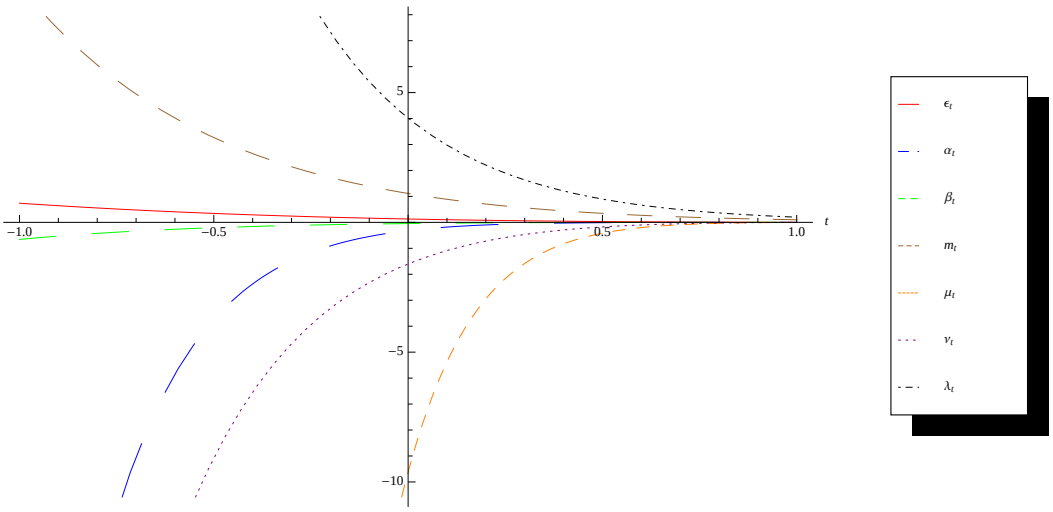

Figure 3.6: RG Flow of the dimensionless couplings $\check{g}_{i,k} = g_{i,k}k^{-d_i}$ from t=1 to t=-1 achieved using the truncation 3.51, 3.53 for the initial conditions $\epsilon_1 = \alpha_1 = \beta_1 = \mu_1 = \nu_1 = 0,\ m_1 = 0.1,\ \lambda_1 = 0.2$ in d=1.

In order to check the accuracy of our truncation, we can make some comparison with some known exact numerical results. Let us consider the vacuum energy solution for the bare potential $\frac{m}{2}\phi^2 + \frac{\lambda}{4!}\phi^4 + \frac{\omega}{6!}\phi^6$, which give the ground state of the QM system, and compare it with the known result ϵ_o^p achieved with other asserted techniques [11],[12]. We can also introduce a truncation of the form 3.51 with higher order potential terms and proceed as before in order to get a more accurate differential system.

$$V_k[\phi] \quad = \quad \sum_{n=0}^{m} g_{2n}\phi^{2n} \qquad\qquad \text{with} \quad m = 2,3,4,5,6 \tag{3.61}$$

If we compare the LPA results ϵ_o^{LPA} given in 2.55 with the results achieved using the truncation containing the non-local ansatz for the 2-point and 4-point vertices ϵ_o^{ANSATZ}, we find that the non-local truncation provides more accurate outcomes than the LPA for many initial conditions and seems to converge to a better result when we increase the maximum polynomial order m of the potential in our truncation. In particular, we find that considering the bare action $S[\phi] = \int dx\ \frac{1}{2}(\partial\phi)^2 + \phi^4$, in the

high m limit the non-local truncation seems to converge to a value with a relative error of about 3 10^{-4}, one order of magnitude more accurate than the one achieved with the LPA. Moreover, we find that both the truncations provides a very accurate result for a particular value of m, that is $m = 3$ for the LPA and $m = 4$ for the non-local truncation, and we find that the most accurate non-local truncation result is again one order of magnitude more accurate than the LPA one. Otherwise, if we consider the bare action $S[\phi] = \int dx\ \frac{1}{2}(\partial\phi)^2 + \phi^6$, we find that both the truncations are less accurate. Despite this, in the high m limit the non-local truncation seems to converge with a relative error of about 2 10^{-2}, more than a 20 percent more accurate than the LPA result. We could try to improve our results by introducing in our truncation a non-local ansatz also of the 6-point vertex together with the 2-point and 4-point ones.

	m=2	m=3	m=4	m=5	m=6
ϵ_o^{LPA}	0,662917	0,667812	0,666432	0,666207	0,666225
ϵ_o^{ANSATZ}	0,664441	0,669317	0,667964	0,667741	0,667755
$\frac{\epsilon_o^{LPA}-\epsilon_o}{\epsilon_o}$	-7,59 10^{-3}	-2,61 10^{-4}	-2,33 10^{-3}	-2,66 10^{-3}	-2,64 10^{-3}
$\frac{\epsilon_o^{ANSATZ}-\epsilon_o}{\epsilon_o}$	-5,31 10^{-3}	1,99 10^{-3}	-3,33 10^{-5}	-3,67 10^{-4}	-3,46 10^{-4}

Table 3.1: Vacuum energy for $S[\phi] = \int dx\ \frac{1}{2}(\partial\phi)^2 + \phi^4$ calculated using the LPA truncation 2.4, 3.61 (LPA) and the non-local truncation 3.51, 3.61 (ANSATZ) for different maximum potential orders $2m$. The results are compared with the exact value $\epsilon_o = 0,66798625916$.

	m=2	m=3	m=4	m=5	m=6
ϵ_o^{LPA}	————	0,682646	0,666403	0,665941	0,665345
ϵ_o^{ANSATZ}	————	0,685881	0,669653	0,669331	0,668714
$\frac{\epsilon_o^{LPA}-\epsilon_o}{\epsilon_o}$	————	2,85 10^{-3}	-2,10 10^{-2}	-2,17 10^{-2}	-2,26 10^{-2}
$\frac{\epsilon_o^{ANSATZ}-\epsilon_o}{\epsilon_o}$	————	7,61 10^{-3}	-1,62 10^{-2}	-1,67 10^{-2}	-1,76 10^{-2}

Table 3.2: Vacuum energy for $S[\phi] = \int dx\ \frac{1}{2}(\partial\phi)^2 + \phi^6$ calculated using the LPA truncation 2.4, 3.61 (LPA) and the non-local truncation 3.51, 3.61 (ANSATZ) for different maximum potential orders $2m$. The results are compared with the exact value $\epsilon_o = 0.6807036117$.

3.6 Discussion

We developed two non-local truncations describing the EAA of a real scalar field theory in d=1 both in the symmetric and in the non-symmetric phase. We compared the vacuum energy results achieved using the Z-2 invariant truncation with the asserted ones achieved with the perturbative expansion approach and we found that the non-local truncation was one order of magnitude more accurate than the LPA truncation. This is quite a good result, if we remember the strong approximations we introduced in order to achieve a consistent Z-2 invariant non-local truncation containing a non-local ansatz both for the 2 and 4 point vertices. Moreover, we only used the zero momentum value and the lowest order high momentum behavior of the vertices flow in order to calibrate the flow for the parameters in the ansatz. This approach strongly simplified our calculations, as we achieved the small momentum behavior of the vertices without introducing an high order derivative expansion for both the 2 and 4 point vertices, which would be quite an hard task, but it could also lead to misleading results.

We investigated the d=1 model, i.e. the QM case, but the generalization to arbitrary d dimensions is straightforward and with some work it is possible to achieve exact analytical results for arbitrary d dimensions. For the sake of brevity we will not write

the $d > 1$ dimensional results in the following, since the β functions are much more complicated expressions, but we will use the 4-dimensional model in chapter 4 in order to check the validity of our truncation also for higher dimensional theories.

Chapter 4

BMW Equation

We will now introduce an alternative method, recently developed, to solve the ERGE and obtain the full momentum dependence of any n-point vertex, in order to check the reliability of the results achieved using the non-local ansatz. This method was firstly developed by J.-P. Blaizot, R. Mendez-Galain and N. Wschebor [6],[2],[4],[7] and exploit some approximations in order to develop a close integro-differential flow equation for the n-point function able to investigate the complete momentum-dependence of any vertex. These integro-differential equations are a priori difficult to solve, but making some more approximations one can reduce them to a more simple differential system that can be finally solved with a reasonable numerical effort.

4.1 The Method

The derivation of the BMW approach to the ERGE proceeds as follow: recalling equation 2.28 and pointing out the field dependence of the n-point vertices, it is possible to write

$$\begin{aligned}\dot{\Gamma}^{(2)}_{k;p;\phi} &= \int \frac{d^dq}{(2\pi)^d} G_{k;q;\phi}\Gamma^{(3)}_{k;p,-p,q-q;\phi} G_{k;q+p;\phi}\Gamma^{(3)}_{k;p+q,-p,-q;\phi} G_{k;q;\phi}\dot{\mathbb{R}}_{k;q} \\ &\quad -\frac{1}{2}\int \frac{d^dq}{(2\pi)^d} G_{k;q;\phi}\Gamma^{(4)}_{k;p,-p,q,-q;\phi} G_{k;q;\phi}\dot{\mathbb{R}}_{k;q}\end{aligned}$$

where

$$G_{k;q;\phi} = \left(\Gamma^{(2)}_{k;q;\phi} + \mathbb{R}_{k;q}\right)^{-1} \tag{4.1}$$

In general, it is possible to find an analogue flow equation for every n-point vertex involving all the m-point functions with $m \leq n+2$. Therefore, it is not possible to achieve a closed system describing the flow of an n-point vertex and we deal with infinite-many integro-differential coupled equations. This problem has been solved by BMW by making some considerations about the integration over the momentum fluctuations. In fact, when working with the optimized cutoff scheme, the $\dot{\mathbb{R}}_{k;q}$ term restrict the integration dominion to all $q \leq k$. Therefore, by assuming the n-point vertices to be smooth for small momenta and the external momenta p to be greater than the scale k, it is possible to approximate $q = 0$ in the n-point vertices in the rhs of the flow equation.

$$\begin{aligned}\dot{\Gamma}^{(2)}_{k;p;\phi} &= \int \frac{d^dq}{(2\pi)^d} G_{k;q;\phi}\Gamma^{(3)}_{k;p,-p,0;\phi} G_{k;q+p;\phi}\Gamma^{(3)}_{k;p,-p,0;\phi} G_{k;q;\phi}\dot{\mathbb{R}}_{k;q} \\ &\quad -\frac{1}{2}\int \frac{d^dq}{(2\pi)^d} G_{k;q;\phi}\Gamma^{(4)}_{k;p,-p,0,0;\phi} G_{k;q;\phi}\dot{\mathbb{R}}_{k;q}\end{aligned}$$

Moreover, recalling that the partial derivative in ϕ corresponds to the functional derivative in a constant field, it is possible to identify

$$\Gamma^{(3)}_{k;p,-p,0;\phi} = \frac{\partial\Gamma^{(2)}_{k;p;\phi}}{\partial\phi} \qquad \text{and} \qquad \Gamma^{(4)}_{k;p,-p,0,0;\phi} = \frac{\partial^2\Gamma^{(2)}_{k;p;\phi}}{\partial\phi^2} \tag{4.2}$$

and, substituting, it is possible to write

$$\dot{\Gamma}^{(2)}_{k;p;\phi} = \mathcal{J}^3_{k;p;\phi}\left(\frac{\partial\Gamma^{(2)}_{k;p;\phi}}{\partial\phi}\right)^2 - \frac{1}{2}\,\mathcal{I}^2_{k;\phi}\frac{\partial^2\Gamma^{(2)}_{k;p;\phi}}{\partial\phi^2} \tag{4.3}$$

with, again,

$$\mathcal{J}^n_{k;a;\phi} = \int \frac{d^dq}{(2\pi)^d} G^{n-1}_{k;q;\phi} G_{k;q+a;\phi}\dot{\mathbb{R}}_{k;q} \tag{4.4}$$

$$\mathcal{I}^n_{k;\phi} = \int \frac{d^dq}{(2\pi)^d} G^n_{k;q;\phi}\dot{\mathbb{R}}_{k;q} = \mathcal{J}^n_{k;a=0;\phi} \tag{4.5}$$

as we already defined in section 3.4. Equation 4.3 present the structure of a close integro-differential equation. Therefore, it is theoretically possible to numerically solve

this equation for given boundary conditions, but it is quite an hard task as we are forced to evaluate it for every p in order to be able to perform the integrations 4.4 and 4.5. BMW have reduced this problem to a much simpler differential equation by separately evaluating the terms $\mathcal{J}^3_{k;a;\phi}$ and $\mathcal{I}^2_{k;\phi}$ after employing another approximation. For example, it is possible to achieve this result by calculating the analytical form of these terms using the LPA next to leading order and then substituting in these expressions the value of the couplings achieved solving the ERGE using a truncation satisfying the LPA, as showed in appendix B. The accuracy of such an approximation has been investigated by Blaizot, Mendez-Galain and Wschebor with good results.

The zero internal momenta approximation is evidently inaccurate when we study the zero external momenta regime and, therefore, it is possible to improve the method by separately evaluating $\Gamma^{(2)}_{k;0} = \frac{\partial^2 V_k}{\partial \phi^2}$. In order to do this, it is useful to introduce the self-energy

$$\Sigma_{k;p;\phi} = \Gamma^{(2)}_{k;p;\phi} - \Gamma^{(2)}_{k;0;\phi} - p^2 \tag{4.6}$$

satisfying

$$\dot{\Sigma}_{k;p;\phi} = \mathcal{J}^3_{k;p;\phi} \left(\frac{\partial \Gamma^{(2)}_{k;p;\phi}}{\partial \phi} \right)^2 - \frac{1}{2}\, \mathcal{I}^2_{k;\phi} \frac{\partial^2 \Gamma^{(2)}_{k;p;\phi}}{\partial \phi^2} - [p \to 0] \tag{4.7}$$

to be solved together with the flow equation for the potential

$$\dot{V}_{k;\phi} = \frac{1}{2} \int \frac{d^d q}{(2\pi)^d} G_{k;q;\phi} \dot{\mathbb{R}}_{k;q} \tag{4.8}$$

with

$$\Gamma^{(2)}_{k;p;\phi} = p^2 + \frac{\partial^2 V_k}{\partial \phi^2} + \Sigma_{k;p;\phi} = G^{-1}_{k;p;\phi} - \mathbb{R}_{k;p} \tag{4.9}$$

It is possible to use the same approach in order to achieve a close integro-differential equation for every n-point vertex with arbitrary $n \geq 2$ [5].

4.2 BMW and non-local 2-point vertex truncation

We will now use the BMW technique results as a test for the results achieved with the non-local truncations we developed in chapter 3. We considered a d-dimensional scalar field theory characterized by the bare action

$$S[\phi] = \Gamma_{k=k_s}[\phi] = \int dx \left(\frac{1}{2}\partial_\mu \phi(x)\partial^\mu \phi(x) + \frac{m_o}{2}\phi(x)^2 + \frac{\rho_o}{3!}\phi(x)^3 + \frac{\lambda_o}{4!}\phi(x)^4 \right) \quad (4.10)$$

and we investigated the RG Flow of the EAA starting from k_s to k_e, focusing on the d=1 and d=4 models.

As a first step, we numerically solved the system of coupled differential equations 3.20-3.26 for the couplings associated to the truncation 3.13, 3.16, generalized to the d-dimensional case. In such a way, we achieved a numerical expression for the effective average 2-point function for $k = k_e$, evaluated in $\phi = 0$

$$\Gamma^{(2)}_{k_e,p} = \sigma_{\alpha_{k_e},\beta_{k_e};p} + m_{k_e} - \rho_{k_e}\hat{\Phi}_{k_e} + \frac{\lambda_{k_e}}{2}\hat{\Phi}^2_{k_e} \quad (4.11)$$

We compared the achieved results with the ones achieved numerically solving the integro-differential BMW equation for the 2-point vertex. We separately evaluated the terms $\mathcal{J}^3_{k;a;\phi}$ and $\mathcal{I}^2_{k;\phi}$ numerically solving the flow equation for the couplings under the LPA and substituting the results in the correspondent analytical expressions, as shown in appendix B. In such a way, we reduced to a standard differential equation, that we autonomously solved for every p implementing the Finite Difference Method on grid.

4.2.1 1-dimensional results

We numerically solved the 1-dimensional differential system 3.20-3.26 considering a scale parameter flow from $k_s = 10$ to $k_e = 0.1$. Such a flow interval is able to guarantee, in d=1, more than the 85 percent of the total flow of the Effective Average Action under the LPA and more than the 99 percent of the flow of the non-local 2-point vertex term in the non-local truncation model we developed.

d=1	$\Gamma^{(2)}_{k_e;p=0}$	$\lim_{p\to\infty}\left(\Gamma^{(2)}_{k_e;p}-p^2\right)$
BMW	0.9987497	1.0000000
N-L Truncation	0.9987499	1.0000023
% err	$1\ 10^{-7}$	$2\ 10^{-6}$

Table 4.1: Numerical results of the low and high momentum 2-point vertex behavior achieved with different techniques in a 1-dimensional scalar field theory with initial conditions as 4.10, where $m_o = 1$, $\rho_o = 0.1$ and $\lambda_o = 0$, and for the scale parameter k flowing from $k_s = 10$ to $k_e = 0.1$. BMW: BMW technique; N-L Truncation: Non-local truncation 3.13, 3.16. The numerical accuracy of the BMW result is 10^{-7}.

Than, we solved the BMW equation in d=1 using the Explicit Euler Finite Difference Method. We considered a domain in the field ϕ from $\phi_s = -5$ to $\phi_e = 5$, that is adequate to provide a final result comfortably independent from the boundary lateral conditions, and we set up the grid partitioning the domain in the scale parameter k in $n_k = 500$ intervals and the field domain in $n_\phi = 51$ intervals. In such a way, we achieved a numerical precision in the final result of about 10^{-7}.

Comparing the outcomes of the two techniques, we find a good agreement of the results and, in particular, we find that the difference between the low momentum 2-point vertex values seems to be compatible with the numerical accuracy of the finite difference method used to solve the BMW equation. The high momentum behavior shows a bigger difference, of the order of 10^{-6}, that is an order of magnitude higher than the numerical accuracy of the results. We can interpret this result as the consequence of the approximate nature of our truncation, and in particular of the local approximation of the 4-point vertex. In fact, the non-local truncation solution introduces a flow for the high momentum 2-point vertex value while, from different considerations, it is possible to show that no flow for this term is present if we solve the ERGE without any truncation. It is nevertheless possible to solve this problem by introducing a non-local 4-point vertex term in our truncation. Finally, we find that the p-dependent shape

of the various 2-point functions achieved with the different techniques shows a good agreement. This is a really comforting result, as the simple analytical function $\sigma_{\mu,\nu,p}$ that we introduced in our ansatz seems to be able to fit with a good accuracy the non-local structure of $\Gamma^{(2)}_{k;p}$ in such a theory. Finally, we also tried to increase the RG interval for the scale parameter, considering an RG flow from $k_s = 50$ to $k_e = 0.05$. In a 1-dimensional scalar theory, such a flow interval guarantees more than the 95 percent of the total flow of the Effective Average Action under the LPA and more than the 99.9 percent of the flow of the non-local 2-point vertex term in the non-local truncation model we developed. We setted $n_k = 2500$ and $n_\phi = 51$ in the Finite Difference Method grid with, again, $\phi_s = -5$ and $\phi_e = 5$ as field dominion. In such a way, we found that the non-local truncation outcomes for a wider RG flow seem to fit the BMW results more accurately than in the case of the previous k-interval.

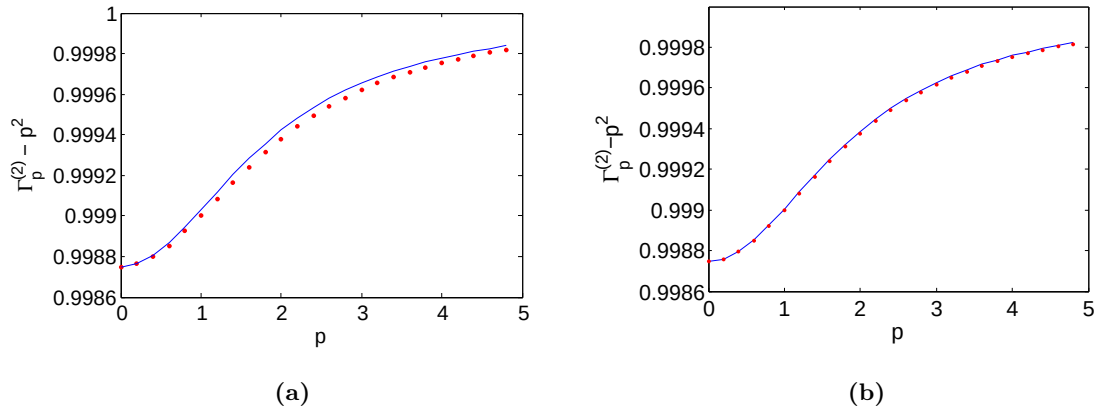

(a) **(b)**

Figure 4.1: Graphical representation of $\Gamma^{(2)}_{k=k_e;p}$ achieved using different techniques in a 1-dimensional scalar field theory with initial conditions as 4.10 with $m_s = 1$, $\rho_s = 0.1$ and $\lambda_s = 0$ and for the scale parameter k flowing from $k_s = 10$ to $k_e = 0.1$ (a) and from $k_s = 50$ to $k_e = 0.05$ (b). Red-dotted line: Finite Difference numerical results of the BMW equation for different p; blue-solid line: Numerical solution of the differential system concerning the non-local truncation 3.13, 3.16.

d=4	$\Gamma^{(2)}_{k_e;p=0}$	$\lim_{p\to\infty}\left(\Gamma^{(2)}_{k_e;p}-p^2\right)$
BMW	0.99990073617	1.00000000
N-L Truncation	0.99990073671	1.00000004
% err	$5\ 10^{-10}$	$4\ 10^{-8}$

Table 4.2: Numerical results of the low and high momentum 2-point vertex behavior achieved with different techniques in a 4-dimensional scalar field theory with initial conditions as 4.10, where $m_o = 1$, $\rho_o = 0.1$ and $\lambda_o = 0$, and for the scale parameter k flowing from $k_s = 10$ to $k_e = 0.1$. BMW: BMW technique; N-L Truncation: Non-local truncation 3.13, 3.16. The numerical accuracy of the BMW result is 10^{-9}.

4.2.2 4-dimensional results

We investigated the 4-dimensional case proceeding as we did in the 1-dimensional one, with the only difference of a higher grid resolution, that is $n_k = 1000$ and $n_\phi = 101$, providing a numerical accuracy of about 10^{-9}. The dependence of the result from the lateral boundary condition is negligible. As it happened in the d=1 case, we found a good numerical agreement between the results achieved using different techniques. In particular we found that the difference between the low momentum behavior results is compatible with the numerical accuracy of the Finite Difference Method, while the high momentum behavior seems to differ more, as it is the case for the 1-dimensional case. Again, the reason for this is to the local approximation of the 4-point vertex in the non-local truncation we developed, which introduce an improper flow of the high-momentum 2-point vertex value. We will address this problem also in the next subsection. Finally, we find that the $\Gamma^{(2)}_{k_e;p}$ p-dependent shape achieved using the non-local truncation differs from the one achieved using the BMW equation more than in the case of d=1. In particular, it result to be lower than the BMW one for $p \lesssim 5$ and higher for $p \gtrsim 5$.

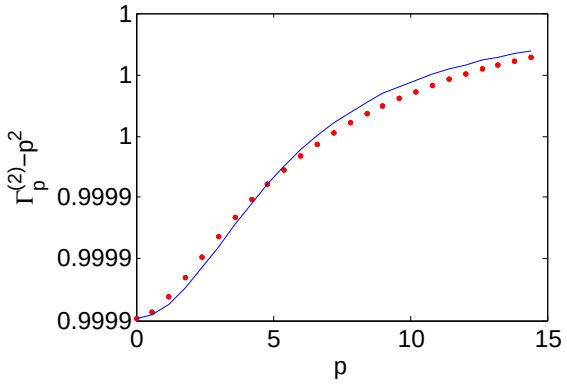

Figure 4.2: Graphical representation of $\Gamma^{(2)}_{k=k_e;p}$ achieved using different techniques in a 4-dimensional scalar field theory with initial conditions as 4.10 with $m_o = 1$, $\rho_o = 0.1$ and $\lambda_o = 0$ and for the scale parameter k flowing from $k_s = 10$ to $k_e = 0.1$. Red-dotted line: Finite Difference results of the BMW equation for different p; blue-continuous line: solution of the differential system concerning the non-local truncation 3.13, 3.16 for d=4.

4.3 BMW and non-local Z-2 invariant truncation

We will now compare the BMW results with the ones achieved using the truncation with non-local 2-point and 4-point vertices in a Z-2 invariant d-dimensional scalar QFT. We considered the bare action

$$S[\phi] = \Gamma_{k=k_s}[\phi] = \int dx \left(\frac{1}{2}\partial_\mu \phi(x) \partial^\mu \phi(x) + \frac{m_o}{2}\phi(x)^2 + \frac{\lambda_o}{4!}\phi(x)^4 \right) \tag{4.12}$$

and, again, we proceeded as in section 4.2 focusing on the d=1 and d=4 cases.

4.3.1 1-dimensional results

We numerically solved the 1-dimensional differential system associated to the Z-2 invariant non-local truncation 3.51, 3.61 both for the maximum potential order $2m = 4$ and $2m = 12$, in order to compare the different outcomes. We considered a flow of the scale parameter from $k_s = 10$ to $k_e = 0.1$, providing more than the 86 percent of the total flow of the EAA under the LPA and more than the 97 percent of the total flow

d=1	$\Gamma^{(2)}_{k_e;p=0}$	$\lim_{p\to\infty}\left(\Gamma^{(2)}_{k_e;p}-p^2\right)$	$\Gamma^{(4)}_{k_e;0,0,0,0}$	$\lim_{p\to\infty}\Gamma^{(4)}_{k_e;p,-p,0,0}$
BMW	1.18938	1.19759	0.7961	0.9228
NLT m=2	1.18876	1.19755	0.7701	0.9234
% err	$5\ 10^{-4}$	$3\ 10^{-5}$	$3\ 10^{-2}$	$6\ 10^{-4}$
NLT m=6	1.18970	1.19857	0.7930	0.9496
% err	$3\ 10^{-4}$	$8\ 10^{-4}$	$4\ 10^{-3}$	$3\ 10^{-2}$

Table 4.3: Numerical results of the low and high momentum 2-point vertex behavior achieved with different techniques in a 1-dimensional Z-2 invariant scalar field theory with initial conditions as 4.12, where $m_o = 1$ and $\lambda_o = 1$, and for the scale parameter k flowing from $k_s = 10$ to $k_e = 0.1$. The numerical accuracy of the BMW 2-point vertex results is $5\ 10^{-5}$ and the one of the 4-point vertex outcomes is $5\ 10^{-4}$. BMW: BMW technique; NLT m=2: Non-local truncation 3.51, 3.53; NLT m=6: Non-local truncation 3.51, 3.61

of the non-local 2-point vertex term in the non-local truncation. Then, we solved the BMW equation considering a domain in the field ϕ from $\phi_s = -5$ to $\phi_e = 5$, sufficient to guarantee a final result independent from the lateral boundary conditions with a good accuracy, and we set up a grid composed by $n_k \times n_\phi = 2000 \times 101$ nodes, providing a numerical accuracy of $5\ 10^{-5}$ for the 2-point vertex results and $5\ 10^{-4}$ for the 4-point vertex ones.

We found that the non-local truncation results for m=2 fit the high momentum behavior of the 2 and 4 point vertices better than the m=6 outcomes and are compatible with the numerical precision of the Finite Difference Method, while the m=6 results are more apt to describe the small momentum behavior of the vertices, although they differ from the BMW result for more than the numerical precision of the latter.This can be interpreted, again, as the consequence of the local approximation we made about the n-point vertices with $n > 4$. In fact, the n-point vertices for large n gives an important contribution to the flow of the low-momentum 2 and 4 point vertices, but, as a

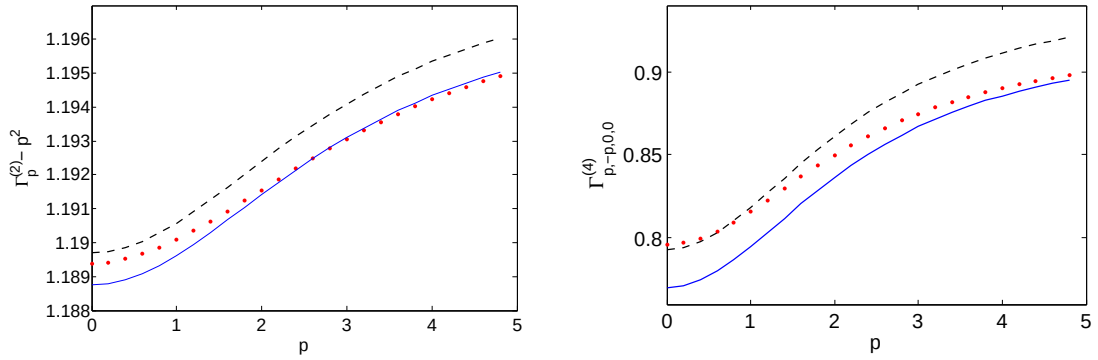

(a) **(b)**

Figure 4.3: Graphical representation of $\Gamma^{(2)}_{k=k_e;p}$ (a) and $\Gamma^{(4)}_{k=k_e;p,-p,0,0}$ (b) achieved using different techniques in a 1-dimensional Z-2 invariant scalar field theory with initial conditions as 4.12 with $m_o = 1$ and $\lambda_o = 0$ and for the scale parameter k flowing from $k_s = 10$ to $k_e = 0.1$. Red-dotted line: Finite Difference results of the BMW equation for different values of p; black-dashed line: Solution of the differential system concerning the non-local truncation with a maximum polynomial order $2m = 4$ in the potential 3.51, 3.53 ; blue-continuous line: Solution of the differential system concerning the non-local truncation with a maximum polynomial order $2m = 12$ in the potential 3.51, 3.61.

consequence of the local approximation we made, they also introduce an improper flow term for the high momentum limit of the vertices. Therefore, it could be reasonable to use the results achieved with m=2 to fix the high momentum 2 and 4 point vertex behavior and the outcomes for m=6 to set the small momentum one. Moreover, it is possible to get a more accurate fit of the outcomes recalling the approximation scheme we used in both the BMW and non-local truncation techniques. In fact, developing the BMW equation, we used the 0 order approximation for high external momenta and in our calculations we did not improve this approximation neither for zero external momenta. Contrarily, in the approximation scheme we introduced when dealing with the non-local 4-point vertex ansatz 3.4, we improved such an approximation by adequately evaluating the zero external momenta 2-point vertex flow. Thus, we can try to remove

such an improvement in the non-local truncation differential system in order to use an approximation scheme more similar to the one we used for the BMW equation. In such a way, we achieve a quite good improvement of the agreement between the results and, specifically, we reduce the difference between the BMW and non-local truncation results of about a factor 3 for both the low and high momentum 2-point vertex limits. In addition, other sources of approximations and errors are present in the non-local truncation approach we used, providing differences from the BMW results. Together with the local approximation of the n-point vertices for high n, also the collinear approximation for the 4-point vertex is a potential source of errors, and for example could lead to an improper flow for the high momentum 2-point vertex limit. Also the high external momenta approximation could lead to discordant results; in fact, despite the same approximation has been used in both the techniques, different approaches could bring to different approximation consequences in different frameworks. Finally, the ansatz we made about the 2 and 4 point vertices could reveal to be inadequate to properly describe the non-local structure of the vertices, but this doesn't seem to be the case, as from 4.3 we can find a quite good agreement between the vertices p-dependent shape we achieved using different techniques.

The d=4 the situation is quite similar to the 1-dimensional case. In particular, we found that the final results are a little less dependent on the maximum potential order we introduced in our non-local truncation but, despite that, the 4-dimensional results seems to reproduce all the features we described about the 1-dimensional ones, and therefore we will not write them in the follow.

4.4 Discussion

We found that the non-local truncation seems to produce predictions quite compatible with the results achieved numerically solving the BMW equation for both a Z-2 invariant and Z-2 non-invariant theory both in d=1 and d=4 and, as a very good result,

it requires a much more little numerical effort. Despite many differences between the results arise in some regimes, they could be interpreted as the consequence of some approximations we introduced in our truncations, and there are many improvements we can bring in the future in order to try to improve our results. Obviously, this can not be considered as a definitive test for the validity of our ansatz. In fact, the BMW equation was developed through many approximations, some coincident with the approximations we used in the non-local truncation approach, and therefore we can not be sure of the validity of the BMW results as a test for our truncations. Moreover, we only tested the RG theory flow for a small interval in the scale parameter dominion, as a consequence of the Finite Difference Method we used to solve the BMW equation. Therefore, we have no information about the full RG flow results, and the only thing we can do in order to check their validity is try to modify such an interval and investigate the consequences on the outcomes.

Chapter 5

Conclusions

In the first part of this work, we tried to give a brief introduction to one of the most useful non-perturbative approach to the Renormalization Group. We compared the results we may achieve in this approach with the perturbative ones, trying to investigate the physical meaning of our equations, and we inserted some simple examples, in order to clarify the introduced concepts. We lingered on some conceptual consequences of this different approach to the renormalization theory, such as the AS scenario and the meaning of fundamental and effective theory, and we tried to understand the deeper meaning of the insertion of a regularization term in the functional integration, exploring the balanced approach to the coarse-graining. Finally, we described the most used truncations, trying to discuss good and bad aspects of them in order to better understand what are the most relevant interacting terms of the EAA to be considered.

In the second part of this thesis, where all our original work is collected, we firstly investigated the 1-loop 2-point vertex structure for a real scalar field theory in order to find a reasonable ansatz describing its momentum-dependence. First, we found that a very simple monotonous function dependent from only two parameters was able to properly fit the 1-loop results at every energy scale k, provided a good choice of the parameters, and we adopted such a function as fundamental ansatz for our truncation. We also investigated the Z-2 invariant real scalar field theory, where it is necessary

to consider the p-dependent structure of the 4-point vertex in order to achieve a non-trivial 2-point vertex, and we developed an approximation scheme that allows us to introduce consistently a non-local ansatz for both the 2 and 4 point vertices. We found that the same function we already used for the non Z-2 invariant model was able to properly describe the momentum dependence of the 2 and 4 point vertices also in a Z-2 invariant theory, and we used it for the construction of a Z-2 invariant truncation.

Using the zero momentum value and the high momentum behavior of the 2 and 4 point vertices in order to calibrate the parameters in our ansatz, we derived the differential system of coupled equations describing the RG flow of the couplings for both the truncations.

We numerically solved them and we compared the vacuum energy outcome for the anharmonic oscillator in QM with the LPA results and with the asserted values achieved using high order perturbative expansion and other techniques. We found that the non-local truncation was able to produce predictions one order of magnitude more accurate than the LPA, that is quite a comforting result. Moreover, we achieved this result using the Z-2 invariant truncation, that was developed introducing many approximations, and try to achieve an improvement to the LPA with a derivative expansion for the 2 and 4 point vertices would be quite an hard task.

Then, we used the BMW technique in order to partially test against this approximate non-perturbative scheme the non-local truncation results in 1 and 4 dimensions for both the Z-2 invariant and Z-2 non-Invariant models. We found that in the Z-2 non-invariant theory, the non-local truncation fits the BMW results with good precision. In particular, the agreement between the two techniques for small momenta is compatible with the numerical precision of the results, while for high momenta they differ of about 10^{-6}-10^{-8}, difference that can be interpreted as the consequence of the local approximation we made about the 4-point vertex. Also the agreement between the BMW and the non-local truncation results in the symmetric phase is quite good, despite not as good as in the previous case.

But this is not a satisfying test for the validity of our truncation: firstly, we compared all the non-local truncation results with the outcomes of the BMW equation, that is not an exact equation. Therefore we are comparing two approximate results. Moreover, with the BMW technique we have not been able to evaluate the complete RG flow but only a small interval of three orders of magnitude, and therefore we don't know if our results keep valid also in the case of a complete flow for the energy scale.

There are many interesting directions we can work in order to improve these truncations and better test their accuracy. As a first step, we could insert a non-local 4-point vertex ansatz also in the non-symmetric phase truncation, in order to improve the results, and we could develop non-local ansatz for the n-point vertices also for $n > 4$ to be inserted in the Z-2 invariant truncation. We could also try to calibrate the flow of the parameters in the ansatz using the low-momentum behavior of the vertices, instead of the high-momentum one. This would lead to more accurate results, as most of the RG flow of the EAA depends on the low-momentum behavior of the vertices. Moreover, we could try to export these results to more complex theories. In particular, there are many theories in which the non-local structure of the EAA plays a very important role. It is the case of massless theories, in which the mass term of the EAA is forced to be null, for example because of Gauge invariance or chirality reasons, and in which the non-local behavior of the 2-point vertex would be fundamental in order to achieve the correct evaluation of the vacuum energy flow. Finally, it could be interesting to investigate the consequences of a non-local truncation on the AS behavior of a theory. For example, it could be possible to evaluation the effect of a local truncation on the Wilson Fisher 3-dimensional IR Fixed Point. The truncation we developed seems to be able to achieve accurate results with a little work, and to predict the p-dependent structure of the vertices with good accuracy, but much remains to be done in order to completely test their validity and to export these results to many other situations.

Appendix A

Loop expansion

As we saw in section 3.1, it is possible to derive a loop expansion for the average effective action starting from the ERGE. If we deal with an optimized regulator term, we are also able to achieve an analytical expression for the first expansion terms. In the following, we are going to evaluate the 1-loop 2-point vertex and the 2-loop vacuum energy term in 1 and d dimensions. The 1-dimensional case is investigated separately from the more general d-dimensional one, as a different approach is used about the integration over the angular variables. We consider a local bare action

$$S[\phi] = \int d^d x \, \frac{1}{2} \left(\partial_\mu \phi(x)\right)^2 + V[\phi(x)] \tag{A.1}$$

A.1 Loop expansion in 1 dimension

As we understand from 3.3, the 1-loop flux of the 2-point vertex can be seen as the sum of a derivative contribution proportional to the 3-point vertex and a non-derivative one proportional to the 4-point vertex.

$$\partial_t \Gamma_k^{(2)1-loop} = \partial_t \Gamma_k^{(2)p-ind} + \partial_t \Gamma_k^{(2)p-dep} \tag{A.2}$$

A.1.1 1-loop momentum independent 2-point vertex

We will firstly calculate the simpler momentum independent contribution

$$\partial_t \Gamma_k^{(2)p-ind} = -\frac{V^{(4)}}{2} \int \frac{dq}{2\pi} G_{k;q} G_{k;q} \dot{R}_{k;q} \tag{A.3}$$

We can write the optimized cutoff term for a constant field strength $z_\phi = 1$

$$R_{k;q} = (k^2 - q^2)\theta(k^2 - q^2) \tag{A.4}$$

$$\begin{aligned} \dot{R}_{k;q} &= 2k^2 \theta(k^2 - q^2) \\ &= \dot{R}^0_{k;q} \theta(k^2 - q^2) \end{aligned} \tag{A.5}$$

and the propagator

$$\begin{aligned} G_{k;q} &= \frac{1}{(q^2 + V'') + R_{k;q}} \\ &= \frac{1}{(k^2 + V'')} \theta(k^2 - q^2) + \frac{1}{(q^2 + V'')} \theta(q^2 - k^2) \\ &= G^m_{k;q} \theta(k^2 - q^2) + G^M_{k;q} \theta(q^2 - k^2) \end{aligned} \tag{A.6}$$

Substituting, we find

$$\partial_t \Gamma_k^{(2)p-ind} = -\frac{k^3 V^{(4)}}{\pi \left(k^2 + V''\right)^2} \tag{A.7}$$

and finally, integrating out the flux, we find

$$\begin{aligned} \Gamma_k^{(2)p-ind} &= -\int_k^\infty \frac{\partial_t \Gamma_s^{(2)p-ind}}{s} ds \\ &= \frac{V^{(4)}}{4\pi} \left(\frac{2k}{k^2 + V''} - \frac{2 \tan^{-1}\left(\frac{k}{\sqrt{V''}}\right)}{\sqrt{V''}} + \pi \sqrt{\frac{1}{V''}} \right) \end{aligned} \tag{A.8}$$

A.1.2 1-loop momentum dependent 2-point vertex

In this section we are going to calculate the $\partial_t \Gamma_k^{(2)}$ one loop momentum dependent contribution

$$\partial_t \Gamma_{k;p}^{(2)p-dep} = (V^{(3)}[\phi])^2 \int \frac{dq}{2\pi} G_{k;p+q} G_{k;q} G_{k;q} \dot{R}_{k;q} \tag{A.9}$$

Firstly, substituting A.6 and A.5 in A.9 we get

$$\begin{aligned}\partial_t\Gamma^{(2)p-dep}_{k;p} =&(V^{(3)}[\phi])^2\int\frac{dq}{2\pi}G^m_{k;p+q}G^m_{k;q}G^m_{k;q}\dot{R}^0_{k;q}\theta(k^2-q^2)\theta(k^2-(q+p)^2)\\ &+(V^{(3)}[\phi])^2\int\frac{dq}{2\pi}G^M_{k;p+q}G^m_{k;q}G^m_{k;q}\dot{R}^0_{k;q}\theta(k^2-q^2)\theta((q+p)^2-k^2)\end{aligned}\tag{A.10}$$

where we can define

$$\begin{aligned}H_{q,p} &= G^m_{k;p+q}G^m_{k;q}G^m_{k;q}\dot{R}^0_{k;q}\\ F_{q,p} &= G^M_{k;p+q}G^m_{k;q}G^m_{k;q}\dot{R}^0_{k;q}\end{aligned}\tag{A.11}$$

Since $(q+p)^2 > k^2$ if $q > -p+k$ or $q < -p-k$, we can write

$$\begin{aligned}\partial_t\Gamma^{(2)p-dep}_{k;p} &= (V^{(3)}[\phi])^2\int_{-k}^{k}\frac{dq}{2\pi}F_{q,p} && \text{if } |p|>2k\\ \partial_t\Gamma^{(2)p-dep}_{k;p} &= (V^{(3)}[\phi])^2\int_{-k}^{k-|p|}\frac{dq}{2\pi}H_{q,|p|} &&\\ &\quad+(V^{(3)}[\phi])^2\int_{k-|p|}^{k}\frac{dq}{2\pi}F_{q,|p|} && \text{if } |p|<2k\end{aligned}\tag{A.12}$$

We can now calculate the indefinite integrals

$$\begin{aligned}\int\frac{dq}{2\pi}H_{q,p} =&\frac{qk^2}{\pi(V''+k^2)^3}\\ \int\frac{dq}{2\pi}F_{q,p} =&\frac{k^2\ \text{ArcTan}\left[\frac{(p+q)}{\sqrt{V''}}\right]}{\pi k^4\sqrt{V''}(V''+k^2)^2}\end{aligned}\tag{A.13}$$

and, finally, we get

$$\begin{aligned}\partial_t\Gamma^{(2)p-dep}_{k;p} =&-\theta\left[4k^2-p^2\right]\frac{k^2(V^{(3)}[\phi])^2\left(\left(k^2+V''\right)\left(\tan^{-1}\left(\frac{k}{\sqrt{V''}}\right)-\tan^{-1}\left(\frac{k+p}{\sqrt{V''}}\right)\right)+\sqrt{V''}(p-2k)\right)}{\pi\sqrt{V''}\left(k^2+V''\right)^3}\\ &-\theta\left[p^2-4k^2\right]\frac{k^2(V^{(3)}[\phi])^2\left(\tan^{-1}\left(\frac{p-k}{\sqrt{V''}}\right)-\tan^{-1}\left(\frac{k+p}{\sqrt{V''}}\right)\right)}{\pi\sqrt{V''}\left(k+V''\right)^2}\end{aligned}\tag{A.14}$$

We can expand in series for small momenta the p-dependence of A.14, finding the known results for the flow of the field strength and of the contribution to the flow of the mass term proportional to the 3-point vertex:

$$\partial_t \Gamma^{(2)p-dep}_{k;p} = \frac{2k^3 (V^{(3)}[\phi])^2}{\pi (V'' + k^2)^3} - \frac{k^3 (V^{(3)}[\phi])^2}{\pi (V'' + k^2)^4} p^2 + O\left(p^3\right) \tag{A.15}$$

We can now integrate the flux of the 2-point vertex in the 1-loop approximation. Firstly we define the functions $t_{k,p}$ and $u_{k,p}$ as follow

$$\frac{\partial_t \Gamma^{(2)p-dep}_{k;p}}{k} = \theta\left[4k^2 - p^2\right] t_{k,p} + \theta\left[p^2 - 4k^2\right] u_{k,p} \tag{A.16}$$

we can write

$$\begin{aligned} \Gamma^{(2)p-dep}_{k;p} &= -\int_{t_{(k)}}^{\infty} \partial_t \Gamma^{(2)p-dep}_{k_{(t)};p} dt \\ &= -\int_{k}^{\infty} \frac{\partial_t \Gamma^{(2)p-dep}_{s;p}}{s} ds \\ &= \theta(2k - p) T[k] + \theta(p - 2k)(T[p/2] + U[k, p/2]) \end{aligned} \tag{A.17}$$

where we have defined

$$T[k] = \int_{k}^{\infty} t_{s,p} ds \;\; ; \qquad U[k^a, k^b] = \int_{k^a}^{k^b} u_{s,p} ds \tag{A.18}$$

and finally we get

$$\begin{aligned}
\Gamma_{k;p}^{(2)p-dep} &= \frac{(V^{(3)}[\phi])^2\theta\left(4k^2-p^2\right)}{4\pi\sqrt{V''}\left(k^2+V''\right)^2\left(4V''+p^2\right)}\times \\
&\left(\sqrt{V''}\left(p-2k\right)\left(4V''+p^2\right)-2\pi\left(k^2+V''\right)^2\right. \\
&-2\left(k^2+V''\right)\left(\left(-k^2+3V''+p^2\right)\tan^{-1}\left(\frac{k+p}{\sqrt{V''}}\right)-\left(k^2+5V''+p^2\right)\tan^{-1}\left(\frac{k}{\sqrt{V''}}\right)\right) \\
&\left.-2\,p^{-1}\sqrt{V''}\left(k^2+V''\right)^2\left(\log\left(k^2+V''\right)-\log\left((k+p)^2+V''\right)\right)\right) \\
&+\frac{(V^{(3)}[\phi])^2\theta\left[-4k^2+p^2\right]}{4\pi\sqrt{V''}\left(k^2+V''\right)^2\left(4V''+p^2\right)}\times \\
&\left(-2\left(k^2+V''\right)^2\left(\pi-2\tan^{-1}\left(\frac{k}{\sqrt{V''}}\right)\right)\right. \\
&-2\left(k^2+V''\right)\left(-k^2+3V''+p^2\right)\left(\tan^{-1}\left(\frac{k-p}{\sqrt{V''}}\right)+\tan^{-1}\left(\frac{k+p}{\sqrt{V''}}\right)\right) \\
&\left.+4\,p^{-1}\sqrt{V''}\left(k^2+V''\right)^2\tanh^{-1}\left(\frac{2kp}{k^2+V''+p^2}\right)\right)
\end{aligned} \tag{A.19}$$

A.1.3 2-loop Effective Average Action

We can now use the formula for the 2-Loop contribution to calculate the average effective action

$$\partial_t\Gamma_k^{2-loop}=\frac{1}{2}\int_0^\infty\frac{dp}{2\pi}\left(G_{k;p}\right)^2\left(\Gamma_{k;p}^{(2)p-ind}+\Gamma_{k;p}^{(2)p-dep}\right)\dot{R}_{k;p} \tag{A.20}$$

We find that, because of the presence of a $\theta(k^2-p^2)$ term in $\dot{R}_{k;q}$, it is sufficient to consider the part of $\Delta\Gamma_{k;q}^{(2)p-dep}$ belonging to the $\theta(4k^2-p^2)$ term. It is possible to achieve an analytical exact result for the flux of the 2-loop average effective action, but it is much more involved than the flux of the 1-loop 2-point vertex and we will not write the result in the following. By evaluating this result for a zero external field $\phi=0$, we get to an analytical expression for the flux of the 2-loop vacuum energy. Finally, we can now integrate out the flux $\partial_t\Delta\Gamma_{k;p}^{2-loop}$ in k, but this is possible only numerically, because of the complexity of the integrand.

A.2 Loop expansion in d dimensions

A.2.1 1-loop momentum independent 2-point vertex

Proceeding as before and using the same definitions introduced in the previous sections with the only exception of a d-dimensional integration with $d > 1$, we find

$$\partial_t \Gamma_k^{(2)p-ind} = -\frac{1}{2^d \pi^{\frac{d}{2}} \Gamma[\frac{d}{2}+1]} \frac{k^{d+2} V^{(4)}}{\left(k^2 + V''\right)^2} \tag{A.21}$$

and integrating out the flux

$$\Gamma_k^{(2)p-ind} = -\frac{V^{(4)}}{2^d \pi^{\frac{d}{2}}} \left(\frac{2\mathrm{k}^{d+2}\, {}_2F_1\left[2, \frac{d}{2}+1; \frac{d}{2}+2; -\frac{\mathrm{k}^2}{m}\right]}{(2d+4)(V'')^2 \Gamma[\frac{d}{2}+1]} - \frac{1}{2}\left(\frac{1}{V''}\right)^{1-\frac{d}{2}} \Gamma\left[1-\frac{d}{2}\right] \right) \tag{A.22}$$

where ${}_2F_1$ represent the Hypergeometric Function.

A.2.2 1-loop momentum dependent 2-point vertex

Let us consider equation A.10 for $d > 1$. It reads

$$\begin{aligned}\partial_t \Gamma_{k;p}^{(2)p-dep} =& \frac{(V^{(3)}[\phi])^2}{(2\pi)^d} \mathrm{Vol}(S^{d-1}) \int_0^\infty dq q^{d-1} \int_{-1}^1 dx G^m_{k;\sqrt{p^2+q^2+2qpx}} G^m_{k;q} G^m_{k;q} \dot{R}^0_{k;q} \theta(k^2-q^2)\theta(k^2-(q^2+p^2+2qpx)) \\ &+ \frac{(V^{(3)}[\phi])^2}{(2\pi)^d} \mathrm{Vol}(S^{d-1}) \int_0^\infty dq q^{d-1} \int_{-1}^1 dx G^M_{k;\sqrt{p^2+q^2+2qpx}} G^m_{k;q} G^m_{k;q} \dot{R}^0_{k;q} \theta(k^2-q^2)\theta((q^2+p^2+2qpx)-k^2)\end{aligned}$$

where $x = \frac{\vec{p}\cdot\vec{q}}{pq} = \cos\theta_{p,q}$. It is convenient to define

$$\begin{aligned} H_{q,p,x} &= d^{D-1} G^m_{k;\sqrt{p^2+q^2+2qpx}} G^m_{k;q} G^m_{k;q} \dot{R}^0_{k;q} \\ F_{q,p,x} &= d^{D-1} G^M_{k;\sqrt{p^2+q^2+2qpx}} G^m_{k;q} G^m_{k;q} \dot{R}^0_{k;q} \end{aligned} \tag{A.23}$$

It is straightforward to show that

$$q^2 + p^2 + 2qpx - k^2 > 0 \iff x > l_{q,p} = \frac{k^2 - q^2 - p^2}{2qp} \tag{A.24}$$

and investigating the behavior of $l_{q,p}$ under the assumptions of q, p and k being positive we find that

$$l_{q,p} \geqslant \begin{cases} 1 & \text{if } q \in (0 \ , \ \text{Max}(k-p,0])] \\ -1 & \text{if } q \in [\text{Max}(p-k,0) \ , \ k+p] \end{cases} \tag{A.25}$$

Finally, denoting for notational simplicity

$$K = \frac{(V^{(3)}[\phi])^2}{(2\pi)^D}\text{Vol}(S^{D-1}) \tag{A.26}$$

we can obtain

$$\begin{aligned} \partial_t \Gamma_{k;p}^{(2)p-dep} = \quad & \text{if } p < k \qquad K\int_{k-p}^{k} dq \int_{l_{q,p}}^{1} dx F_{q,p,x} \\ & \qquad\qquad +K\int_{0}^{k-p} dq \int_{-1}^{1} dx H_{q,p,x} + K\int_{k-p}^{k} dq \int_{-1}^{l_{q,p}} dx H_{q,p,x} \\ & \text{if } k \leq p < 2k \qquad K\int_{0}^{p-k} dq \int_{-1}^{1} dx F_{q,p,x} + K\int_{p-k}^{k} dq \int_{l_{q,p}}^{1} dx F_{q,p,x} \\ & \qquad\qquad +K\int_{p-k}^{k} dq \int_{-1}^{l_{q,p}} dx H_{q,p,x} \\ & \text{if } 2k \leq p \qquad K\int_{0}^{k} dq \int_{-1}^{1} dx F_{q,p,x} \end{aligned} \tag{A.27}$$

We have obtained the corresponding analytical expression for 1-loop $\partial_t \Gamma_{k;p}^{(2)p-dep}$ in arbitrary d-dimensions, but the result is much more complex than the 1-dimensional one, and we will not report it in this work. Finally, it is possible to perform the integration of the 2-point vertex flux in order to get $\Gamma_{k;p}^{(2)p-dep}$ and, proceeding as we did in the 1-dimensional case, it is possible to achieve a flow expression for the average effective action.

Appendix B

BMW Tools

As we see in section 4.1, the integro-differential equation 4.3 can be strongly simplified by evaluating separately

$$\mathcal{J}^3_{k;a;\phi} = \int \frac{d^d q}{(2\pi)^d} G^2_{k;q;\phi} G_{k;q+a;\phi} \dot{\mathbb{R}}_{k;q} \tag{B.1}$$

$$\mathcal{I}^2_{k;\phi} = \int \frac{d^d q}{(2\pi)^d} G^2_{k;q;\phi} \dot{\mathbb{R}}_{k;q} = \mathcal{J}^n_{k;a=0;\phi} \tag{B.2}$$

This can be easily achieved under the LPA. As a first step, we can solve the ERGE adopting the LPA truncation 2.4 - 2.5; for brevity purposes we will only consider all potential terms up to the 4-order in ϕ.

$$V[\phi] = \epsilon_k + \frac{m_k}{2}\phi^2 + \frac{\rho_k}{3!}\phi^3 + \frac{\lambda_k}{4!}\phi^4 \tag{B.3}$$

As we saw in chapter 2, the derivation of the d-dimensional RG flow equations for the couplings is straightforward

$$\partial_t z_k = -\frac{2^{1-d}\pi^{-d/2}k^3\rho_k^2 z_k^2}{d\Gamma\left(\frac{d}{2}\right)\left(k^2 z_k + m_k\right)^4} \tag{B.4}$$

$$\partial_t \hat{\phi}_k = \frac{2^{-2d-1}\pi^{-d}k^{d+2}\rho_k z_k\left(2^{d+1}\pi^{d/2}\left(k^2 z_k + m_k\right)^4 - \frac{k^3\rho_k^2 z_k}{\Gamma\left(\frac{d}{2}+2\right)}\right)}{\Gamma\left(\frac{d}{2}+1\right) m_k \left(k^2 z_k + m_k\right)^6} \tag{B.5}$$

$$\partial_t \epsilon_k = \frac{2^{-2d-1}\pi^{-d}k^d z_k\left(k^2\left(z_k-1\right)+m_k\right)\left(\frac{k^3\rho_k^2 z_k}{\Gamma\left(\frac{d}{2}+2\right)} - 2^{d+1}\pi^{d/2}\left(k^2 z_k + m_k\right)^4\right)}{\Gamma\left(\frac{d}{2}+1\right)\left(k^2 z_k + m_k\right)^5} \tag{B.6}$$

$$\partial_t m_k = -\frac{2^{1-d}\pi^{-d/2}k^{d+2}z_k\left(m_k\left(k^2\lambda_k z_k - 3\rho_k^2\right) - k^2\rho_k^2 z_k + \lambda_k m_k^2\right)}{d(d+2)\Gamma\left(\frac{d}{2}\right) m_k \left(k^2 z_k + m_k\right)^3}\times$$
$$\left(-\frac{2^{1-d}\pi^{-d/2}k^3\rho_k^2 z_k}{d\Gamma\left(\frac{d}{2}\right)\left(k^2 z_k + m_k\right)^4} + d + 2\right) \tag{B.7}$$

$$\partial_t \rho_k = \frac{(4\pi)^{-d}k^{d+2}\rho_k z_k\left(\lambda_k\left(k^2 z_k + m_k\right)\left(k^2 z_k + 7m_k\right) - 6m_k\rho_k^2\right)}{d\Gamma\left(\frac{d}{2}+2\right)\Gamma\left(\frac{d}{2}\right) m_k\left(k^2 z_k + m_k\right)^8}\times$$
$$\left(2^{d+1}\pi^{d/2}\Gamma\left(\frac{d}{2}+2\right)\left(k^2 z_k + m_k\right)^4 - k^3\rho_k^2 z_k\right) \tag{B.8}$$

$$\partial_t \lambda_k = \frac{3\ 2^{1-2d}\pi^{-d}k^{d+2}z_k\left(-6\lambda_k\rho_k^2\left(k^2 z_k + m_k\right) + \lambda_k^2\left(k^2 z_k + m_k\right)^2 + 4\rho_k^4\right)}{(d+2)\Gamma\left(\frac{d}{2}+1\right)^2\left(k^2 z_k + m_k\right)^9}\times$$
$$\left(2^{d+1}\pi^{d/2}\Gamma\left(\frac{d}{2}+2\right)\left(k^2 z_k + m_k\right)^4 - k^3\rho_k^2 z_k\right) \tag{B.9}$$

and, therefore, it is sufficient to numerically solve the system of coupled differential equations in order to achieve the k-dependent value of the flowing couplings. It is now possible to get an analytical expression for $\mathcal{I}^n_{k;\phi}$ and $\mathcal{J}^n_{k;a;\phi}$ proceeding as in A.1.2 and A.2.2 for non-trivial anomalous dimensions $\eta_k = -\frac{\partial_t z_k}{z_k}$

$$\mathcal{I}^2_{k;\phi} = \frac{2^{2-d}\pi^{-d/2}z(d-\eta+2)k^{d+2}}{d(d+2)\Gamma\left(\frac{d}{2}\right)\left(k^2 z + \mathrm{V}"\right)^2} \tag{B.10}$$

d=1

$$
\begin{aligned}
\mathcal{J}^3_{k;p;\phi} \quad = \quad & \frac{\theta\left[p^2-4k^2\right]}{2\pi\sqrt{z}\sqrt{V''}\left(k^2z+V''\right)^2}\times \\
& \left(\left(\eta(z(k-p)(k+p)+\mathrm{V"})-2k^2z\right)\left(\tan^{-1}\left(\frac{\sqrt{z}(p-k)}{\sqrt{\mathrm{V"}}}\right)-\tan^{-1}\left(\frac{\sqrt{z}(k+p)}{\sqrt{\mathrm{V"}}}\right)\right)\right. \\
& \left.+\eta\sqrt{z}\sqrt{V''}\left(p\log\left(z(k-p)^2+V''\right)-p\log\left(z(k+p)^2+V''\right)+2k\right)\right) \\
& +\frac{z\theta\left[4k^2-p^2\right]}{6\pi\left(k^2z+V''\right)^3}\times \\
& \left(\sqrt{\mathrm{V"}}\sqrt{z}\left(z\left(-4(\eta-3)k^3+3(\eta-2)k^2p+3\eta kp^2-\eta p^3\right)+3\eta p\mathrm{V"}\right)\right. \\
& +3\left(k^2z+V''\right)\left(\left(\eta(z(k-p)(k+p)+\mathrm{V"})-2k^2z\right)\left(\tan^{-1}\left(\frac{k\sqrt{z}}{\sqrt{\mathrm{V"}}}\right)-\tan^{-1}\left(\frac{\sqrt{z}(k+p)}{\sqrt{\mathrm{V"}}}\right)\right)\right. \\
& \left.\left.+\eta p\sqrt{\mathrm{V"}}\sqrt{z}\left(\log\left(k^2z+\mathrm{V"}\right)-\log\left(z(k+p)^2+\mathrm{V"}\right)\right)\right)\right)
\end{aligned}
\tag{B.11}
$$

Proceeding as in subsection A.2.2 it is possible to achieve an analytical expression for $\mathcal{J}^3_{k;a;\phi}$ also in a general d-dimensional framework, but it is much more complex than in the 1-dimensional case, and we will not write it in this work. We can finally substitute the value obtained for the running couplings in the analytical expressions for $\mathcal{I}^n_{k;\phi}$ and $\mathcal{J}^n_{k;a;\phi}$ in order to achieve the required terms to be inserted in equation 4.3.

Appendix C

Sommario della Tesi

Nella prima parte della tesi vengono introdotti alcuni concetti fondamentali riguardo uno dei piú utilizzati approcci non perturbativi al Gruppo di Rinormalizzazione.

Nel capitolo 1, dopo una breve escursione sull'interpretazione fisica dell' azione efficace, viene introdotto il concetto di azione efficace media e viene derivata un' equazione integro-differenziale che ne controlla il flusso, chiamata Equazione Esatta del Gruppo di Rinormalizzazione (ERGE). Viene inoltre introdotto lo scenario di Salvezza Asintotica, che si propone come una generalizzazione non-perturbativa del concetto di rinormalizzabilitá. Tutti i risultati ottenuti vengono confrontati con i loro corrispondenti in teoria perturbativa, nel tentativo di comprendere meglio il significato fisico di questo approccio. Infine, vengono dati alcuni semplici esempi.

Nel capitolo 2, viene introdotto un troncamento per l'azione efficace media utilizzando l'approssimazione di potenziale locale. Il caso di un campo scalare reale interagente in d-dimensioni viene approfondito e, attraverso la ERGE, vengono derivate le equazioni di flusso per gli accoppiamenti. la ERGE viene inoltre utilizzata per investigare le dimensioni anomale del campo e il flusso del valore di aspettazione del vuoto. Infine, i risultati ottenuti per l'energia di vuoto nel caso di una teoria interagente in 1 dimensione, corrispondente all'oscillatore anarmonico quantistico, vengono confrontati con i corrispondenti risultati in teoria perturbativa.

Nel capitolo 3 é raccolta la maggior parte del nostro lavoro originale. Come prima cosa, utilizzando i risultati perturbativi al primo ordine per il vertice efficace medio a 2 punti come riferimento (raccolti nell'appendice A), viene introdotto un ansatz non locale per quest'ultimo nel caso di un campo scalare reale in una dimensione. Tale ansatz viene poi utilizzato per definire un troncamento non locale e, attraverso la ERGE, vengono calcolate le equazioni di flusso per gli accoppiamenti. Viene poi proposto uno schema di approssimazioni utile per introdurre un troncamento non locale consistente anche nel caso di una teoria Z-2 invariante e, sotto tale troncamento, vengono nuovamente derivate le equazioni di flusso per gli accoppiamenti. Sempre nel caso di una teoria Z-2 invariante, i risultati ottenuti attraverso il nostro troncamento non locale e attraverso il troncamento definito nel capitolo 2 sono confrontati con i risultati esatti, mostrando un miglioramento di un ordine di grandezza dei risultati ottenuti con l'ansatz non locale rispetto a quelli ottenuti nell'approssimazione di potenziale locale.

Infine, nel capitolo 4 viene descritta una tecnica che permette di ottenere, attraverso alcune approssimazioni, un' equazione integro-differenziale chiusa per il vertice efficace medio a 2 punti, chiamata BMW in onore dei primi ricercatori che la ottennero. Abbiamo risolto su griglia tale equazione utilizzando un metodo alle differenze finite e abbiamo utilizzato i valori ottenuti come test per i corrispondenti risultati ottenuti attraverso il troncamento non locale da noi introdotto. Tale confronto ha evidenziato un buon accordo tra risultati ottenuti nei due diversi approcci e, in particolare, sembra mostrare come, in una teoria di questo tipo, il nostro ansatz sia in grado di descrivere la struttura non locale delle funzioni a due e quattro punti con buona precisione.

Nelle conclusioni sono raccolti i piú significativi risultati ottenuti insieme ad alcune proposte riguardo ulteriori test, possibili miglioramenti e interessanti applicazioni future per i troncamenti non locali introdotti in questa tesi.

Acknowledgements

Durante questi cinque anni che ho trascorso come studente di fisica presso l'universitá di Bologna, molte sono le persone cui sento di essere grato. Ho avuto modo di imparare da grandi "maestri", che con estrema eleganza hanno saputo guidarmi, trasmettendomi entusiasmo e serietá. Ma prima di ogni altra persona, desidero ringraziare il mio correlatore, Gian Paolo Vacca. Mai avrei pensato che scrivere una tesi avrebbe potuto appassionarmi tanto, e questo lo devo completamente a lui. Egli mi ha guidato con grande esperienza e disponibilitá mentre andavo a tentoni in un mondo che non conoscevo, e pur sapendo fin dall'inizio quale sarebbe stata la meta ha lasciato che percorressi passo a passo la strada, correggendomi con pazienza tutte le volte che per qualche ragione deviavo e sembravo perdermi. Per aver reso tutto cosí naturale gli sono immensamente grato. Desidero inoltre ringraziare il prof. Giovanni Venturi, per avermi accolto con grande disponibilitá nel suo gruppo di lavoro quando mi sono recato da lui e per aver saputo guidarmi tutte le volte che gli ho chiesto consiglio. Sono contento di avere codiviso con colleghi e amici questo percorso, e per questo prima di tutti vorrei ringraziare Cesco e Soncio. Grazie per le camminate trascorse a raccontarci i problemi e le soddisfazioni che nel lavoro incontravamo, quando si scopriva di essere in fondo tutti nella stessa barca ed ogni cosa, in un certo qual modo, appariva piú semplice. Non posso non sentirmi grato verso le persone con cui ho vissuto in questi anni, e che hanno reso questo percorso cosí ricco. Grazie Marta, Fabi, un grazie immenso Lore e Mike, grazie alla grande Anna e, anche se aggiunta clandestinamente, grazie Ludo. Grazie a Massa 46 e alla saggia Terrazza.

Un grazie particolare va alla mia famiglia, che ha sempre creduto in me e mi ha sempre spinto a seguire i miei sogni, qualunque essi fossero. Grazie Mamma e grazie Babbo, grazie davvero, perché se sto per laurearmi lo devo unicamente e completamente a voi. Infine grazie Ilenia, grazie per come sei. Grazie per vivere insieme a me questo momento, grazie per renderlo quello che é.

Bibliography

[1] L.F. Abbott. Introduction to the Background Field Method. *Acta Phys.Polon.*, B13:33, 1982.

[2] F. Benitez, J.-P. Blaizot, H. Chaté, B. Delamotte, R. Méndez-Galain, and N. Wschebor. Solutions of renormalization-group flow equations with full momentum dependence. *Phys. Rev. E*, 80:030103, Sep 2009.

[3] Jurgen Berges, Nikolaos Tetradis, and Christof Wetterich. Non-perturbative renormalization flow in quantum field theory and statistical physics. *Physics Reports*, 363(4-6):223 – 386, 2002.

[4] J.-P. Blaizot, R. Méndez-Galain, and N. Wschebor. A new method to solve the non-perturbative renormalization group equations. *Physics Letters B*, 632(4):571 – 578, 2006.

[5] J.-P. Blaizot, R. Méndez-Galain, and N. Wschebor. Non perturbative renormalization group and momentum dependence of n-point functions. II. *Phys.Rev.*, E74:051117, Nov 2006.

[6] J.-P. Blaizot, R. Méndez-Galain, and N. Wschebor. Non-perturbative renormalization group calculation of the scalar self-energy. *European Physical Journal B*, 58:297–309, August 2007.

[7] J.-P. Blaizot, R. Méndez-Galain, and N. Wschebor. Perturbation theory and

non-perturbative renormalization flow in scalar field theory at finite temperature. *Nucl.Phys.*, A784:376–406, 2007.

[8] Bryce S. DeWitt. Quantum Theory of Gravity. II. The Manifestly Covariant Theory. *Phys. Rev.*, 162(5):1195–1239, Oct 1967.

[9] D. Dou and R. Percacci. The running gravitational couplings. *Classical and Quantum Gravity*, 15:3449–3468, November 1998.

[10] H. Gies. Introduction to the functional RG and applications to gauge theories. 2006.

[11] M. Jafarpour. Energy Levels for the Pure λx^{2m} Potentials. *Journal of Sciences*, 18:75–81, 2007.

[12] M. H. Macfarlane. A High-Precision Study of Anharmonic-Oscillator Spectra. *Annals of Physics*, 271:159–202, February 1999.

[13] A Morozov and A J Niemi. Can renormalization group flow end in a big mess? *Nucl. Phys. B*, 666(hep-th/0304178. ITEP-TH-2003-23):311–336. 40 p, Apr 2003.

[14] R. Percacci. The renormalization group, systems of units and the hierarchy problem. *Journal of Physics A Mathematical General*, 40:4895–4913, May 2007.

[15] Roberto Percacci and Daniele Perini. Asymptotic safety of gravity coupled to matter. *Phys. Rev. D*, 68(4):044018, Aug 2003.

[16] A. Codello; R. Percacci; C. Rahmede. Investigating the ultraviolet properties of gravity with a wilsonian renormalization group equation. *Annals of Physics*, 324(2):414 – 469, 2009.

[17] M. Reuter. Nonperturbative Evolution Equation for Quantum Gravity. *Phys. Rev.*, D57:971–985, 1998.

[18] M. E. Peskin; D. V. Schroeder. *An Introduction to Quantum Field Theory*. Westview Press, Perseus Books Group,, 1995.

[19] R. Soldati. Intermediate relativistic quantum field theory. September 2010.

[20] S. Weinberg. *The quantum theory of fields*, volume 1-2. Cambridge University Press, 1995.

[21] C. Wetterich. Average action and the renormalization group equations. *Nuclear Physics B*, 352(3):529 – 584, 1991.

[22] C. Wetterich. Exact evolution equation for the effective potential. *Physics Letters B*, 301(1):90 – 94, 1993.

[23] K. G. Wilson. Renormalization group and critical phenomena. i. renormalization group and the kadanoff scaling picture. *Phys. Rev. B*, 4(9):3174–3183, Nov 1971.

[24] G. P. Vacca; L. Zambelli. Functional RG flow equation: Regularization and coarse-graining in phase space. *Phys. Rev. D*, 83(12):125024, June 2011.

[25] L. Zambelli. Effective average actions and rg flows of gravity-matter systems. Master's thesis, University of Bologna, 2007-2008.

[26] O. Zanusso. *Selected applications of functional RG*. PhD thesis, 2010.

[27] O. Zanusso, L. Zambelli, G. P. Vacca, and R. Percacci. Gravitational corrections to Yukawa systems. *Physics Letters B*, 689:90–94, May 2010.

[28] A. Zee. *Quantum Field Theory in a Nutshell*. Princeton University Press, 2010.